No. 118
December 1971

LOADING OF THE HULL GIRDER

J. Moe
Translated by: F. C. Michelsen

THE DEPARTMENT OF NAVAL ARCHITECTURE AND MARINE ENGINEERING

THE UNIVERSITY OF MICHIGAN
COLLEGE OF ENGINEERING

ACKNOWLEDGEMENT

The cost of typing and reproducing these notes was covered in part by a grant from Frederic Gibbs.

L O A D I N G O F T H E

H U L L G I R D E R

by: J. Moe*

translated by: F.C. Michelsen**

DEPARTMENT OF NAVAL ARCHITECTURE AND MARINE ENGINEERING
COLLEGE OF ENGINEERING
THE UNIVERSITY OF MICHIGAN
ANN ARBOR, MICHIGAN
1971

* Prof. N.T.H. Trondheim, Norway

** Prof. University of Michigan

TABLE OF CONTENTS

P R E F A C E

Current progress in ship structure analysis is extremely rapid. Until the middle of the 1950's, all computations of external longitudinal stresses in ships were done using the quasistatic method which is discussed in section 1.3. In 1953, St. Denis and Pierson published a work in the Transactions of SNAME under the title: "On the Motions of Ships in Confused Seas." This work came to represent the introduction to a new era on the subject, since following its publication statistical methods were introduced in the mathematical description of ships' motion and the resulting loading when operating in a storm sea. This method of approach has proved very useful. Even though we most likely are still in the early stages of development of a rational set of dimensioning rules based on statistical methods, it must be characterized as fortunate that these new methods were introduced in time to be of value in establishing strength requirements for the very large ships built today.

The amount of loading of the hull is closely related to the motions. For precise computations, the inertia forces must be included. For this reason it has been necessary to include in the following presentations some basic theory of waves and ship motion which actually belongs elsewhere. These discussions are short, so readers with special interest in ship motion are referred to the special literature, e.g.:

Korvin-Kroukovsky, B.V.: "Theory of Seakeeping." Ship Structures Committee, SNAME, New York, 1961.

Vossers, G.: "Behaviour of Ships in Waves." Haarlem (The Netherlands), 1962.

A lot of the basics for the material in sections 1.2, 1.3, and 1.4, was collected and revised by Heesch and is presented in the book:

Heesch, F.G.: "Ytre Langskipspåkjenninger." Institutt for Skipsbygging II, NTH, 1964.

In the above book a number of worked examples in connection with the material presented here in section 1.4 can be found.

Readers with special interest for the statistical treatment of wave motion and resulting motion and stresses on ships, are referred to the literature given under the respective sections. A great deal on this subject will be found in the above-mentioned books by Korvin-Kroukovsky and Vossers.

Trondheim, Spring 1965.

1. Longitudinal stresses.

1.1 Introduction

One of the most important problems of strength analysis of ships is to determine the longitudinal stresses the hull experiences when being regarded as a floating beam of box-shaped cross-section. The hull girder is loaded by vertical downward forces produced by its own weight, equipment, cargo, etc., and oppositely directed buoyancy forces. When the ship is moving in waves, the hull girder also experiences dynamical stresses. For large ships, the magnitude and type of these static and dynamic longitudinal stresses become decisive in the design and dimensioning of a very significant part of the hull's structure, and it is therefore economically important to arrive at the most realistic values for the longitudinal stresses in the hull.

When determining the external longitudinal stresses, the hull is regarded as rigid. The changes in the buoyancy distribution, etc., that occur due to hull girder deflections caused by external loading, are generally disregarded. The elastic(or plastic) properties of the design must in special cases be taken into consideration, e.g. when calculating the loading caused by hull vibrations, local impacts, slamming, etc.

The loading of the hull girder arises from the difference between oppositely directed external forces. We differentiate between loadings parallel to the following planes (see Fig. 1.1):

1) A longitudinal plane through the center-line of the bottom and deck, the so-called center-line-plane.

2) A longitudinal plane perpendicular to the center-line-plane, the so-called lateral plane.

The external loading generally causes shear forces and bending moments in both longitudinal planes as well as torsion moments in the transverse plane.

It will be convenient to distinguish between stresses caused by the following (partly hypothetical) loading conditions:

a) The ship is positioned in static equilibrium in calm water.

b) The ship is positioned in static equilibrium on a stationary regular wave of a simple geometrical form (sinusoidal, trochoidal). For this loading condition, the buoyancy forces are usually corrected for the water particles own motion in the wave. (The orbital motion of the particles gives a reduction of the specific weight of the water at the wave crest and an increase at the wave through caused by the centrifugal effect, the so-called Smith's effect). This method of calculating the wave loads is referred to as being quasi-static.

c) Dynamic equilibrium in regular waves. In this case the motion of the ship as well as the wave is taken into consideration. The motions are assumed to be harmonic.

d) The ship moves in irregular waves. In this case the ship will experience rapid and quite irregular motions and stresses. Quantitatively the stresses may, under special conditions, still be derived, using statistical methods.

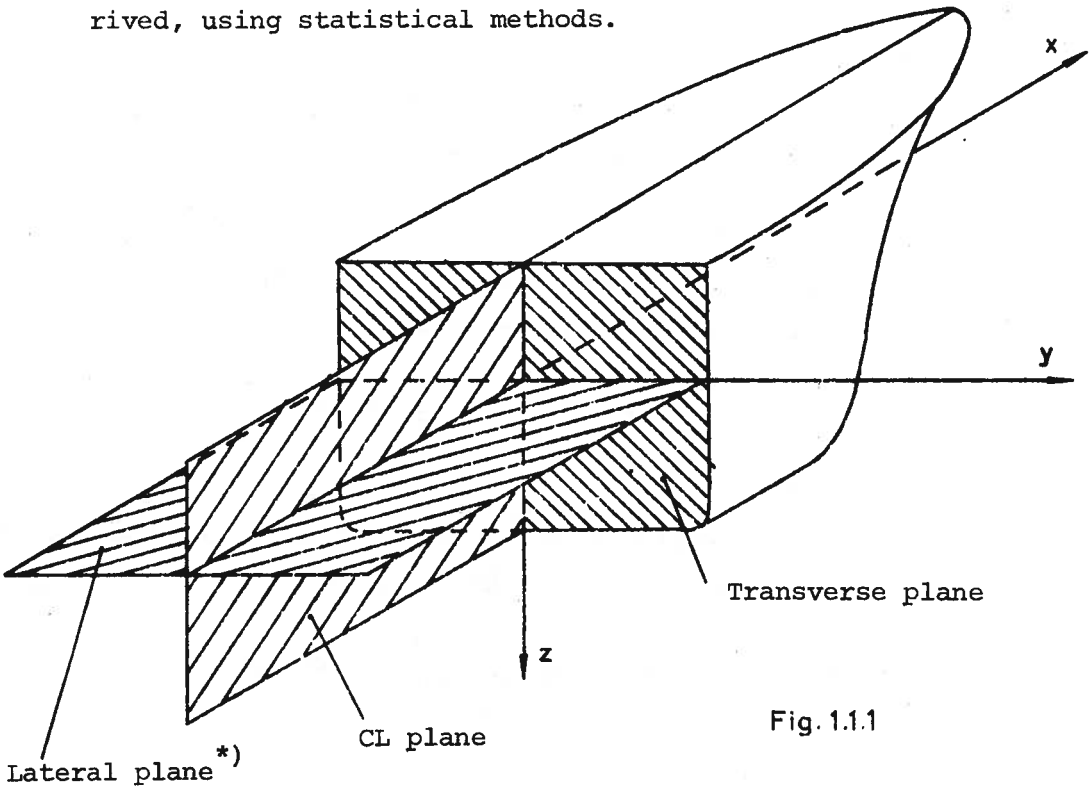

Fig. 1.1.1

*) "Waterline plane" might be a better term since the "lateral plane" also has another meaning in the literature.

The force and motion conditions are three-dimensional in nature. To describe them it is convenient to introduce three coordinate systems:

i) A system (ξ, η, ζ) which is fixed in space.

ii) A system (x, y, z) which is fixed in the vessel, see fig. 1.1.1. Origin in the (x, y, z) system is placed at the center of gravity of the vessel, at the center of flotation, or at other convenient places depending on the problem at hand.

iii) A system (x', y', z') that follows the vessel (see fig. 1.3.16) such that the (x', y', z') plane coincides with the water surface in calm water.

The vessel performs non-oscillating and oscillating translational and rotational motions. The motions are decomposed in the usual manner into three components. The result is 6 possible motions (degrees of freedom); in addition we consider the motion of the rudder. In reality, all these motions are coupled (depending upon each other), but for the time being only the stresses due to uncoupled phenomenon will be studied.

1.2 Still water loading

1.2.1 Buoyancy

1.2.1.1 Fundamentals

The distribution of the buoyancy forces on the hull and resulting loading can only be decided when the equilibrium position of the vessel in the water is known. The equilibrium position is usually determined in the following way:

a) The ship is first assumed placed in a chosen position which is assumed to be as close as possible to the equilibrium position.

b) The necessary corrections to this arbitrarily chosen position are then determined to obtain complete equilibrium.

Let

- $/q_z^b/$ represent the resultant buoyancy force, per unit length in the x-direction.*

q_z^w represent the resulting downwards loading per unit length

$q_z = q_z^b + q_z^w$

$\overline{y^b}$ $\overline{(y^w)}$ represent the distance transversely from the CL-plane to the point of action for q_z^b and q_z^w respectively, see fig. 1.2.1.

---

* Forces acting upwards are taken to be negative.

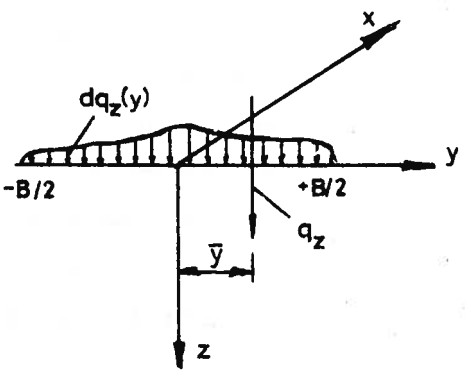

Fig. 1.2.1

$$q_z = \int_{-\frac{B}{2}}^{+\frac{B}{2}} dq_z(y) \qquad (1.2.1)$$

$$\bar{y} = \frac{1}{q_z} \int_{-\frac{B}{2}}^{+\frac{B}{2}} y \cdot dq_z(y)$$

If the vessel is in equilibrium, the following relations must be valid:

Force equilibrium in the z-direction:

$$\int_L q_z \, dx = \int_L q_z^w \, dx + \int_L q_z^b \, dx = 0 \qquad (1.2.2a)$$

Moment equilibrium in the CL-plane ($\Sigma M_y = 0$):

$$\int_L q_z x \, dx = \int_L q_z^w x \, dx + \int_L q_z^b x \, dx = 0 \qquad (1.2.2b)$$

Moment equilibrium transversely ($\Sigma M_x = 0$):

$$\int_L q_z \bar{y} \, dx = \int_L q_z^w \bar{y}^w \, dx + \int_L q_z^b \bar{y}^b \, dx = 0 \qquad (1.2.2c)$$

The equilibrium position is usually not to be achieved on the first attempt. Instead of zero, after the integrations above, δP , δM_y , and

δM_x repectively are obtained on the right hand side of the eqns. 1.2.2a,b, and c. This means that the vessel in the chosen position is acted on by the resulting forces and moments δP , δM_y , and δM_x with positive directions as shown in fig. 1.2.2. To reach equilibrium, the vessel must be immersed deeper and at the same time trim by the bow (the bow is immersed relative to the afterbody) and heeled to starboard.

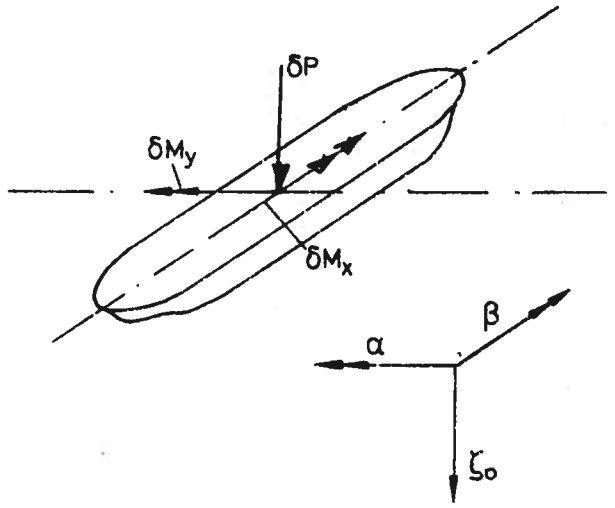

Fig. 1.2.2

1.2.1.2 Vessels with approximately vertical sides.

The effect of parallel immersion, trim and heeling will now be determined, since the analysis is based on the following assumptions:

1) The vessel is initially positioned such that the (ξ,η,ζ) axis coincide with the (x,y,z) axis. The (ξ,η) plane is in addition coinciding with the free-surface of the water with origin at the center of floatation.

2) Original and new floatation water-planes have same area with the center of floatation unchanged.

3) Trim and heeling angles (α and β) are positive when the draft increases in the first quadrant of the $\xi\eta$-plane . The angles α and β are smaller than approximately 0.1 radians (5.7°) such that $\tan\alpha \sim \sin\alpha \sim \alpha$, $\tan\beta \sim \sin\beta \sim \beta$, $\cos\alpha \sim \cos\beta \sim 1$.

The second assumption will always be satisfied if the vessel has vertical sides in the region between the two floatation planes.

The vessel which is floating at equilibrium in an upright condition, is now assumed displaced from the equilibrium condition by:

a) The draft of the floatation center is increased by the amount ζ_o .

b) The vessel is trimmed by an angle α .

c) The vessel is heeled by an angle β .

The forces applied to the vessel to give the above displacements are wanted. The changes in the buoyancy forces that develop during the displacements will depend on the location of the new floatating plane relative to the (x,y) plane (see fig. 1.2.3). When α and β are small, the location of (x,y,z) may be expressed approximately by the point $(\xi,\eta,0)$ in the original floatating plane by the following equations:

$$\begin{aligned} x &= \xi \\ y &= \eta \\ z &= -(\zeta_o + x\alpha + y\beta) \end{aligned} \qquad (1.2.3)$$

The buoyancy force on a surface element $dA = dxdy$ of the floatation plane is changed by the additional force

$$dq_z^b = \gamma z dA$$

where positive dq_z^b corresponds to the reduction in the buoyancy according to earlier sign convention and γ is the specific weight of the water.

Forces and moments that result from the displacements ζ_o, α, and β are thus:

$$dP = \int_{-\frac{B}{2}}^{+\frac{B}{2}} \int_{L} dq_z^b = -\gamma \int_{-\frac{B}{2}}^{+\frac{B}{2}} \int_{L} (\zeta_o + x\alpha + y\beta)\, dxdy$$

$$dP = -\gamma\,(A_{WL}\,\zeta_o + S_y\alpha + S_x\beta) \qquad (1.2.4a)$$

$$dM_x = \int_{-\frac{B}{2}}^{+\frac{B}{2}} \int_{L} y\,dq_z^b = -\gamma \int_{-\frac{B}{2}}^{+\frac{B}{2}} \int_{L} (y\,\zeta_o + xy\alpha + y^2\beta)\,dxdy$$

$$dM_x = -\gamma(S_x\,\zeta_o + I_{xy}\alpha + I_x\beta) \qquad (1.2.4b)$$

$$dM_y = \int_{-\frac{B}{2}}^{+\frac{B}{2}} \int_{L} x\,dq_z^b = -\gamma \int_{-\frac{B}{2}}^{+\frac{B}{2}} \int_{L} (x\,\zeta_o + x^2\alpha + xy\beta)\,dxdy$$

$$dM_y = -\gamma(S_y\,\zeta_o + I_y\alpha + I_{xy}\beta) \qquad (1.2.4c)$$

The following notation is used:

$A_{WL} = \iint_{BL} dxdy$ = area of the floatation plane

$S_x = \iint_{BL} y\,dxdy$ = the static moment of the floatation plane relative to the x-axis.

$S_y = \iint_{BL} x\,dxdy$ = the static moment of the floatation plane relative to the y-axis

$I_x = \iint_{BL} y^2 dxdy$ = the moment of inertia of the floatation plane relative to the x-axis.

$I_y = \iint_{BL} x^2 dxdy$ = the moment of inertia of the floatation plane relative to the y-axis.

$I_{xy} = \iint_{BL} xy\,dxdy$ = the product of inertia of the floatation plane.

Letting the (x,y) axis coincide with the principal axis of the flotation plane, the origin will be located at the center of floatation (the center of gravity of the floatation plane) giving:

$$I_{xy} = S_x = S_y = 0$$

The equations (1.2.4a-c) then become:

$$\begin{aligned} dP &= -\gamma A_{WL} \zeta_o \\ dM_x &= -\gamma I_x \beta \\ dM_y &= -\gamma I_y \alpha \end{aligned} \qquad (1.2.5a\text{-}c)$$

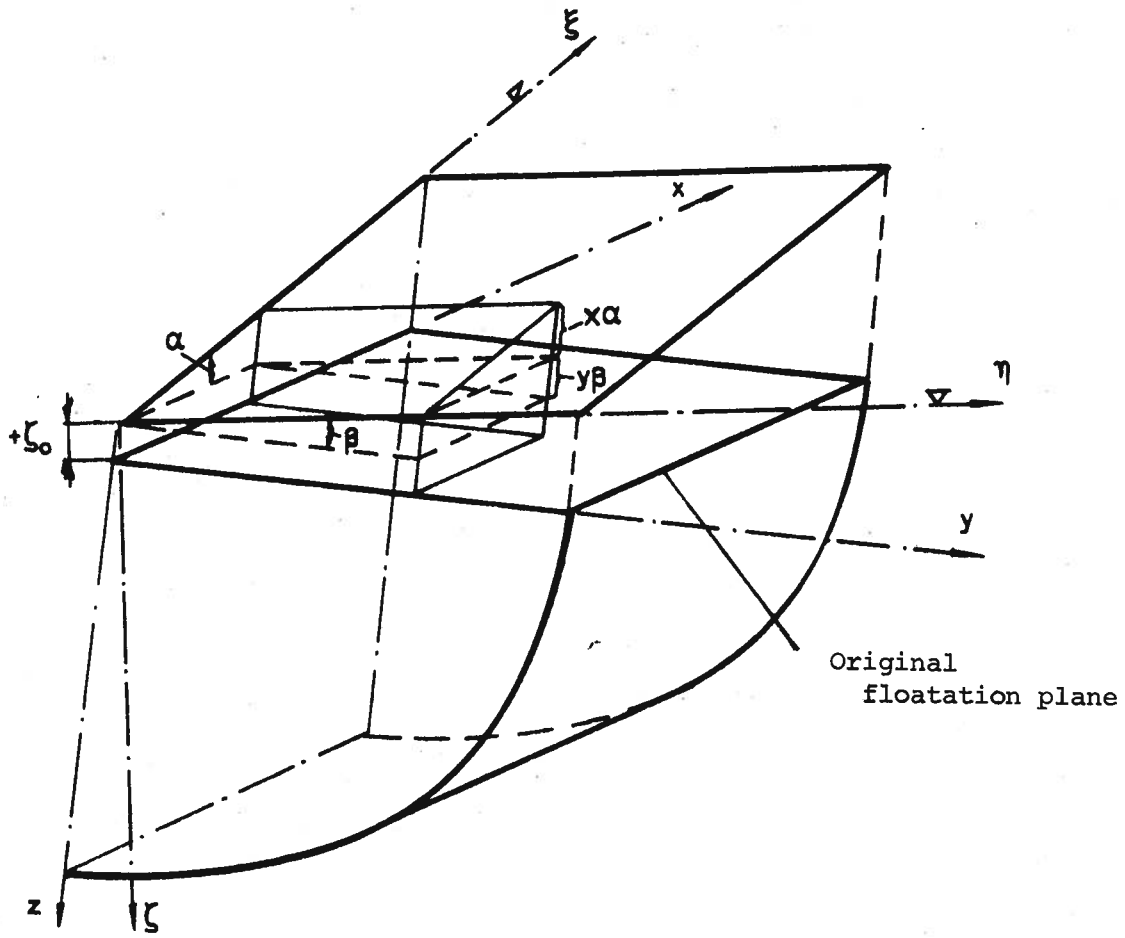

Fig. 1.2.3

The equations (1.2.5) describe the relationships between the vessel's displacements (immersion ζ_o , heeling angle β , and trim angle α) and the corresponding changes in the external forces and moments. These are totally due to changes in buoyancy. Positive direction for forces, moments, displacements, and rotations are shown in Fig. 1.2.2.

We are ready to return to the problem of finding the equilibrium position of the vessel. Relative to the initially assumed position the vessel must be immersed, heeled and trimmed such that

$$\delta P + dP = 0$$
$$\delta M_x + dM_x = 0$$
$$\delta M_y + dM_y = 0$$

which with the aid of equations (1.2.5a-c) give:

$$\zeta_o = \frac{\delta P}{\gamma A_{WL}}$$

$$\beta = \frac{\delta M_x}{\gamma I_x} \qquad (1.2.6a\text{-}c)$$

$$\alpha = \frac{\delta M_y}{\gamma I_y}$$

After these changes in the position of the vessel are made, it may be desirable to check again the equilibrium equations (1.2.2a-c) with the new distribution of the buoyancy forces.

Example 1.2.1

A box-shaped vessel with dimensions L x B x d and $C_B = C_{WL} = 1$ is floating upright on even-keel*. A weight P is taken onboard and positioned at $(\frac{L}{4}, \frac{B}{4})$ in a coordinate system with origin at the center of floatation.

---

* The block-coefficient is defined by the equation $C_B = \frac{\nabla}{BdL}$. The waterline coefficient is defined by the equation $C_{WL} = \frac{A_{WL}}{BL}$ where ∇ = the immersed volume of the vessel. A_{WL} = the area of the waterline plane. d = draft. B = the maximum beam of the floatation plane. L = length of vessel (usually LBP).

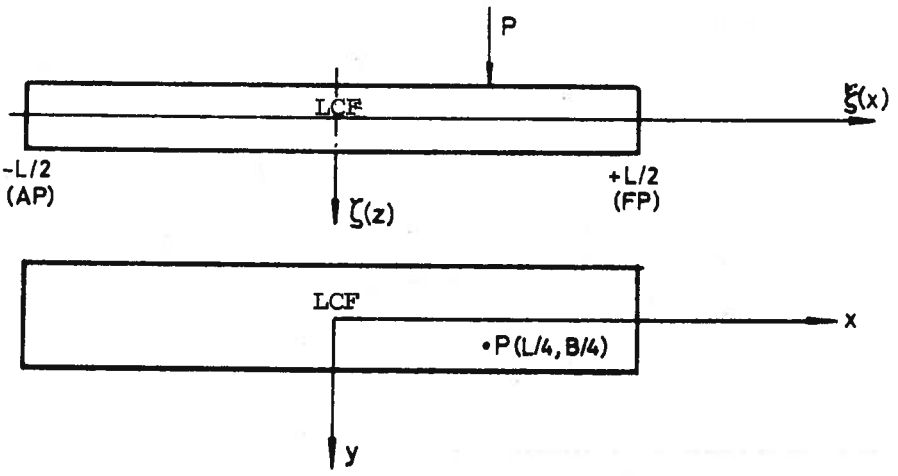

Fig. 1.2.4

The weight P gives:

Displacement increase equal to P.

Heeling moment $\delta M_x = P \frac{B}{4}$

Trimming moment $\delta M_y = P \frac{L}{4}$

The vessel sinks, heels and trims until equilibrium between cargo and buoyancy forces is reestablished. By using the equations (1.2.5a-c) the equilibrium conditions may be written:

$$P - \gamma BL\zeta_o = 0$$

$$P \frac{B}{4} - \gamma L \frac{B^3}{12} \beta = 0$$

$$P \frac{L}{4} - \gamma B \frac{L^3}{12} \alpha = 0$$

Thus:

$$\zeta_o = \frac{P}{\gamma BL} \; ; \quad \beta = \frac{3P}{\gamma LB^2} \; ; \quad \alpha = \frac{3P}{\gamma BL^2}$$

It is assumed here that the center of buoyancy and the center of gravity have the same vertical position above the keel. (See stability theory.).

1.2.1.3 Vessels with varying frame width.

For a hull form with curved U and V-shaped frames, the changes in buoyancy associated with a change in equilibrium form a position (I) to another position (II) must usually be established by using the hydrostatic curves; see fig. 1.2.5.

The equilibrium position is obtained as before after parallel immersion followed by trim and heel. But the displacements ζ_o , α and β depend now on the floatation planes both at the initial condition and the end condition. For example, adding the weight P at the center of floatation for straight V-frames will give:

$$\zeta_o = \frac{P}{\frac{\gamma}{2}(A_I + A_{II})} = \frac{P}{\gamma A_{WL\ avg.}} \qquad (1.2.7)$$

The expressions in 1.2.6 may be used where changes in the WL-area from condition I to II are small and where angles of rotation are less than approximately 0.1 rad. The inaccuracies this introduces are easily estimated using the hydrostatic curves (fig. 1.2.5). A_{WL} , I_x , and I_y for the conditions I and II can actually be estimated using the formulas:

$\gamma A_{WL} = a =$ "tonn pr. cm. immersion".

$\frac{\gamma I_x}{\Delta} = b =$ "the distance from the center of buoyancy to (original) metacenter" - usually denoted BM_T . (= KM_T - KB in fig. 1.2.5).

$\frac{\gamma I_y}{L} = c =$ "trim moment pr. cm. trim at the perpendiculars.

The quantities a, b, and c can be read directly from the hydrostatic curves for the conditions I and II. For an approximate determination of the buoyancy distribution after trim (heel) and simultaneous parallel immersion, the moment of inertia of the floatation plane for condition II should be used.

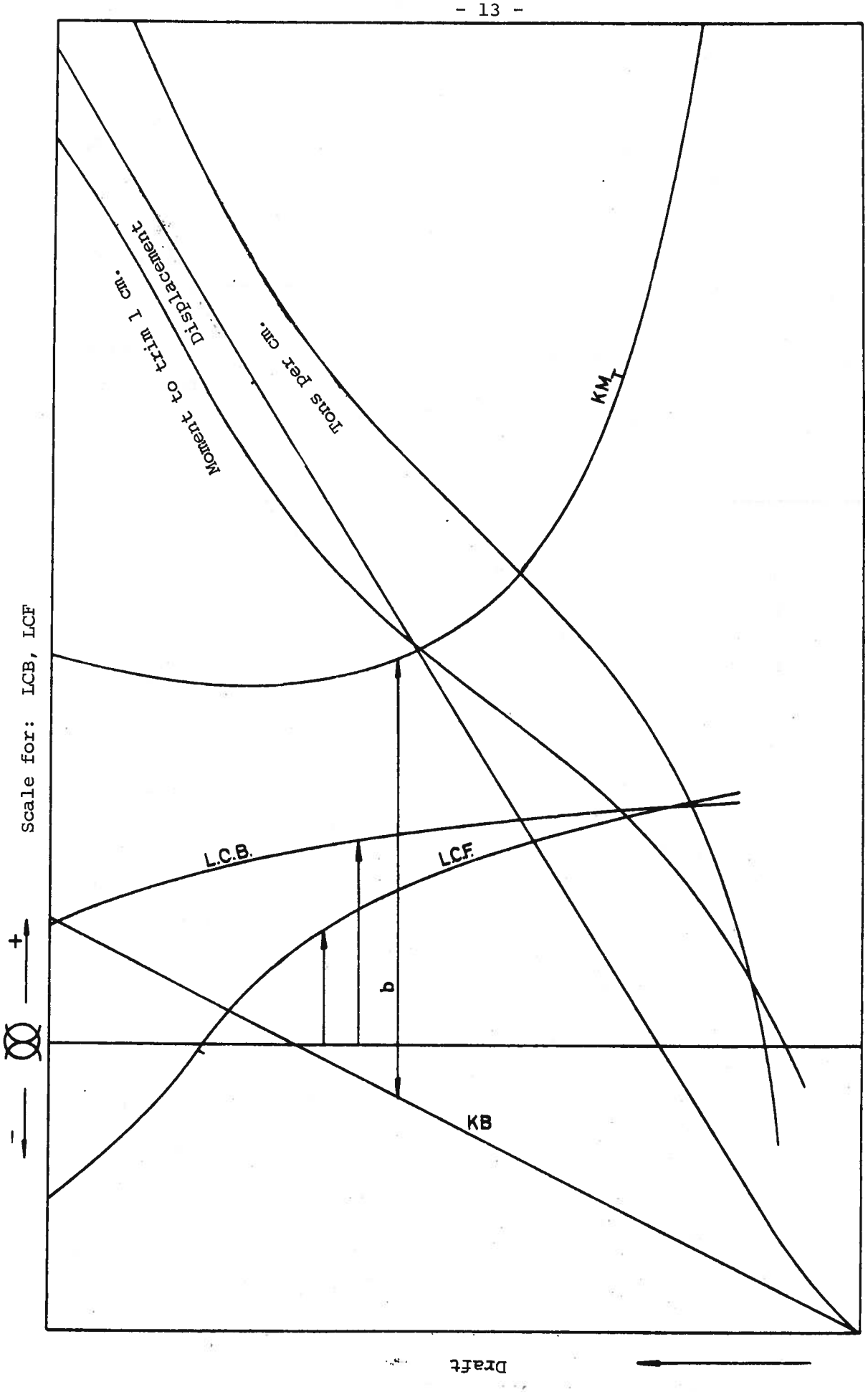

Scale for: KB, KM_T, Tons per cm. immersion, Displacement, Moment to trim 1 cm.

Fig. 1.2.5

Muckle[1,2] found it convenient to use the Bonjean curves for determining the mean breadth B_m of the floatation plane within a limited region, see Fig. 1.2.6. For instance, if the distance $\overline{Z}_2 - \overline{Z}_1$ is chosen equal to 1.0 m, B_m will in magnitude be equal to the distance $A_{2s} - A_{1s}$ *) . The computations must be done numerically for the actual hull form. If it is desired, for instance, to find the equilibrium position for the vessel in fig. 1.2.7 in the wave indicated in the figure, the procedure is as follows: As a trial, the ship is positioned as shown in the figure with the ξ-axis coinciding with the floatation plane that corresponds to equilibrium in calm water**) . The floatation plane is now curved and given by the following equation:

$$z = h(x) - (\zeta_0 + \alpha x) \tag{1.2.8}$$

where $h(x)$ denotes the coordinates of the wave in relation to the fixed coordinate system in the space ($\xi \simeq x$).

If $\overline{Z}_1$ in fig. 1.2.6 is chosen to correspond to the draft to the floatation plane in still water for all the Bonjean-Curves, and if the distance $(\overline{Z}_2 - \overline{Z}_1)$ is made equal to z according to eqn. (1.2.8), then $A_{s2} - A_{s1}$ will directly indicate the change in immersed area at the respective frame, and the conditions for statical equilibrium may be written as

$$\int_L (A_{s2} - A_{s1})\, dx = 0$$

$$\int_L (A_{s2} - A_{s1})\, x dx = 0$$

---

1. W. Muckle: "The bouyancy curve in longitudinal strength calculations". The Shipbuilder and Marine Engine Builder. Vol. 61, Feb. 1954.
2. W. Muckle: "A note on the buoyancy curve for a ship in the inclined condition". The Shipbuilder and Marine Engine Builder, Aug. 1962. p.473-474.

*) A_{1s} = the frame area at draft $\overline{Z}_1$, and similarly for A_{2s} .

**) ξ-axis and x-axis coincide in still water.

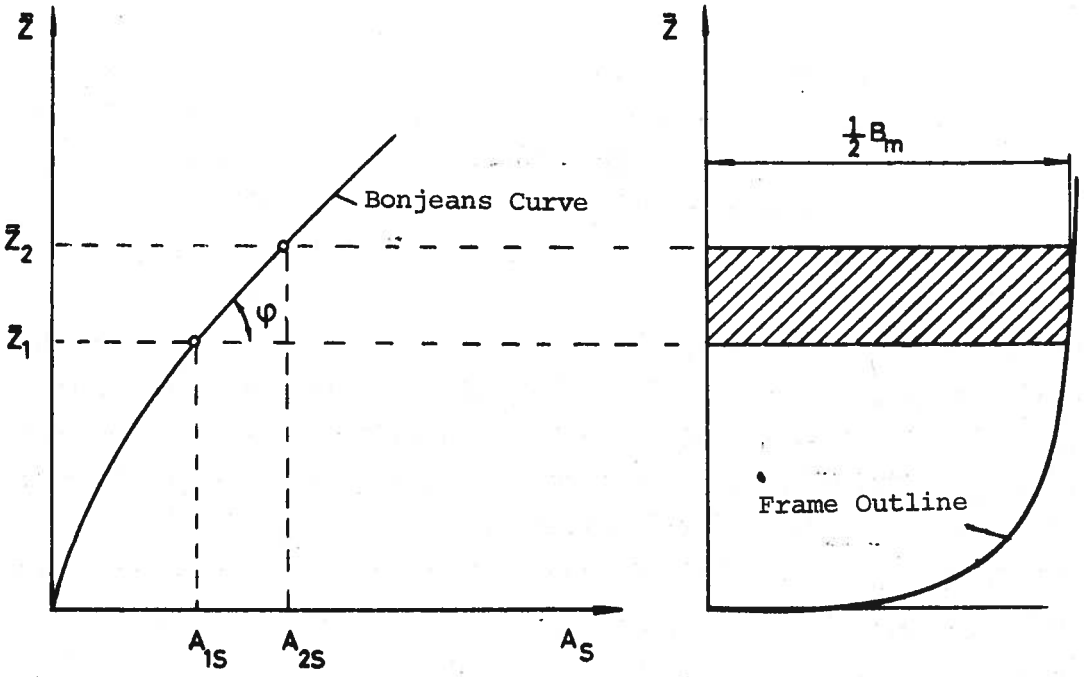

Fig. 1.2.6

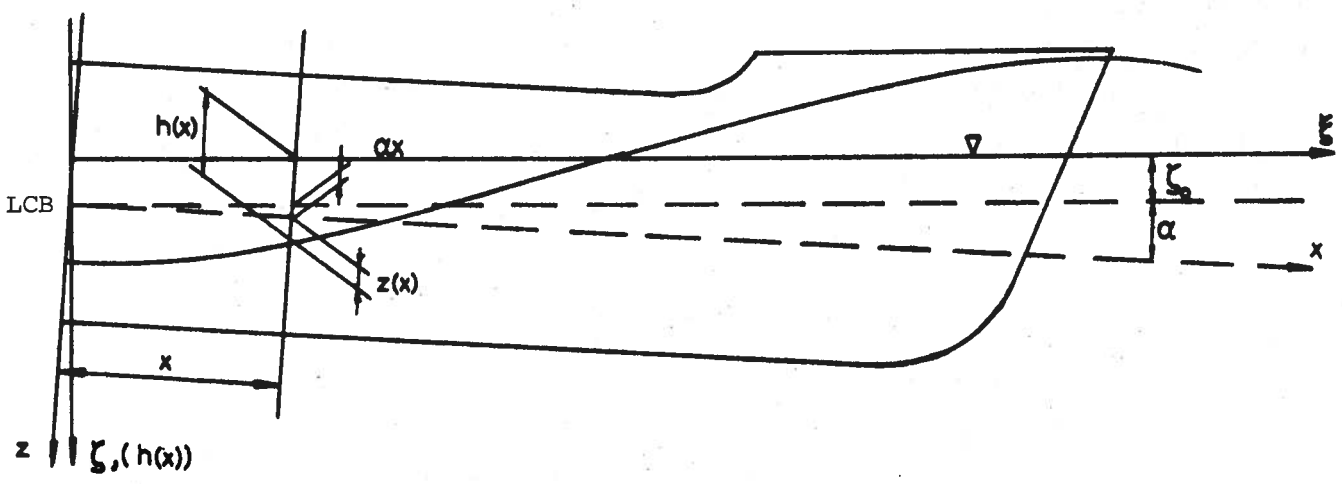

Fig. 1.2.7

The integration is done numerically and the position of the vessel is adjusted until both equilibrium conditions are satisfied with adequate accuracy. "The sectional area curve (SAC) " gives the final distribution of the buoyancy forces longitudinally, see fig. 1.2.8b.

When the hull sides are not vertical, a coupling between heel and trim will normally occur. If the vessel is heeled by moving a load transversally, a change of trim will occur simultaneously. The equilibrium position is obtained (most easily by first estimating the heel without taking into consideration the change in trim and then trimming the vessel until equilibrium is reestablished in the XZ-plane too. It is actually necessary to go back and adjust the heel angle, but the computations converge rapidly so this will for small angles of heel be unnecessary.

1.2.2 Weight Calculations

Since the static loading of the hull girder in any place is found as the difference between two quantities (weight and buoyancy) which are approximately equally large, it is very important that these quantities seperately are established as accurately as possible. Estimating q_x^w is of course no real trouble. The computations of accurate weight calculations represents a sizable task, however. By effectively utilizing the computer, it is expected that accurate weight calculations will be carried out more frequently in the future than is the case today.

The weights are split into two main groups:

A. Light ship weight $\dot{W}_\ell$

B. Deadweight W_d

Together, these weights give the total weight of the vessel (displacement):

$$\Delta = W_\ell + W_d$$

Each main group consists of 3 sub-groups:

A. Light Ship

1) Hull weight (including superstructure (except outfitting), foundations, rudder, bilge keel, etc.): W_H

2) Engine room weights *) (including piping arrangement, steering gear, shafting, propeller): W_M

3) Outfitting and equipment (wood panels, furniture, deck covering, sanitary installations, winches, davits, anchors, etc.) : W_o

B. Deadweight

1) Bunker (fuel oil, lubricating oil, feed water): W_b

2) Storage (fresh water, provisions, crew, passengers, etc.) : W_s

3) Cargo : W_c

Consequently the light ship weight is: $W_\ell = W_H + W_M + W_o$

and the deadweight $W_d = W_b + W_s + W_c$

The weight distribution gives weight/length and is denoted q with subscripts h, m, o, etc. Fig. 1.2.8a shows the longitudinal distribution of the 6 weight groups for a steamship with the machinery midships.

The discontinuities in the steel weight curve (q_h) represent changes in frame form, deck houses or increased or reduced steel cross-sections. The peaks indicate the contribution of the transverse bulkheads. Roughly estimated it can be seen that the steel weight pr. meter frame section up to the upper continuous deck , varies as the SAC (to the same deck) with local deviations dictated by strengthenings due to external loadings, cargo,

*) "Wet" system. "Dry" system: Weight with empty pipes and boilers.

and internal arrangements (cargo hold and engine room positioning, superstructures, deck equipment, etc.).

Consequently, the distribution of the hull weight depends on the type of vessel and arrangement. Almost the same applies for the curve q_o which in fig. 1.2.8a indicates, amongst other things, that the cargo hold is fitted with wooden ceiling and battens. This does not apply for tankers which, on the other hand, have piping, whereas for refrigerated ships we have to account for the weight of insulation.

From fig. 1.2.8b it appears that the ship has no parallel middle body. For vessels with parallel middlebody, another distribution of the steel weights is likely.

The curve for machinery weight distribution q_{in} shows the machinery with piping, etc., casing and funnel, plus three boiler rooms, where the weights are distributed trapezoidally with the right area (total weight) and center of gravity.

The cargo distribution q_c is partly given by the size of the holds (from the capacity plan) and partly by the types of cargo, e.g. general cargo, ore, grain, sugar, oil, petroleum, etc.

Even though the weight varies with vessel type, trade area amd yard practice, it is possible by systematic analysis to obtain functional relationships between the weights referred to above and the parameters such as L, B, D, C_B, SHP, etc. which are depending upon the type of vessel. General weight data may be found in the articles given in the literature list in Appendix A. This Appendix furthermore, contains some discussions and data concerning estimating the weight distribution for light ship. The distribution of the deadweight depends upon the cargo condition, machinery size, route, number of passengers, crew size, etc. Data may be found from the capacity plan, the machinery manufacturer's data on fuel-consumption, feed-water consumption, etc. Quite often, a number of loading conditions must be checked. For ballast conditions, there is a minimum draft requirement (e.g. 0.027 L forward and 0.042 L aft),(see the rules of the classification societies).

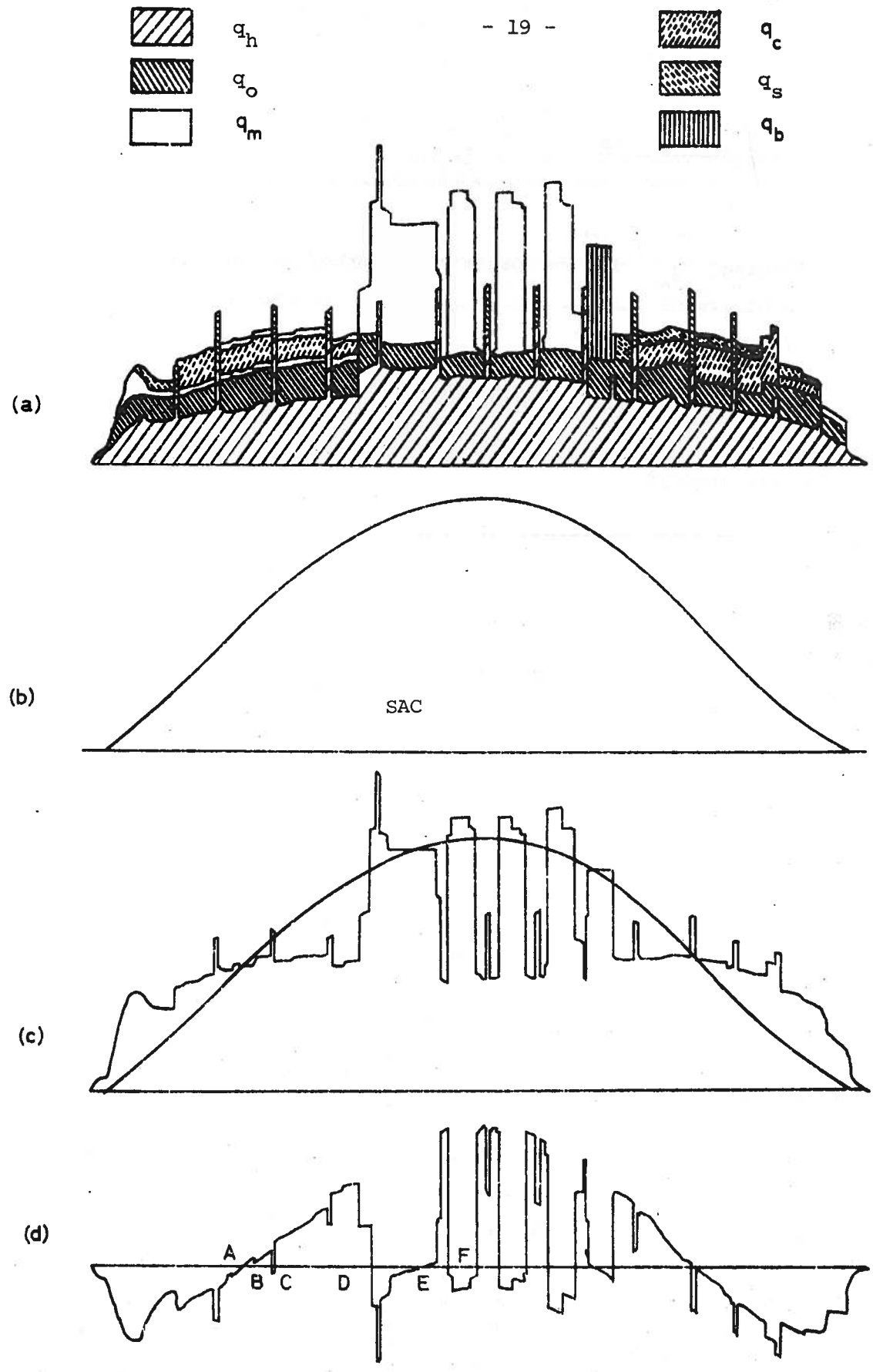

Fig. 1.2.8

1.2.3 Shear forces and moments

1.2.3.1 Fundamentals

In the following, q_z will represent the loading pr. unit length of the hull, unless otherwise stated. Loading as well as moments and shear forces will be functions of x.

The following sign convention is chosen:

a) Loading (as previously)

Weights positive: $q_z^w > 0$

Buoyancy negative: $q_z^b < 0$

$$q_z = q_z^w + q_z^b$$

b) Shear forces acting in the center line plane;

$$Q_z = -\int q_z^b \, dx \qquad (1.2.9a)$$

which corresponds to the sign convention shown in fig. 1.2.9a.

c) Moments acting in the center line plane;

$$M_y = \int Q_z \, dx = -\iint q_z dxdx \qquad (1.2.9b)$$

which corresponds to the sign convention shown in fig. 1.2.9b.

Positive bending moment defined as above usually denotes a "sagging" moment in ship-technical literature, whereas a negative moment is called a "hogging" moment, see fig. 1.2.9c-d.

In the upright static condition the vessel is subjected to a loading q_z with associated shear force Q_z and moment M_y (z is the vertical axis, positive downwards). These forces act in the CL-plane as long as buoyancy and weights individually and at every section are symmetrically distributed with respect to this plane. The buoyancy in calm water in this

condition is always symmetrically distributed (for ordinary hull forms), whereas the weights may be unsymmetrically distributed, e.g. the starboard double-bottom tank being full, while the port tank is empty. This produces a torsion moment in addition to the "vertical" loading.

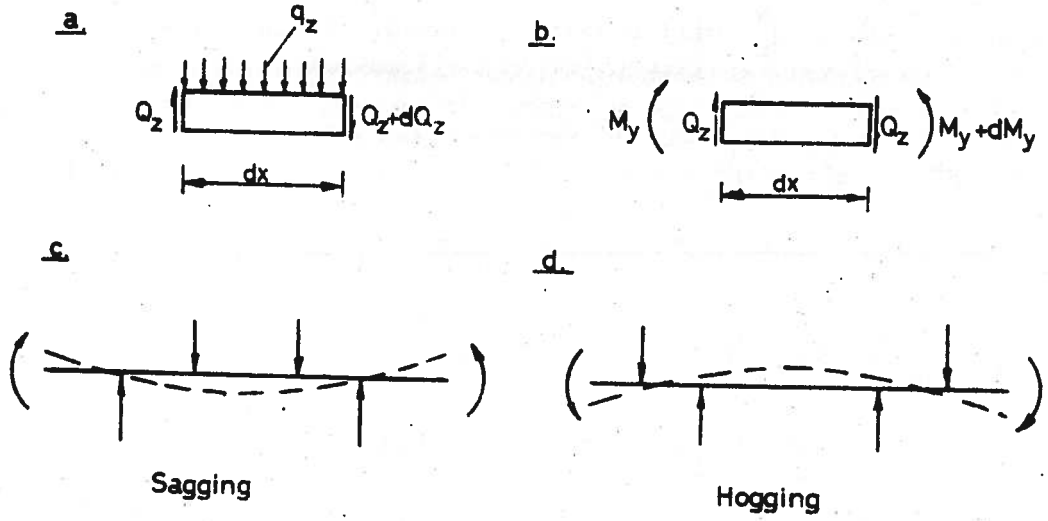

Fig. 1.2.9

The buoyancy in waves may be unsymmetrically distributed, i.e. the starboard wave is out of phase with the port side wave. The vessel may still be assumed to be upright under special conditions, but with the addition of torsion and horizontal loadings, q_y , Q_y , M_z . The static loading caused by external fluid pressure in a transverse section is then as shown in fig. 1.2.10.

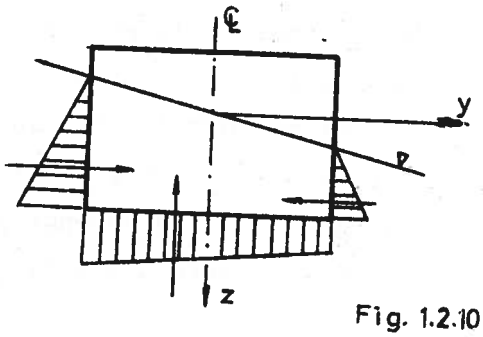

Fig. 1.2.10

When heeled, the vessel becomes subjected to buoyancy loading with components in the y- and z-directions. The same applies to the weights. The torsion loading consists now of the moment with respect to the shear center of <u>all</u> forces acting on the hull girder-element (of length dx)

If the horizontal water line plane is changed to a wave-formed surface, q_z^b will also change, whilst q_z^w will remain unchanged. It is convenient to set

$$q_z^b = q_{sz}^b + q_{wz}^b \tag{1.2.10}$$

where

q_{sz}^b = the buoyancy in still water

q_{wz}^b = additional buoyancy by waves

The folowing equations must be satisfied:

$$\int_L (q_{sz}^b + q_{wz}^b)\, dx = \int_L q_{sz}^b\, dx = \Delta \quad \text{(Displacement)}$$

$$\int_L (q_{sz}^b + q_{wz}^b)\, x\, dx = \int_L q_{sz}^b\, x\, dx = M_\alpha \quad \text{(Trim moment)}$$

It follows that:

$$\int_L q_{wz}^b\, dx = \int_L q_{wz}^b\, x\, dx = 0 \tag{1.2.11}$$

The above equations imply that the wave induced loadings must represent a system of forces which are themselves in equilibrium. The loading in still water can therefore be calculated first followed by the superposition of the loading caused by the waves. This porcedure is very convenient and is commonly used in practice. Whilst the still water loading depends upon the weight distribution as well as the buoyancy distribution, the wave loading will only

depend upon the form of the wave and the external form of the hull in the region near the floatation plane. It is therefore relatively simple to develop approximate formulas for wave induced loading that applies to larger classes of ships of relatively similar hull forms.

It is not always necessary to find the longitudinal distribution of the hull loading. It is often sufficient to know the bending moment at certain sections of the hull girder, e.g. amidships.

With the notation (fig. 1.2.11)

W_f = weight forward of amidships;

W_a = weight aft of amidships;

$\gamma\nabla_f$ = buoyancy forward of amidships in still water,

$\gamma\nabla_a$ = buoyancy aft of amidships in still water,

$s_{f(a)}$ = location of the resultant of the weights forward (aft) of amidships;

$\ell_{f(a)}$ = location of the resultant of the buoyancy forward (aft) of amidships;

the bending moment midships in still water becomes:

$$\overline{M}_{sy} = - W_a s_a + \gamma\nabla_a \ell_a = - W_f s_f + \gamma\nabla_f \ell_f \qquad (1.2.12)$$

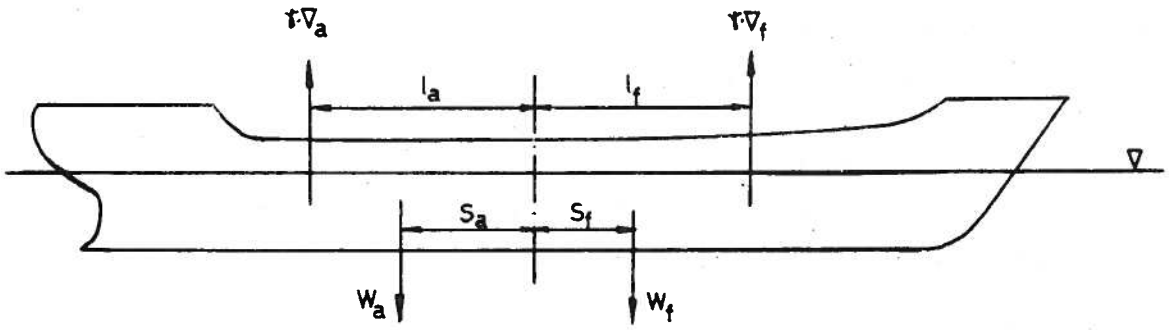

Fig. 1.2.11

This can also be written as

$$\overline{M}_{sy} = \frac{\gamma}{2}(\nabla_f \ell_f + \nabla_a \ell_a) - \frac{1}{2}(W_f s_f + W_a s_a)$$

$$= \overline{M}^{b}_{sy} + \overline{M}^{w}_{sy} \qquad (1.2.13)$$

where the buoyancy moment is only dependent upon form (immersed hull) whilst the weight moment is form-and arrangement dependent, and further,

$$\overline{M}^{b}_{sy} = \frac{\gamma}{2}(\nabla_f \ell_f + \nabla_a \ell_a)$$

$$\overline{M}^{w}_{sy} = -\frac{1}{2}(W_f s_f + W_a s_a) \qquad (1.2.14)$$

If the same calculations are done for wave formed free surface (floatation plane) and denote the new buoyancy condition by the notation ∇' and ℓ' , the total moment in waves becomes equal to:

$$\overline{M}_y = \frac{\gamma}{2}(\nabla_f' \ell_f' + \nabla_a' \ell_a') - \frac{1}{2}(W_f s_f + W_a s_a) \qquad (1.2.15)$$

The wave bending moment is now equal to:

$$\overline{M}_{wy} = \overline{M}_{y} - \overline{M}_{sy}$$

Substituting equations (1.2.13) and (1.2.15), we obtain:

$$\overline{M}_{wy} = \frac{\gamma}{2} \{(\nabla_f' \ell_f' - \nabla_f \ell_f) + (\nabla_a' \ell_a' - \nabla_a \ell_a)\} \qquad (1.2.16)$$

The wave bending moment is thus equal to the arithmetic mean value of the moments caused by the waves alone respectively forward and aft of midships, with $\nabla_f' = \nabla_f$ and $\nabla_a' = \nabla_a$, then

$$\overline{M}_{wy} = \frac{\gamma}{2} (\nabla_f (\ell_f' - \ell_f) + \nabla_a (\ell_a' - \ell_a)) \qquad (1.2.17)$$

At the ends of the hull, the shear force, bending moment, and torsion moment must be equal to zero. In practice when integrating from one end of the hull one frequently obtains an unblanced shear force δQ and/or bending moment δM at the opposite end. This is caused either by equilibrium for weights and buoyancy not being completely satisfied, or inaccuracies in the arithmetic during the integrations.

If now $\frac{\partial Q}{Q_{max}} \leq 0.03$ and $\frac{\partial M}{M_{max}} \leq 0.06$ the inaccuracy can with good results be corrected by drawing a new straight base-line between the end points such that ∂Q respectively ∂M are made zero at the ends, see fig. 1.2.12 [1,2]. A possible remaining shear force ∂Q must of course be corrected before the bending moment curve is obtained. If the remaining shear force or remaining moment is larger than the allowable according to the above, new calculations must be performed in order to determine the equilibrium position more accurately.

---

1) Henschke: Schiffbautechnisches Handbuch, Bd. 1,2. Aufl., s. 886.
2) Schultz, H.: Das Restmoment bei Langsfestigkeitsrechnungen. Schiffbau, Bd. 20 (1919).

Fig. 1.2.12

Example 1.2.2

A box-shaped vessel has a displacement $\Delta = \gamma BdL$ where γ is equal to 1 t/m^3 . Light weight of the ship is $0.25\ \Delta$ and is uniformly distributed over the ship length. The cargo is $0.75\ \Delta$ which is uniformly distributed over the tank section, the length of which is 0.62 L. The cargo distribution is such that the vessel is subjected to a trim moment by the stern:

$$M_\alpha = -\frac{\Delta L}{205}$$

We also have that

$$\frac{L}{D} = 17$$

The length of the tank aft of L/2 is denoted aL and forward of L/2 is denoted bL .

Find:

1) a and b,
2) Trim angle α,
3) the loading curve,
4) the shear force curve,
5) the moment curve.

Solution:

1) Box shaped vessels have the center of floatation located amidships.

The cargo 0.75Δ acts x meters from LCF. (x positive forward).

$$M_\alpha = 0.75\ \Delta\ x = -\frac{\Delta\ L}{205}$$

$$x = -\ 0.0065\ L$$

$$a = \frac{0.62}{2} - \frac{x}{L} = 0.3165$$

$$b = \frac{0.62}{2} + \frac{x}{L} = 0.3035$$

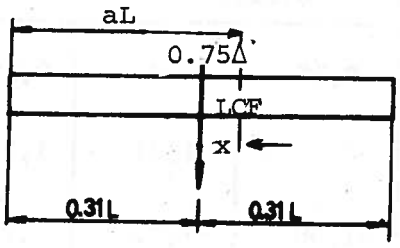

Fig 1.2.13

2) The trim angle becomes:

$$\alpha = +\frac{M_\alpha}{\gamma I_{LCF}} = -\frac{12}{205}\ \frac{BL^2 d}{BL^3} = -\ 0.00345\ \text{rad.}$$

3) The loading consists of:

a) Light weight: $q_1 = 0.25\ \frac{\Delta}{L}$ for $-\ 0.5\ L \leqq x \leqq 0.5\ L$

b) Cargo: $q_2 = \frac{0.75}{0.62}\ \frac{\Delta}{L} = 1.21\ \frac{\Delta}{L}$ for $-\ aL \leqq x \leqq bL$

c) Buoyancy "even keel": $q_3 = -\ \frac{\Delta}{L}$ for $-\ 0.5\ L \leq x \leq 0.5\ L$

d) Buoyancy from the trim wedges: $q_4 = -\ \gamma B x \alpha = 0.0585\ \frac{x}{L}\ \frac{\Delta}{L}$

for $-\ 0.5\ L \leq x \leq 0.5\ L$

Total loading: $q_z = \sum_{n=1} q_n$

In the following table

$$\bar{q}_z = \frac{q_z}{\Delta/L}\ ,\ \bar{Q}_z = Q_z/\Delta \text{ and } \bar{M}_y = M_y/\Delta \cdot L$$

as these are obtained from the data above being substituted into equations (1.2.9). The results are shown graphically in fig. 1.2.14.

x	-0,5 L	-0,3165 L		0	+0,3035 L		0,5 L
$\bar{q}_1$	0,25	0,25	0,25	0,25	0,25	0,25	0,25
$\bar{q}_2$	0	0	1,21	1,21	1,21	0	0
$\bar{q}_3$	-1,00	-1,00	-1,00	-1,00	-1,00	-1,00	-1,00
$\bar{q}_4$	-0,03	-0,02	-0,02	0	+0,02	+0,02	+0,03
$\bar{q}_z$	-0,78	-0,77	+0,44	+0,46	+0,48	-0,73	-0,72
x	-0,5 L	-0,3165L	-0,1583L	0	+0,1517L	+0,3035L	+0,5 L
$\bar{Q}_z$	0	+0,1423	+0,072	0	0,0705	-0,1427	0
$\bar{M}_y$	0	+0,013	+0,030	+0,0357	+0,0304	+0,0142	0

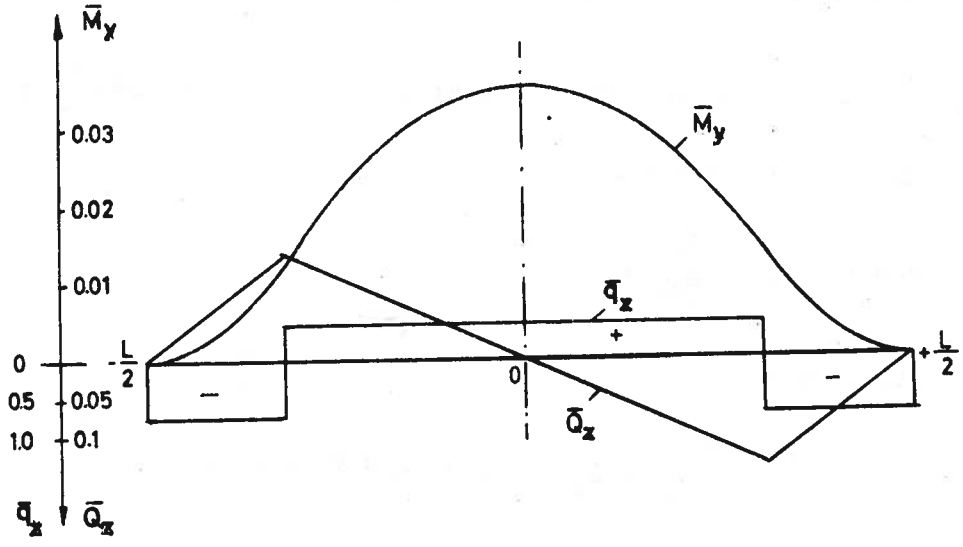

Fig. 1.2.14

Example 1.2.3

Onboard a box shaped vessel on "even-keel" are brought two weights, each of P tons which are distributed uniformly over the hatched areas of the deck, see fig. 1.2.15a. Find 1) the change in the still water moment midships, and 2) the torsion moments.

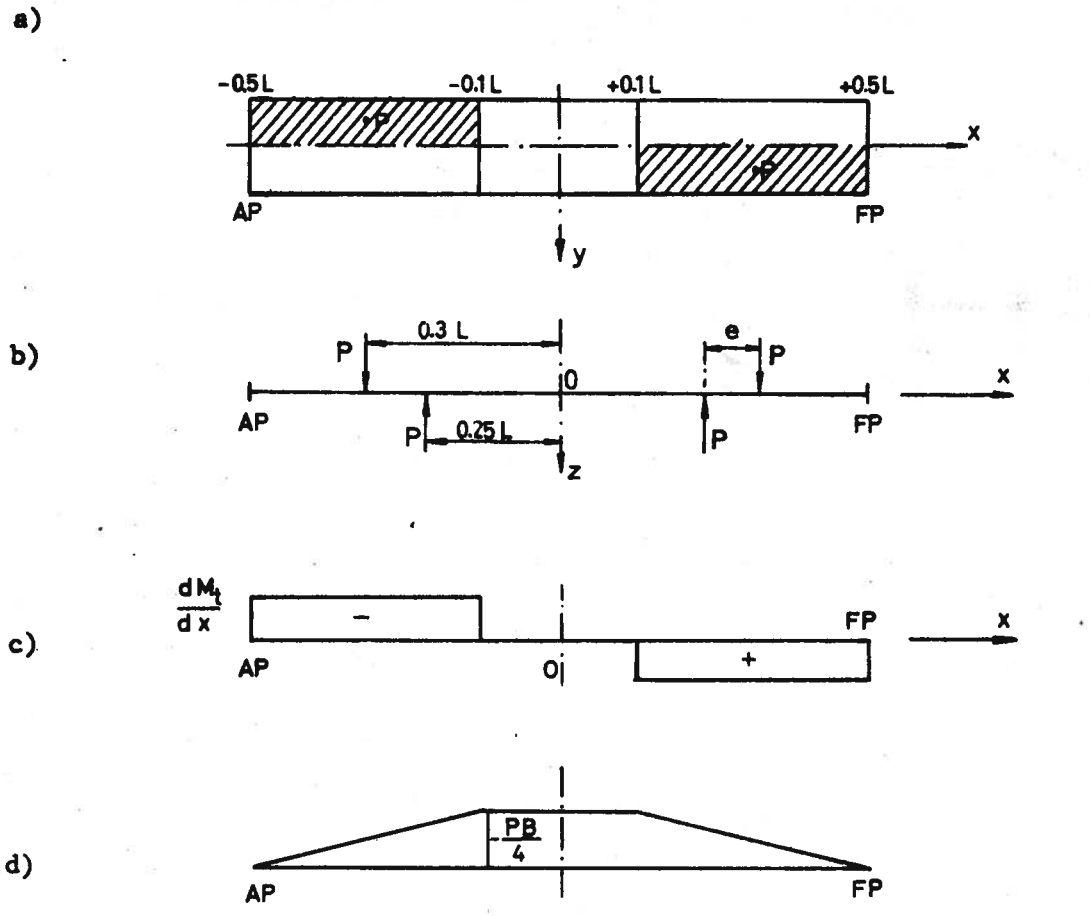

Fig. 1.2.15

1) The resulting vertical loading (the CL-plane) is as shown in fig. 1.2.15b The additional moment amidships ($\overline{M}_{sy}$) in still water:

$$\overline{M}_{sy} = -P \cdot e = -0.05\ PL$$

(Hogging moment since the weights act outside the buoyancy resultants).

2) The unsymmetrical cargo distribution (about the CL-plane) produces at section x a torsion moment (fig. 1.2.15c):

$$\frac{dM_t}{dx} = \pm q_z^w \frac{B}{4} \quad \text{for} \quad 0.1\ L \leq |x| \leq 0.5\ L$$

The torsion moment $M_{tx} = \int_{-L/2}^{x} \frac{dM_t}{dx}\, dx$ is then as shown in fig. 1.2.15d.

Example 1.2.4

A vessel has vertical sides and rectangular floatation plane with principal dimensions BL. Find the wave induced shear force (Q_{wz}) and bending moment (M_{wy}) when the vessel is assumed on a static wave of height $h(x)$ given by the formula

$$h(x) = r \cos \frac{2\pi x}{L}$$

where $x = 0$ at the middle of the ship and $h(x)$ is positive downwards (wave through midships).

Such a wave will for this hull form not cause change in trim or sinkage of the vessel, and we have immediately

$$q_{wz} = \gamma B h(x) = \gamma B\, r \cos \frac{2\pi x}{L}$$

$$Q_{wz} = - \int_{-L/2}^{x} \gamma B\, r \cos \frac{2\pi x}{L}\, dx = - \frac{\gamma B r L}{2\pi} \sin \frac{2\pi x}{L}$$

Maximum shear force is obtained at $x = \pm \frac{L}{4}$ where

$$(Q_w)_{max} = \mp \frac{\gamma B r L}{2\pi}$$

Similarly:

$$M_{wy} = - \int_{-L/2}^{x} \frac{\gamma BrL}{2\pi} \sin \frac{2\pi x}{L} \, dx = \frac{\gamma BrL^2}{4\pi^2} \left(1 + \cos \frac{2\pi x}{L}\right)$$

Maximum wave bending moment occurs at $x = 0$ and is equal to:

$$(M_{wy})_{max} = + 0.051 \, \gamma BrL^2 \qquad \text{(Sagging)}$$

1.2.3.2 Influence lines

The influence upon shear force and bending moment of a variation in arrangement (e.g. the location of the engine room, the bridge, etc.) or a change in the cargo distribution, can easily be established by the use of influence lines. Influence lines can therefore be used beneficially during the design phase, since it is then desireable to compare a number of alternative arrangements in order to obtain favorable shear force-and moment distributions.

The influence line for a statics variable (Q, M, etc.) at a section $x = x_o$ has the following property: The coordinate at any arbitrary point $x = \mu$ indicates the magnitude of the statics variable under consideration due to a unit load placed at $x = \mu$.

In the following, it will be shown how to find influence lines for Q and M when a weight P is brought onboard at an arbitrary point in the CL-plane (no heeling).

A. Influence lines for shear force.

A load P is brought onboard and located as shown in fig. 1.2.16. The vessel will then sink and trim such that:

$$\zeta_o = + \frac{P}{\gamma A_{WL}}$$

$$\alpha = + \frac{P \, \mu}{\gamma I_{LCF}}$$

Shear force in section x_o is found by considering the fore body:

$$Q_o = \int_{x_o}^{L_f} q_z^b \, dx + \varepsilon_f P = \gamma \int_{x_o}^{L_f} B_x z \, dx + \varepsilon_f P$$

Where $\varepsilon_f = 0$ if $\mu < x_o$

$\varepsilon_f = 1$ if $\mu > x_o$

z = the distance from original to new floatation plane (positive downwards).

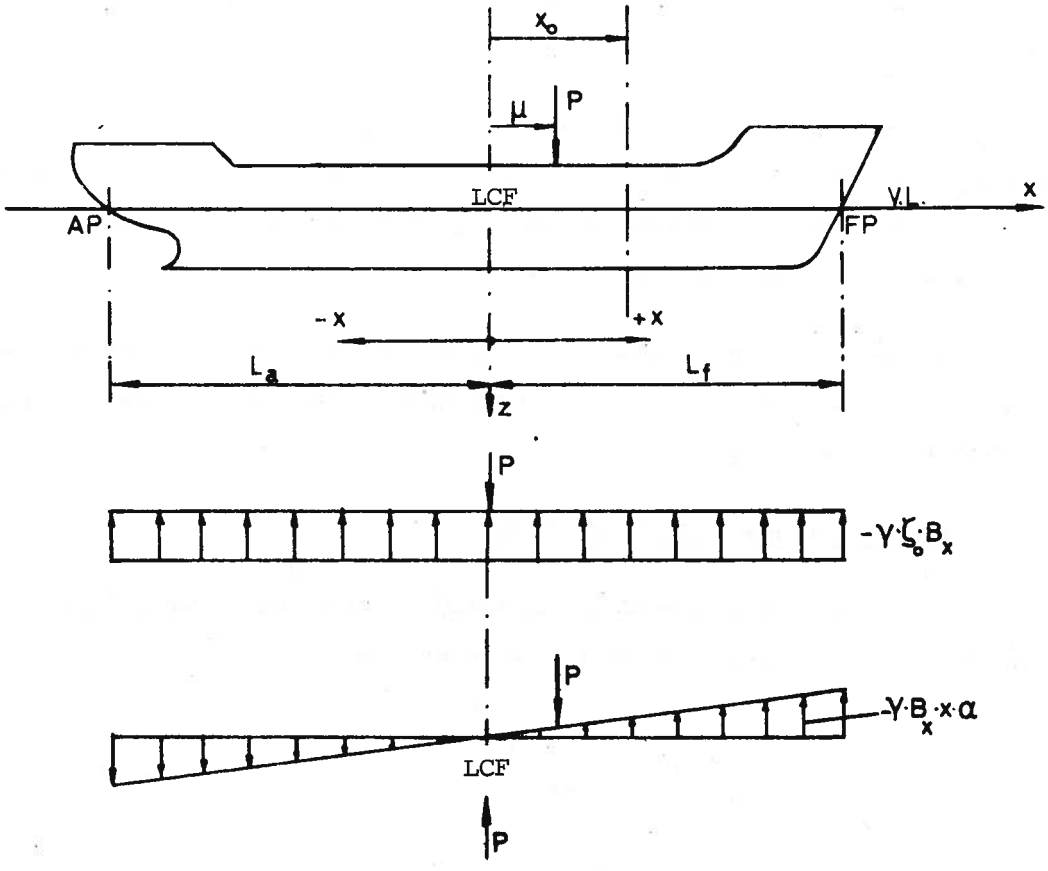

Fig. 1.2.16

Now;

$$z = -(\zeta_o + x\alpha) = -\left(\frac{P}{\gamma A_{WL}} + \frac{P\mu}{\gamma I_{LCF}} x\right)$$

Such that:

$$Q_o = -\gamma \int_{x_o}^{L_f} B_x(\zeta_o + x\alpha)\, dx + \varepsilon_f P$$

$$= -P\left(\frac{A_{o1}}{A_{WL}} + \frac{S^F_{o1}}{I_{LCF}}\mu - \varepsilon_f\right)$$

Where:

A_{o1} = WL-area forward section x_o .

S^F_{o1} = the A_{o1}-area's statical moment with respect to LCF . (x = 0)

Consequently, the two cases must be distinguished

1) $\mu < x_o$ (The weight P aft of considered section),

2) $\mu > x_o$ (the weight P forward of considered section).

Thus:

$$\text{for } \mu < x_o \;;\quad \frac{Q_o}{P} = -\left(\frac{A_{o1}}{A_{WL}} + \frac{S^F_{o1}}{I_{LCF}}\mu\right)$$

$$\text{for } \mu > x_o \;;\quad \frac{Q_o}{P} = \left(\frac{A_{o2}}{A_{WL}} + \frac{S^F_{o2}}{I_{LCF}}\mu\right) \qquad (1.2.18)$$

where the following relations have been used:

$$A_{o1} + A_{o2} = \int_{x_o}^{L_f} B_x dx + \int_{-L_a}^{x_o} B_x dx = A_{WL}$$

$$S^F_{o1} + S^F_{o2} = \int_{x_o}^{L_f} B_x x dx + \int_{-L_a}^{x_o} B_x x dx = \int_{-L_a}^{L_f} B_x x dx = 0$$

The influence line for the shear force at section x_o consequently gives the change $\frac{Q_o}{p}$ at section x_o when P is brought onboard and moved along the vessel from forward to aft:

$$-L_a \leqq \mu \leqq L_f$$

Example 1.2.5A

Q-influence line (QIF) is desired for section $x_o = 0$ by bringing on board the weight P on a box-shaped vessel: L x B x d. Here:

$$A_{o1} = A_{o2} = \frac{BL}{2}$$

$$S^F_{o1} = -S^F_{o2} = \frac{BL^2}{8}$$

$$I_{LCF} = \frac{BL^3}{12}$$

Substituting into equation 1.2.18 gives:

1) $\mu < 0$; $\frac{Q_o}{P} = -\left(\frac{1}{2} + \frac{3}{2}\frac{\mu}{L}\right)$

2) $\mu > 0$; $\frac{Q_o}{P} = \left(\frac{1}{2} - \frac{3}{2}\frac{\mu}{L}\right)$

$\left(\frac{Q_o}{P} = 0 \text{ for } \mu = \pm\frac{1}{3}L\right)$

The influence lines for the shear force midships is then as shown in fig. 1.2.17a.

a)

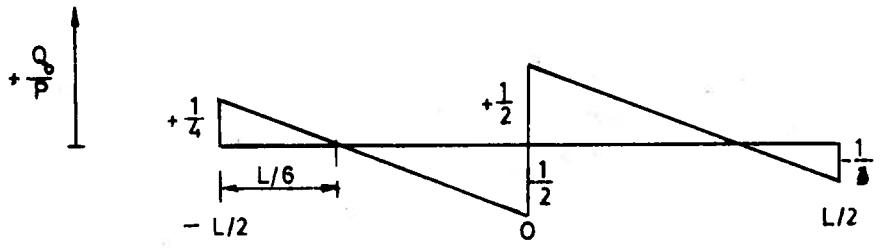

b)

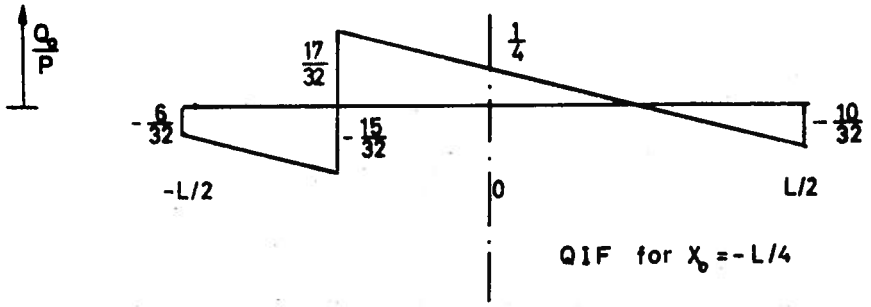

Fig. 1.2.17

Example 1.2.5B

For the same vessel as in example 1.2.5A QIF is desired for $x_o = -\frac{L}{4}$. In this case:

$$A_{o1} = \frac{3}{4} BL$$

$$A_{o2} = \frac{1}{4} BL$$

$$S^F_{o1} = \int_{-L/4}^{L/2} Bx dx = \frac{3}{32} BL^2$$

$$S^F_{o2} = \int_{-L/2}^{-L/4} Bx dx = -\frac{3}{32} BL^2$$

$$I_{LCF} = \frac{BL^3}{12}$$

Consequently:

1) $\mu < -\frac{L}{4}$; $\frac{Q_o}{P} = -\left(\frac{3}{4} + \frac{9}{8}\frac{\mu}{L}\right)$

2) $\mu > -\frac{L}{4}$; $\frac{Q_o}{P} = \left(\frac{1}{4} - \frac{9}{8}\frac{\mu}{L}\right)$ (See fig. 1.2.17 b).

If a weight is moved from μ_I to μ_{II} (fig. 1.2.18), a weight deduction is obtained for point I , and a corresponding weight addition for point II . The influence diagram can of course be used to determine changes in the shear force (dQ_o) for section $x = x_o$ caused by this shift of cargo.

a)

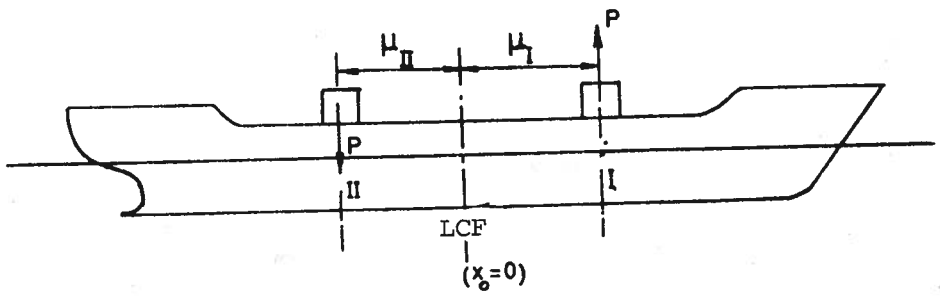

b)

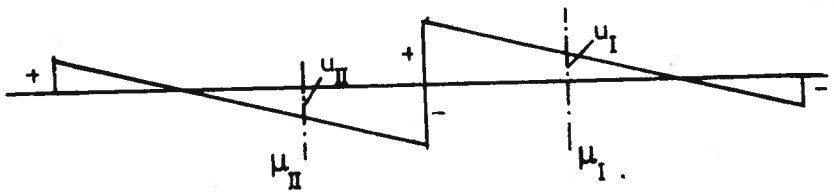

Fig. 1.2.18

We have that

$$dQ_o = P \left(u_{II} - u_I \right)$$

where

u_{II} = the coordinate for the influence line at μ_{II}

u_I = the coordinate for the influence line at μ_I .

B. Influence lines for moments

The change in bending moment at a certain section x_o when a weight P is brought on board and placed at an arbitrary point, may be determined in a similar manner.

It is necessary to distinguish between the two cases again (see fig. 1.2.16):

1) $\mu < x_o$

2) $\mu > x_o$

The bending moment in x_o then becomes (where sagging-moment is taken as positive):

$$M_o = - \int_{-L_a}^{x_o} q_z^b \, (x_o - x) \, dx - \varepsilon_a P \, (x_o - \mu)$$

where

$\varepsilon_a = 1$ for $\mu < x_o$

$\varepsilon_a = 0$ for $\mu > x_o$

Substituting now as before for q_z^b ;

$$M_o = \int_{-L_a}^{x_o} B_x \left(\frac{P}{A_{WL}} + \frac{P\mu}{I_{LCF}} x \right) (x_o - x)\, dx - \varepsilon_a P (x_o - \mu) \tag{1.2.19}$$

$$\frac{M_o}{P} = \frac{S_{o2}}{A_{WL}} - \frac{\mu}{I_{LCF}} \left(I^F_{o2} - S^F_{o2} \cdot x_o \right) - \varepsilon_a (x_o - \mu)$$

Subscript 01 denotes here values which refer to the water line area forward of section x_o . Subscript o2 similarly denotes values which refer to the water line area aft of section x_o .

$$S_{o2} = \int_{-L_a}^{x_o} B_x (x_o - x)\, dx = \text{the statical moment of the area } A_{o2} \text{ with respect to } x_o . \quad (S_{o2} > 0)$$

$$S^F_{o2} = \int_{-L_a}^{x_o} B_x x dx = \text{the statical moment of the area } A_{o2} \text{ with respect to the center of floatation.} \quad (S^F_{o2} < 0)$$

Similarly

$$S_{o1} = \int_{x_o}^{L_f} B_x (x - x_o)\, dx$$

$$I^F_{o2} = \int_{-L_a}^{x_o} B_x x^2 dx = \text{moment of inertia with respect ot the center of floatation of the area } A_{o2} ,$$

and so forth.

Note that:

$$A_{o1} + A_{o2} = A_{WL}$$

$$S^F_{o1} + S^F_{o2} = 0$$

$$S_{o1} = S^F_{o1} - A_{o1}x_o \quad ; \quad S_{o2} = -S^F_{o2} + A_{o2}x_o$$

$$I^F_{o1} + I^F_{o2} = I_{LCF}$$

The equations for the influence lines for the bending moment at $x = x_o$ may consequently also be written as:

$$\mu < x_o \; ; \; \frac{M_o}{P} = \frac{S_{o1}}{A_{WL}} + \frac{I^F_{o1} - S^F_{o1}\, x_o}{I_{LCF}}\, \mu$$

$$\mu > x_o \; ; \; \frac{M_o}{P} = \frac{S_{o2}}{A_{WL}} - \frac{I^F_{o2} - S^F_{o2}\, x_o}{I_{LCF}}\, \mu \qquad (1.2.20)$$

Example 1.2.6A

M-influence line is desired for section $x_o = 0$ by bringing on board the weight P in a box shaped vessel: L x B x d .

Solution:

$$A_{o1} = A_{o2} = \frac{BL}{2}$$

$$S_{o1} = S_{o2} = \frac{BL^2}{8} \; ; \; S^F_{o1} = -S^F_{o2} = \frac{BL^2}{8}$$

$$I^F_{o1} = I^F_{o2} = \frac{1}{2} I_{LCF} = \frac{BL^2}{24}$$

$$\mu < 0 \; ; \; \frac{M_o}{P} = \frac{S_{o1}}{A_{WL}} + \frac{\mu}{2} = \frac{L}{8} + \frac{\mu}{2}$$

$$\mu > 0 \; ; \; \frac{M_o}{P} = \frac{S_{o2}}{A_{WL}} - \frac{\mu}{2} = \frac{L}{8} - \frac{\mu}{2}$$

The influence diagram for this case is shown in fig. 1.2.19a.

a)

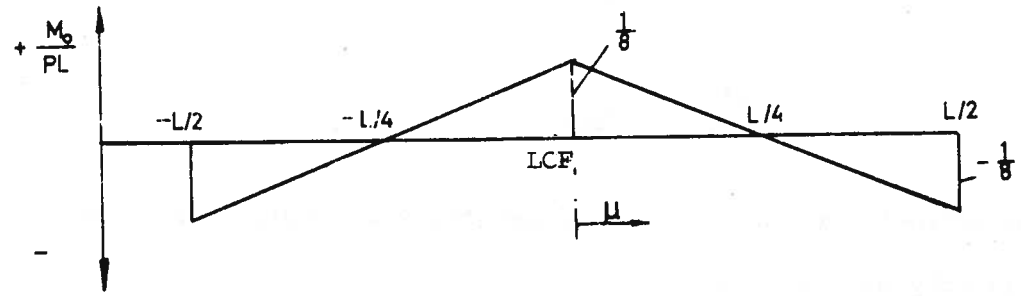

b)

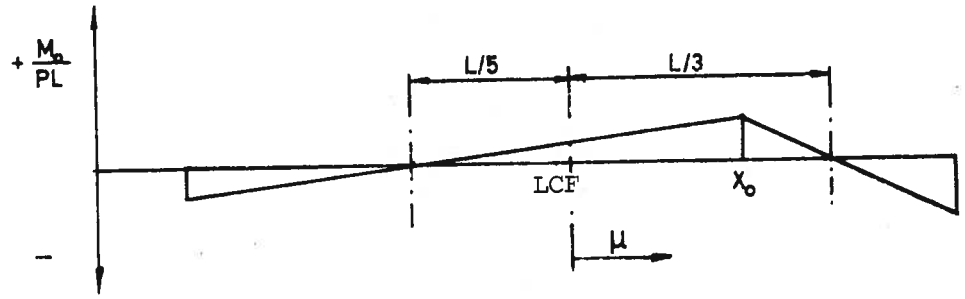

Fig. 1.2.19

Note that:

$\frac{PL}{8}$ is the bending moment at LCF caused by buoyancy forces resulting from parallel sinkage.

$\frac{1}{2} P\mu$ is equal to half the trim moment ($\frac{1}{2} M_\alpha$).

For vessels with double symmetrical WL-plane, the bending moment at LCF ($x_o = 0$) can always be expressed as follows:

$$\text{for } \mu < 0 \; ; \; M_o = P \frac{S_{ol}}{A_{WL}} + \frac{M_\alpha}{2} \qquad \text{(Here } M_\alpha \text{ is negative)}$$

$$\mu > 0 \; ; \; M_o = P \frac{S_{ol}}{A_{WL}} - \frac{M_\alpha}{2} \qquad \text{(Here } M_\alpha \text{ is positive)} \qquad (1.2.21)$$

Example 1.2.6B

For the same vessel as in example 1.2.6A MIF is sought for $x_o = \frac{L}{4}$.

Solution:

$$A_{o1} = \frac{BL}{4} \quad ; \quad A_{o2} = \frac{3BL}{4}$$

$$S_{o1} = \frac{BL^2}{32} \quad ; \quad S_{o2} = \frac{9}{32} BL^2$$

$$S^F_{o1} = \int_{L/4}^{L/2} Bx\, dx = \frac{3BL^2}{32} = - S^F_{o2}$$

$$I^F_{o1} = \int_{L/4}^{L/2} Bx\, dx = \frac{7}{3 \cdot 64} BL^3$$

$$I^F_{o2} = I_{LCF} - I^F_{o1} = \frac{9}{3 \cdot 64} BL^3$$

$$S^F_{o1} \cdot x_o = \frac{3BL^3}{4 \cdot 32} = - S^F_{o2}\, x_o$$

The coordinates of the influence are given by equation (1.2.20):

$$\text{for } \mu < x_o \qquad \frac{M_o}{P} = \frac{L}{32} + \frac{5\mu}{32}$$

$$\text{for } \mu > x_o \qquad \frac{M_o}{P} = \frac{9L}{32} - \frac{27\mu}{32} \qquad \text{(fig. 1.2.19b)}$$

If a weight is moved from μ_I to μ_{II}, there is a weight reduction at point I and a weight increment at point II with resulting trim-moment $M_\alpha = P(\mu_{II} - \mu_I)$. The change in the magnitude of the moment at a section $x = x_o (dM_o)$ can also in this case be easily read from the influence lines

for the moment at that point. This makes (see fig. 1.2.20)

$$\frac{dM_o}{P} = u_{II} - u_I \tag{1.2.22}$$

The influence diagram may also be used to determine the change in shear force or moment caused by an additional load which is distributed over a certain length. This gives for instance

$$dM_o = \int_x q(x)\, u(x)\, dx \tag{1.2.23}$$

where

$u(x)$ = the coordinate of the influence line

$q(x)$ = the loading intensity.

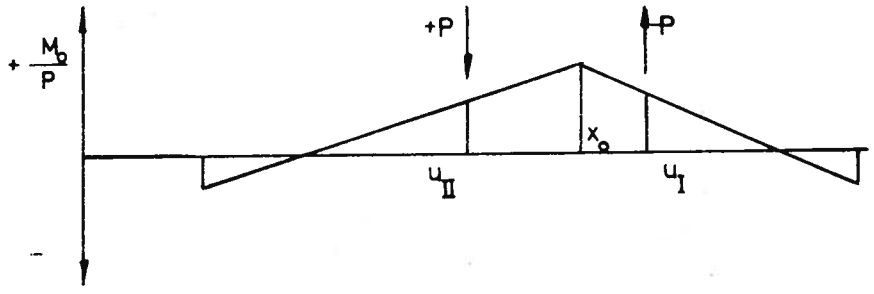

Fig. 1.2.20

Example 1.2.7

Fig. 1.2.21 and 1.2.22 show an ore carrier with $C_B = 0.72$. The change in the midships bending moment in still water (dM_o) is to be determined for the transition from ballast to fully loaded condition.

This change can be determined approximately using influence lines by studying the effects of emptying the ballast tanks and loading the ore separately.

The expressions for the moment influence lines for a symmetrical vessel with parabola-shaped water plane and $C_{WL} = 0.83$ are applied here, which gives:

$$\frac{dM_o}{P} = 0.107\ L - \frac{1}{2}\ /\mu/$$

Or by n weight changes:

$$dM_o = L \sum_{n=1}^{n} P_n \left(0.107 - \frac{1}{2} / \frac{\mu_n}{L} / \right)$$

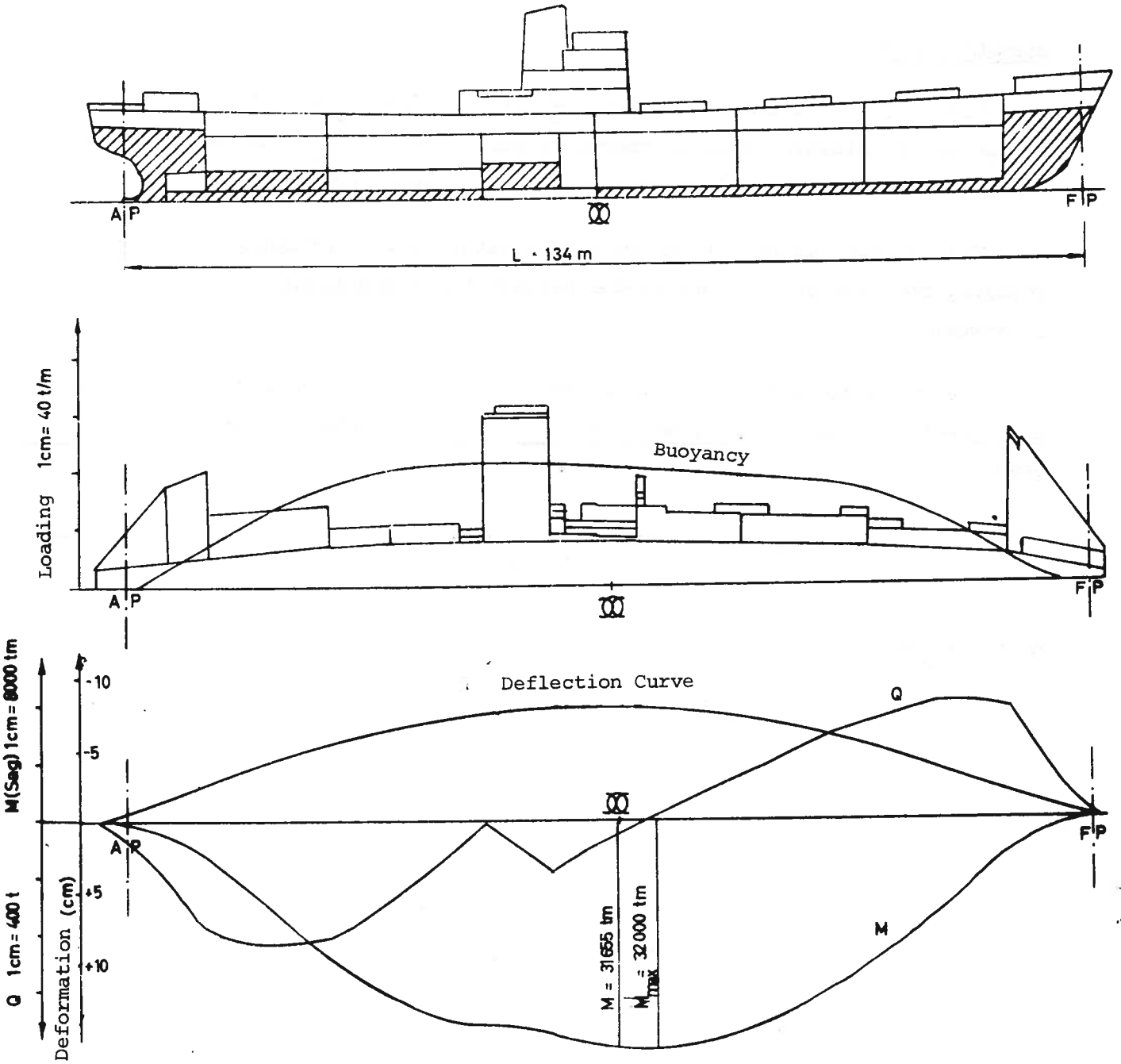

Ballast Condition

Fig. 1.2.21

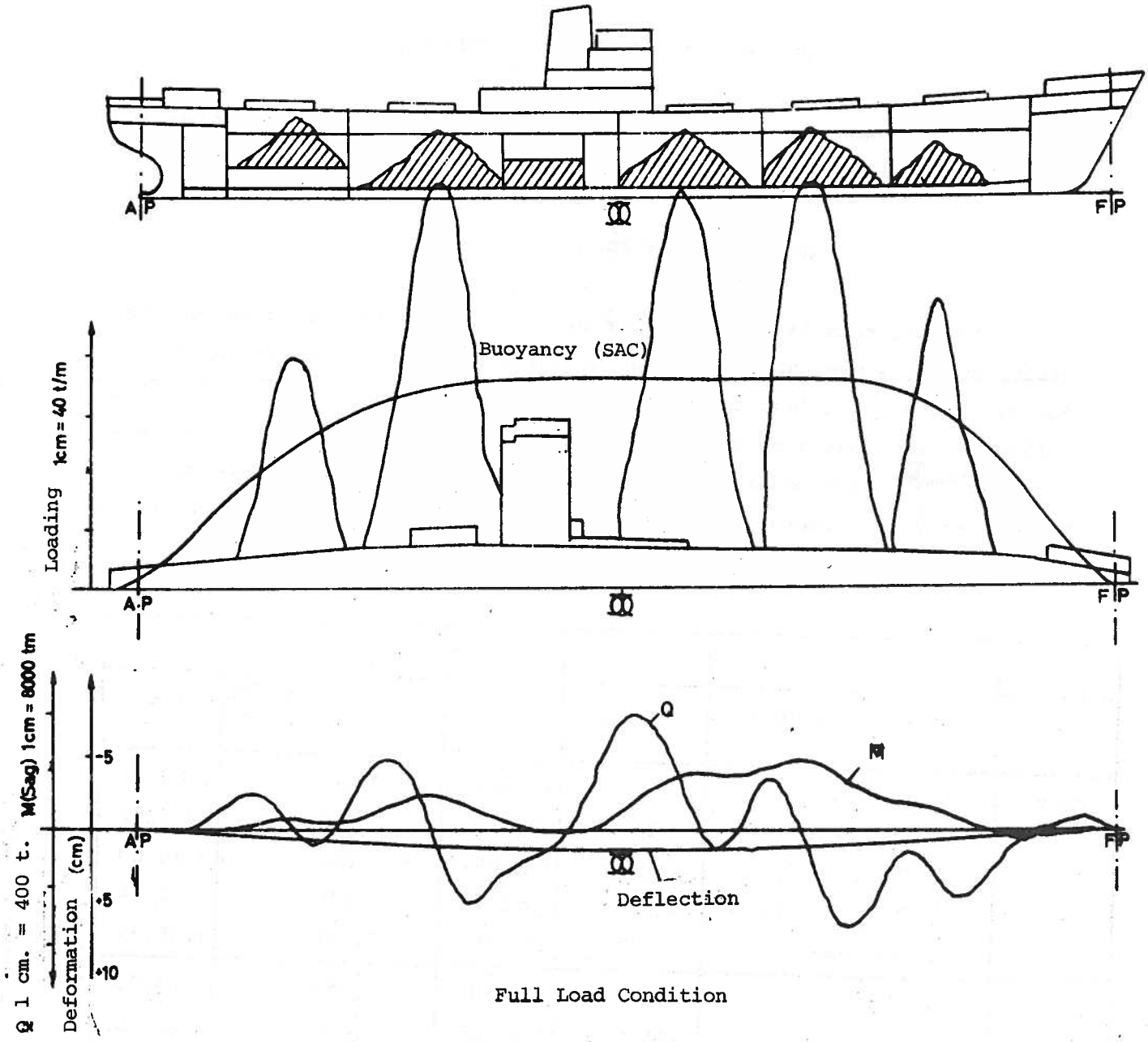

Full Load Condition

Fig. 1.2.22

The calculations are tabulated in table 1.2.1 and give:

$$dM_o = L \cdot 187.75 = + 25159 \text{ tm}$$

Through an ordinary graphical longitudinal calculation of the moments, the following was found:[1)]

$$dM_o = 23814 \text{ tm.}$$

The estimate is therefore off by 6% . Here, the calculations are pretty rough, since the changes in the water line shape between the draft for respectively ballast and full load are disregarded. By using two-three influence lines based on the actual water line shapes in 1) ballast condition and 2) loaded condition, and 3) probably in an intermediate draft, the accuracy will improve. But for a quick check, the method is good enough.

Table 1.2.1

1	2	3	4	5	6
	Tank or Cargo Hold	P_n tonn	$\frac{\mu_n}{L}$	$0{,}107 - 0{,}5 \cdot \frac{\mu_n}{L}$	3 x 5
Empty Tanks	Force Peak	-547	+0,446	- 0,116	+ 63,42
	D.B. Tank 2	-347	+0,212	+ 0,001	- 0,35
	" 3	-300	+0,089	+ 0,062	- 18,60
	" 5	-117	-0,253	- 0,020	+ 2,34
	After Peak	-270	-0,488	- 0,137	+ 36,99
Cargo	Hold 1	+1300	+0,320	- 0,053	- 68,90
	" 2	+2650	+0,194	+ 0,010	+ 26,50
	" 3	+2600	+0,059	+ 0,077	+200,20
	" 4	+2550	-0,195	+ 0,009	+ 22,95
	" 5	+1200	-0,342	- 0,064	- 76,80
					+187,75

1) Seyderhelm, H.: "Langsfestigkeitsfragen und Ergebnisse einer Reise mit Erzladung". Schiff und Hafen, H. 12, 1965.

1.2.3.3 Practical determination of the still water loads.

Scientists were engaged as early as 1746 (Bouget) and 1759 (Euler) with the determination of weight and buoyancy bending moments on ships. But not until this century has the calculation of statical longitudinal loads been performed systematically and routinely. (See for instance, J.M. Murray, IESS, 1947).

The determination of the statical longitudinal loads in still water does not cause any difficulties in principle. But since this, as mentioned previously, has to be done accurately, the work is very time consuming and can profitably be done with the aid of computers *). For "manual" calculations a simplification is aimed at by using approximate formulas for the different types of vessels. These formulae are either based on an analysis of built ships or an analysis of standard ships with information on corrections required for deviations from the standard conditions.

The calculations are performed as part of the project design of a new ship, at launching, at rebuilding, for determination of favorable cargo distribution in a ship in operation, or in cases of investigation of shipwrecks. During the design stage it is often difficult to determine the weights. After a damage, the exact cargo distribution may not be known.

During normal operation of a ship the weight distribution as well as the buoyancy will change from voyage to voyage and also during one voyage as the supplies are used up. It is further possible to distinguish between full load or ballast conditions.

This has generally led to the longitudinal loading in still water being checked for certain standard operating conditions which may be as follows:

Fully loaded departure

Fully loaded arrival

Fully loaded with partially used fuel & stores (Lloyd's)

Loaded to the summer freeboard on even keel (DNV)

Ballast (min. draft forward approx. 0.027 L and min. draft aft approx. 0.042 L).

*) Judd, P.H. "Longitudinal Strength and Vibration of Ships by Electronic Computers". NECI, Vol. 77, 1960.

The conventional calculation consists of a laborious determination of the loading curve q_z , which is then integrated twice and the associated integral curves are drawn. The integration can be performed numerically (Simpson's rules or other) or graphically (integraph).

The still water loadings are strongly influenced by the following factors:

a) The length of the machinery room.
b) The location of the machinery room.
c) Machinery weight.
d) The location of the cargo holds and their contents.
e) Block-coefficient.
f) The location and content of deep tanks.
g) The location of ballast tanks.

In fig. 1.2.23 a and b are shown the static longitudinal loading in still water for a passenger ship with machinery room respectively midships, and aft[1)]. It can be seen that the bending moment is greatest when the machinery room is aft. The wave loading midships are calculated for a wave height equal to $1.1\sqrt{L}$ (ft.). The following maximum shear forces (tons) and moments (ft. tons) were obtained.

Vessel	Still Water		Wave	
	Shear force	Moment	Shear force	Moment
Fig. 1.23	2.257	430.770	4.694	985.850
Fig. 1.23	2.811	567.700	5.458	1.133.820

Fig. 1.2.21 and 1.2.22 show the still water loading of an ore carrier (bridge and machinery room midships) in ballast and full load respectively.[2)] A

1) R.V. Turner et. al.: "Some aspects of pasenger liner design". TINA, Vol. 105, 1963.

2) Seyderhelm, Schiff und Hafen 1956, H. 12.

comparison shows that the ballast condition (with filled tanks forward and aft) gives the greatest bending moment. In the full load condition the maximum bending moment occurs relatively for forward (hatch no. 2). Especially for bulk carriers which carry heavy cargo (ore), the still water loading may be unfavorable. These ships often sail in loaded condition with some holds empty. The maximum bending moments will then not necessarily occur close to midships, and it will be necessary to determine shear force as well as bending moment curves for the whole length of the ship in order to determine the unfavorable sections.

Dry cargo ships with machinery room midships are normally subjected to hogging moments in the loaded condition since there is reserve buoyancy in the area around the machinery room. Larger tankers always have the machinery room aft and are in loaded condition normally exposed to sagging bending moment midships.

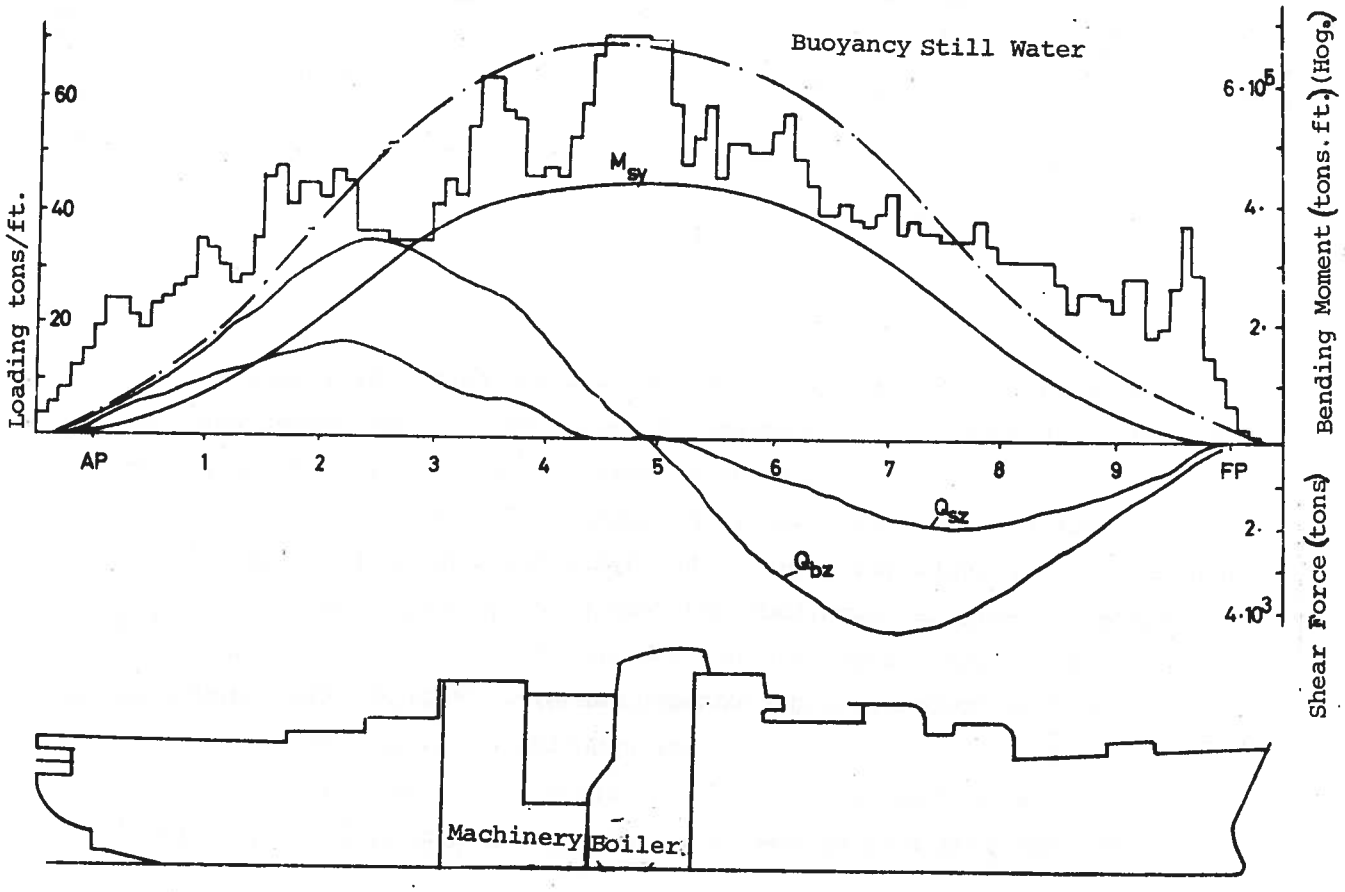

Fig. 1.2.23a

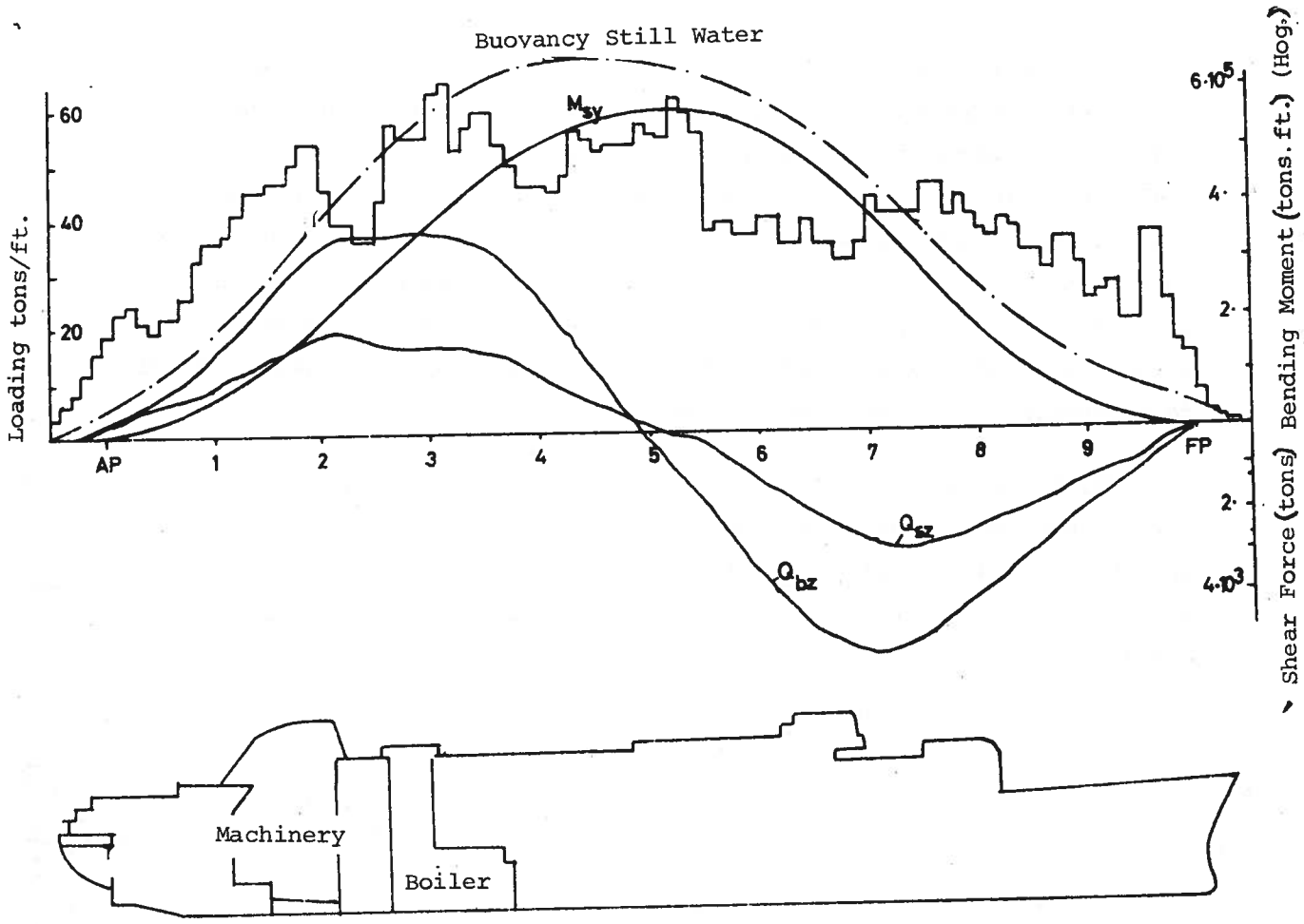

Fig. 1.2.23b

Every large ship is exposed to considerable danger by irrational cargo distribution. It is therefore common practice that larger ships are equipped with a load-indicator which shows whether the cargo distribution is permissible. This indicator is basically an analogue calculator whose electrical components are tuned to the hydrostatic data of the vessel and the permanent weights' magnitude and centers of gravity. On the console of the instrument every cargo hold has its own reostat, which by a change in cargo stored is correspondingly changed manualy. With all the weights recorded correctly, a strain difference corresponding to shear force, bending moment or trim is registered, on a calibrated potensiometer. The apparatus is checked for each ship by the classification society which gives upper

limit for permissible loading.

For practical calculations it may be convenient to indicate the still water moment (M_s) at an arbitrary section by the formula:

$$M_s = M_s^{w\ell} + M_s^b + M_s^{wd} + M_s^t$$

where

- $w\ell$ indicates the contribution of the light weight
- b indicates the contribution of the buoyancy at varying draft and even keel.
- wd indicates the contribution of the deadweight onboard
- t indicates the contribution of the trim.

We can once and for all determine $M_s^{w\ell} + M_s^b$ at varying drafts. Figure 1.2.24 which is produced by Loeser [1] shows curves of this type. These are determined by integration from both ends of the vessel towards the middle. The discontinuity in the curves midships is a result of the fact that buoyancy and light weight are not alone in equilibrium. The deadweight moments are found by simple moment-calculations when the center of gravity of the individual cargoes are determined. This can also in most cases be done once and for all by varying stowage heights and cargo types.

The simplest is perhaps to determine influence lines for bending moments at the transverse bulkheads for different drafts. Corresponding calculations can be done in order to determine the shear forces. Then either the curves follow the vessel, or an analogue calculator is made from the calculated data.

---

[1] Harrison T. Loeser; "Notes on Longitudinal Bending Moments". Marine Engineering and Shipping Review, Aug. 1949.

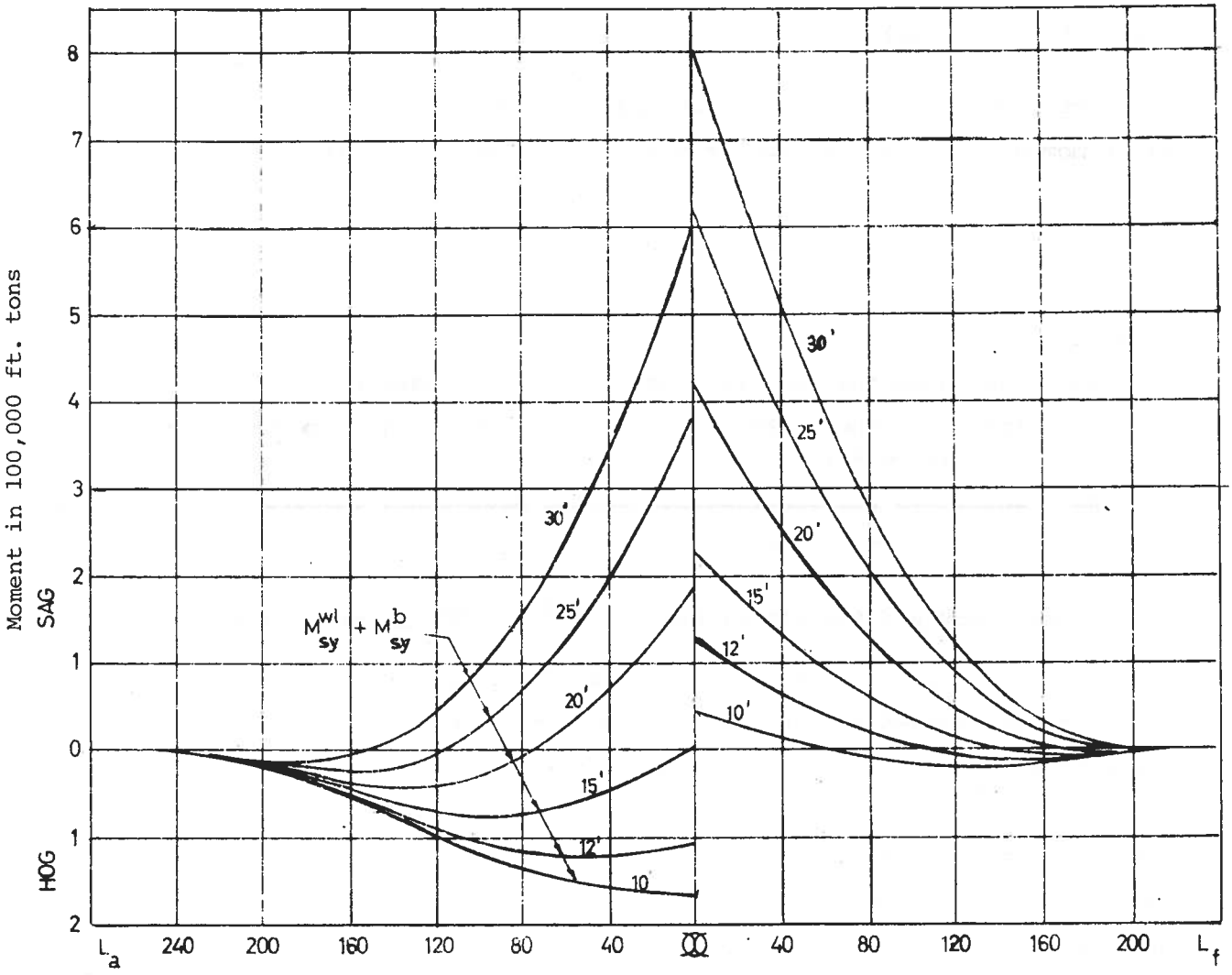

Fig 1.2.24

For a doubly symmetrically loaded and shaped hull girder, the weight and buoyancy resultants forward and aft respectively form two equally large and oppositely directed force couples (fig. 1.2.25) which give the still water moment amidships *).

*) The notataion $\overline{M}$ indicates that the quantity refers to the section amidships.

$$\bar{M}_{sy} = e_o \frac{\Delta}{2} \tag{1.2.24}$$

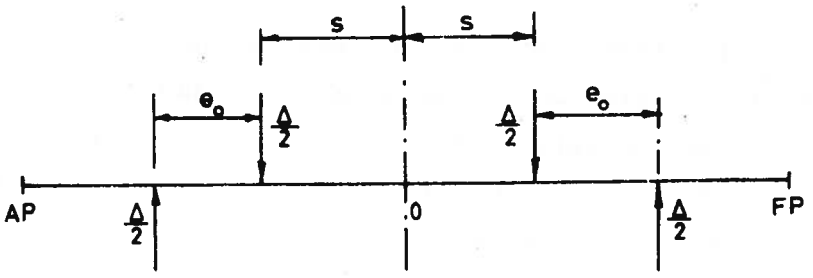

Fig. 1.2.25

For a vessel which is unsymmetric about the midship, the bending moment will be approximately given by[1] (see also eqn. 1.2.13 and fig. 1.2.11):

$$\begin{aligned} \bar{M}_{sy} &= \frac{\Delta}{4} (e_a + e_f) \\ &= \frac{\Delta L}{2} \left(\frac{\ell_a + \ell_f}{2L} - \frac{s_a + s_f}{2L} \right) = \bar{M}^b_{sy} - \bar{M}^w_{sy} \end{aligned} \tag{1.2.25}$$

where

$$\begin{aligned} \bar{M}^b_{sy} &= \frac{\Delta L}{2} \frac{\ell_a + \ell_f}{2L} \\ \bar{M}^w_{sy} &= \frac{\Delta L}{2} \frac{s_a + s_f}{2L} \end{aligned} \tag{1.2.26}$$

The contribution of the buoyancy forces to the still water moment depends only upon the hull form, draft and trim, and can be set equal to:

$$\bar{M}^b_{sy} = \gamma \, B \, d \, L^2 \cdot C^b_s \tag{1.2.27}$$

Fig. 1.2.26 shows some applied relations between the moment coefficient C^b_s and the block coefficient C_B. Buchanan in Lloyd's Register [2] goes one step further with the simplifications, since for cargo ship with machinery room near midships he sets:

---

1) Murray: "Longitudinal Bending Moments". IESS 1947.

2) Murray: "A Hundred Years of Lloyd's Register Ship Rules". TINA, 1955.

$$\overline{M}_{sy} = e \frac{\Delta L}{2} \qquad \text{(Units: tons and feet)} \qquad (1.2.28)$$

where the coefficient e is taken from figures 1.2.27 a and b. The diagrams are based on the cargo distribution at "standard arrival condition". The vessel was assumed to be homogeneously loaded in all holds. One fouth of the tank volume for fuel and water supply was assumed onboard, and located in the double bottom near midships. If the distribution of cargo or bunker is considerably different from the above, then the figures 1.2.27 a and b can only be used together with certain corrections [1], which can, for instance, be made by means of influence lines.

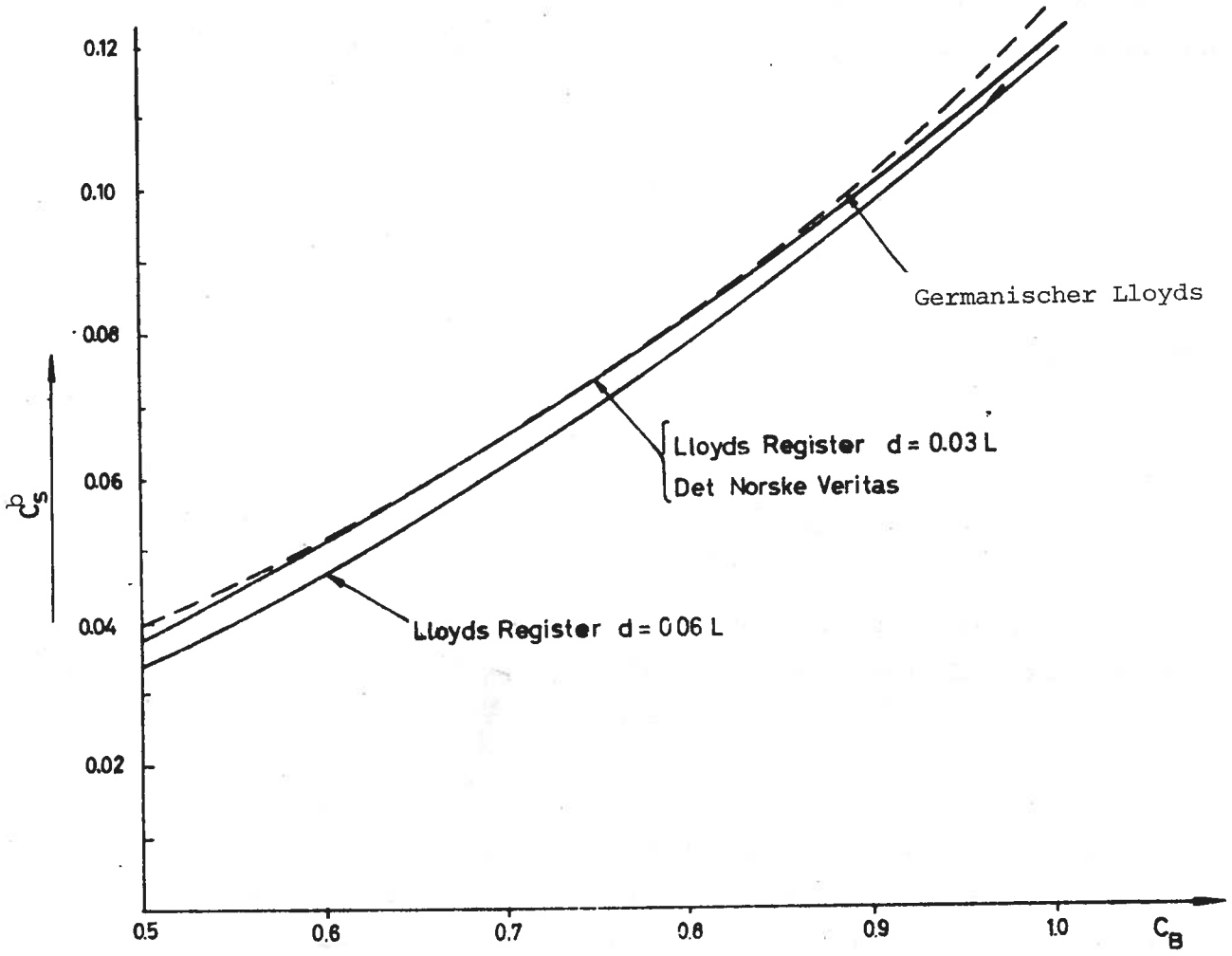

Fig. 1.2.26

1) Buchanan, G.: "Longitudinal Stresses in Cargo Ships". Lloyd's Register of Shipping, 1958.

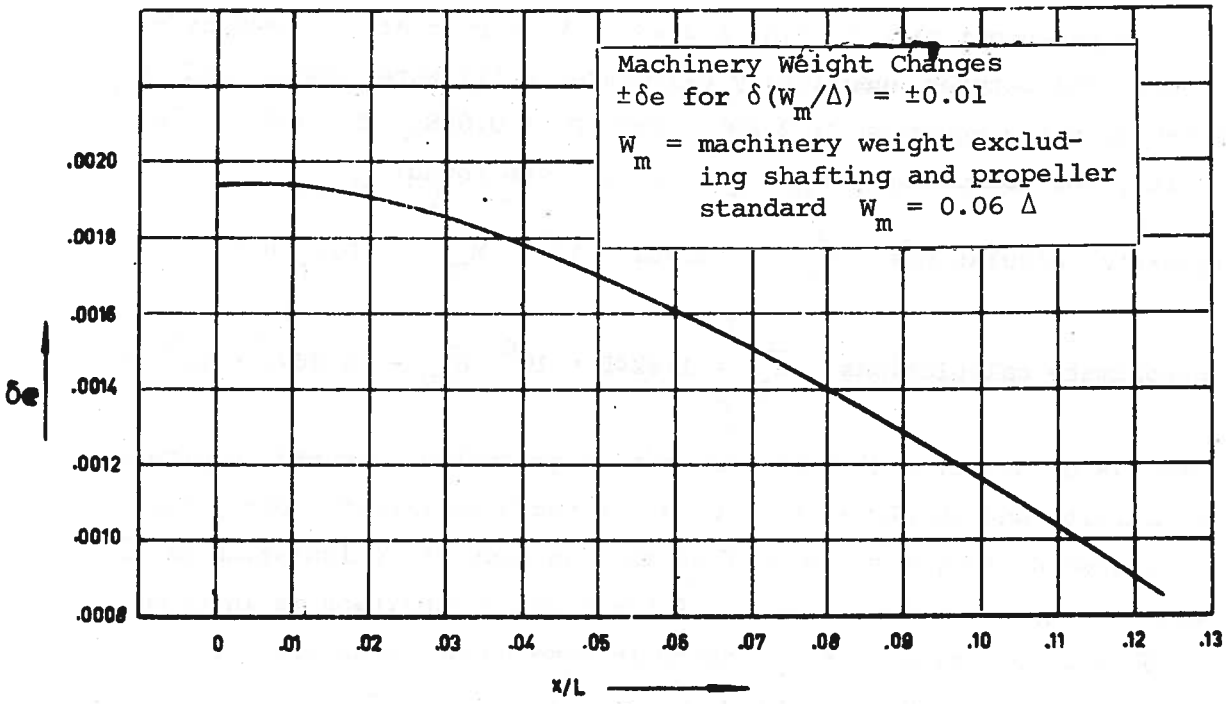

Fig. 1.2.27 a

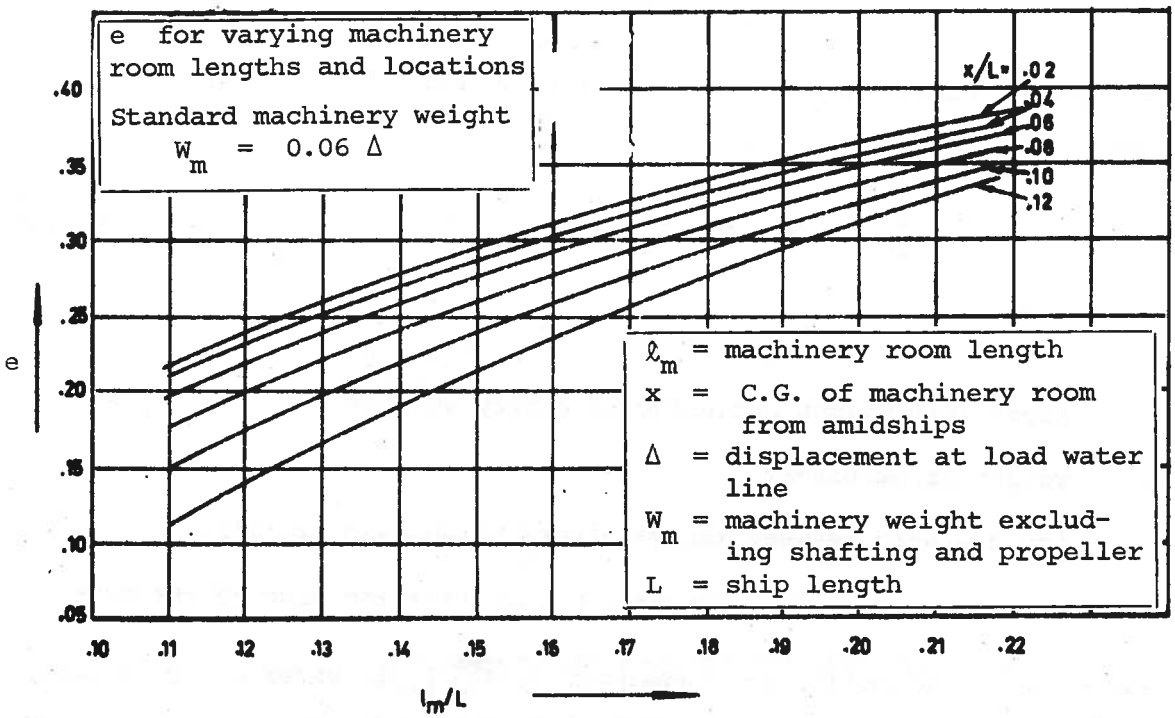

Fig. 1.2.27 b

For the passenger ship in fig. 1.2.23, R.V. Turner et.al. have carried out a comparison between numerically calculated still water moment and $\bar{M}_{sy}$ calculated by using equation (1.2.28). For $C_B = 0.658$, $d = 0.06\ L$ and $L = 600$ ft., the following moments (ft. tons) were found:

Accurate calculations: $\bar{M}^b_{sy} = 1.961 \cdot 10^6$ $\bar{M}_{sy} = 0.4308 \cdot 10^6$

Approximate calculations: $\bar{M}^b_{sy} = 1.9245 \cdot 10^6$ $\bar{M}_{sy} = 0.4673 \cdot 10^6$

Formulas of the type (1.2.28) can not in general be assumed to give dependable results and should only be used for rough estimates. Det Norske Veritas recommends in the rules of 1964 that an accurate calculation of the still water moments should be made. If the loading condition is inhomogeneous (high concentration of heavy cargo in some holds) such accurate calculations are mandatory. A simplified formula of the type (1.2.25) is in some cases allowed to be used. M^b_{sy} is then determined by using curves in fig. 1.2.26. The contribution of the weight moment is then set equal to:

$$\bar{M}^w_{sy} = \bar{M}^{w\ell}_{sy} + \bar{M}^{wd}_{sy} \tag{1.2.29}$$

where the moment contribution from light ship weights ($\bar{M}^{w\ell}_{sy}$) can be set equal to:

$$\bar{M}^{w\ell}_{sy} = c \cdot P \cdot L + M \cdot m \tag{1.2.30}$$

where:

P = light ship weight exclusive machinery weights

M = weight of machinery

m = the distance between the machinery weight and midships

c = a given factor which depends on ship type and size of the ship (L).

The moment contribution of deadweight ($\bar{M}^{wd}_{sy}$) is under any circumstances required to be calculated accurately with the deadweights taken as single

loads at ballast tanks, bunker, fresh water, supplies, cargo, etc. The rules dictate which loading conditions are to determine scantlings.

1.3 Quasi-static analysis of loads in regular waves.

1.3.1 Potential theory for two-dimensional waves in deep water.

1.3.1.1 Hydrodynamic fundamentals.

For studies in wave induced loads on ships, it is convenient to start from the theory of waves in an incompressible, frictionless liquid. It will later appear that this theory also is the basis for studies related to the irregular seaway.

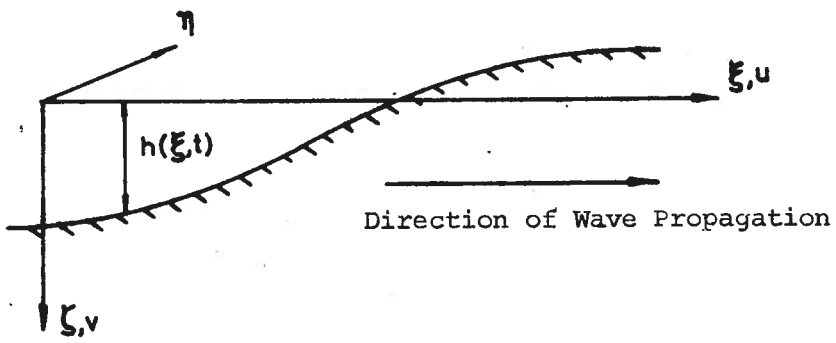

Fig. 1.3.1

From the general theory of hydrodynamics it is known that the continuity condition for an incompressible liquid in motion may be expressed by the Laplace partial differential equation

$$\frac{\partial^2\phi}{\partial\xi^2} + \frac{\partial^2\phi}{\partial\zeta^2} = 0 \qquad (1.3.1)$$

where

ϕ = a velocity potential, defined by:

$$-\frac{\partial\phi}{\partial\xi} = u$$

$$-\frac{\partial\phi}{\partial\zeta} = v \qquad (1.3.2)$$

with

u = the liquid particles' motion velocity in the ξ-direction.

v = the liquid particles' motion velocity in the ζ-direction.

Equation (1.3.1) applies only for a pure two-dimensional motion): no particle motion in the η-direction, see fig. 1.3.1.

From hydrodynamics theory it is further known that when the gravitation forces represent the only external influence, Euler's equations of motion (force = mass x acceleration) will be satisfied if:

$$\frac{p}{\rho} = \frac{\partial \phi}{\partial t} + g\zeta - \frac{1}{2} q^2 \qquad (1.3.3)$$

where

g = gravitational acceleration
ρ = density
p = pressure
q = $(u^2 + v^2)$ = velocity

1.3.1.2 Determination of wave motion.

The problem is now to find a function $\theta(\xi\ \zeta)$ which satisfies equation (1.3.1), and certain boundary conditions.

It is convenient to write the solution of euqation (1.3.1) as follows:

$$\phi = \sum_n \phi_n = \sum_n F_n\ (\zeta)\ \sin k_n\ (\xi - c_n t) \qquad (1.3.4)$$

where

$$k_n = \frac{2\pi}{\lambda_n}$$

$$k_n c_n = \frac{2\pi}{T_n}\ ):\ c_n = \frac{\lambda_n}{T_n} \qquad (1.3.5)$$

Here:

λ_n = wave length for the n'th harmonic component

T_n = wave period for the n'th harmonic component

c_n = celerity of the wave. (n'th harmonic component).

By substituting from equation (1.3.4) in (1.3.1) it is found that $F_n(\zeta)$ must satisfy the following ordinary differential equation:

$$\frac{d^2F_n}{d\zeta^2} - k_n^2 F_n = 0 \qquad (1.3.6)$$

From here on, one part of the series for ϕ will be treated separately and we can drop the index n. The solution of equation (1.3.6) is then:

$$F(\zeta) = A\, e^{k\zeta} + B\, e^{-k\zeta} \qquad (1.3.7)$$

where A and B are constants of integration which must be determined from the boundary conditions.

Since only surface waves in deep water are discussed here, it follows that $A = 0$ such that $F(\zeta) = 0$ when $\zeta \to \infty$. Thus, according to eq. (1.3.4) and (1.3.7):

$$\phi = B\, e^{-k\zeta} \sin k\,(\xi - ct) \qquad (1.3.8)$$

Here it is advantageous to introduce a new constant, by writing equation (1.3.8):

$$\phi = r_o\, c\, e^{-k\zeta} \sin k\,(\xi - ct) \qquad (1.3.8a)$$

The quantities r_o and c are constants of integration which are determined from the boundary conditions on the free surface. For all particles along the surface, where $\zeta = h(\xi,t)$ the following conditions must apply:

1) The pressure in the liquid is equal to the atmospheric pressure. In the following we disregard the atmospheric pressure and set

$$p_{\zeta=h} = 0$$

2) The liquid particles on the surface move with a velocity:

$$v_{\zeta=h} = \frac{\partial h}{\partial t}$$

(This equation is valid only in a linearized theory).

From equations (1.3.2), (1.3.3) and (1.3.8a) the following general relationships are obtained:

$$\begin{aligned} u &= -\frac{\partial \phi}{\partial \xi} = -k\, r_o\, c\, e^{-k\zeta} \cos k(\xi - ct) \\ v &= -\frac{\partial \phi}{\partial \zeta} = k\, r_o\, c\, e^{-k\zeta} \sin k(\xi - ct) \\ q^2 &= u^2 + v^2 = (k\, r_o\, c)^2\, e^{-2k\zeta} \\ \frac{\partial \phi}{\partial t} &= -k\, r_o\, c^2\, e^{-k\zeta} \cos k(\xi - ct) \end{aligned} \qquad (1.3.9)$$

$$p = \rho \{ g\zeta - \frac{1}{2} (k\, r_o\, c)^2\, e^{-2k\zeta} - k\, r_o\, c^2\, e^{-k\zeta} \cos k(\xi - ct) \} \qquad (1.3.10)$$

First boundary condition.

The first boundary condition may by (1.3.10) be written:

$$gh - \frac{1}{2} (k\, r_o\, c)^2\, e^{-2kh} - k\, r_o\, c^2\, e^{-kh} \cos k(\xi - ct) = 0$$

This equation is difficult to solve exactly. It is therefore convenient to set [x]

$$e^{-2kh} \sim 1 - 2kh$$

---

x) Here $2kh = 4\,\pi/\lambda$. At $h_{max}/\lambda = \frac{1}{40}$, which is a representative value, $e^{-2kh} = e^{-0.314} = 0.730$, whereas $1 - 2kh = 0.686$. The accuracy is sufficient, especially since the part $1/2\ q^2$ is small compared to the other terms.

The boundary condition then becomes

$$(g + k^3 r_o^2 c^2)\, h - \frac{1}{2}(k\, r_o\, c)^2 - k\, r_o\, c^2\, e^{-kh} \cos k(\xi - ct) = 0$$

which gives:

$$h = \frac{kc^2}{g + k^3 r_o^2 c^2} \left\{\frac{1}{2} k\, r_o^2 + r_o\, e^{-kh} \cos k(\xi - ct)\right\} \qquad (1.3.11)$$

Second boundary condition.

From the equations (1.3.9), (1.3.11) and the second boundary condition, we find that:

$$\frac{kc^2}{g + k^3 r_o^2 c^2} = 1$$

and consequently (since $k^2 r_o^2 << 1$):

$$c^2 = \frac{g}{k(1 - k^2 r_o^2)} \sim \frac{g}{k}(1 + k^2 r_o^2) \qquad (1.3.12)$$

We can now write

$$h = \frac{1}{2} k\, r_o^2 + r_o\, e^{-kh} \cos k(\xi - ct) \qquad (1.3.11a)$$

Equation (1.3.11a) defines the free surface $h(\xi,t)$ as an implicit function. The coordinate h is measured from the still water level. If the ξ-axis is positioned a distance $\frac{1}{2} k\, r_o^2$ below the still water level, eqn. (1.3.11a) can without any significant loss of accuracy be written:

$$h = r_o\, e^{-kh} \cos k(\xi - ct) \qquad (1.3.11b)$$

This is the classical Stoke's wave[1]. Fig. 1.3.2 and table 1.3.1 give a few data to be used for drawing the Stoke's wave for varying ratioes r_o/λ.

---

1) Stokes, G.G.: "On the Theory of Oscillatory Waves". Trans. Cambridge Philos. Soc. Vol. 7, pp. 441-457, 1847.

From equation (1.3.5) it is evident that the quantity c is the wave celerity ($\frac{\lambda}{T}$) .

1.3.1.3 The wave surface.

In order to better be able to interpret the form of the gravitational wave, the expression (1.3.11) will be expanded in a series. Setting:

$$e^{-kh} = 1 - kh + \frac{1}{2}(kh)^2 - \frac{1}{3!}(kh)^3 + \ldots\ldots$$

On the right hand side of this expression we introduce (see eqn. (1.3.11a))[x]:

$$kh = k\, r_o\, e^{-kh} \cos k(\xi - ct)$$

and a new series expansion is made in a similar manner. Equation (1.3.11a) may then be written as:

$$h(\xi,t) = r_o \{(1 + \frac{3}{8} k^2 r_o^2) \cos k(\xi - ct) - \frac{1}{2} k\, r_o \cos 2k(\xi - ct) +$$

$$+ \frac{3}{8} k^2 r_o^2 \cos 3k(\xi - ct) \ldots\ldots\} \qquad (1.3.13)$$

The gravitation wave may thus be taken to be the sum of harmonic components. This feature will be utilized extensively later. Thus, from now on, when nothing else has been specifically stated, only one harmonic component will be treated.

$$h(\xi, t) = r_o \cos k(\xi - ct) \qquad (1.3.14)$$

This wave may furthermore be interpreted as a first approximation to equation (1.3.11a), since it is assumed that:

---

[x] Actually

$$kh = \frac{1}{2} k^2 r_o^2 + k\, r_o\, e^{-kh} \cos k(\xi - ct)$$

but here the first part on the right hand side is of minor importance.

1) The term $\frac{1}{2} k r_o^2 << r_o$ and may be neglected.

2) $e^{-kh} = 1 - kh + ... \sim 1$. This is proper if the first approximation is acceptable.

From equation (1.3.12) it is immediately evident that by using equation (1.3.14) we obtain:

$$c^2 = g/k \qquad (1.3.15)$$

It is further possible to show that the gravitational wave (1.3.11a) is very similar to the trocoidal wave, which has been widely used and can be found described in a number of well known text books[1)2)]. If the equation for the trocoidal wave is expanded in a series, the three first terms correspond to those of equation (1.3.13).

Fig. 1.3.3 shows the form of gravitational wave compared to that of the cosine-wave. The trocoidal wave coincides with the gravitational wave. It can be seen from equation (1.3.13) that the height of the gravitational wave is equal to $2r_o$. Further, it appears that:

a) The wave-crest is $r_o(1+ \frac{1}{2} k r_o)$ above the still water level.

b) The trough is $r_o(1 - \frac{1}{2} k r_o)$ below the still water level.

If the cosine-wave (1.3.14) is to correspond to the gravitation wave, the ξ-axis of the first wave must be located $\frac{1}{2} k r_o^2$ <u>above</u> the still water level. In fig. 1.3.3, then:

Line I : Absissa for wave eqn. (1.3.11c) = still water level.

---

1) "Principles of Naval Architecture". SNAME, N.Y., 1967.

2) Robb, A. : "Theory of Naval Architecture". London, 1952.

Line II : Absissa for Stoke's wave eqn. (1.3.11b).

Line III : Absissa for the cosine wave, eqn. (1.3.14).

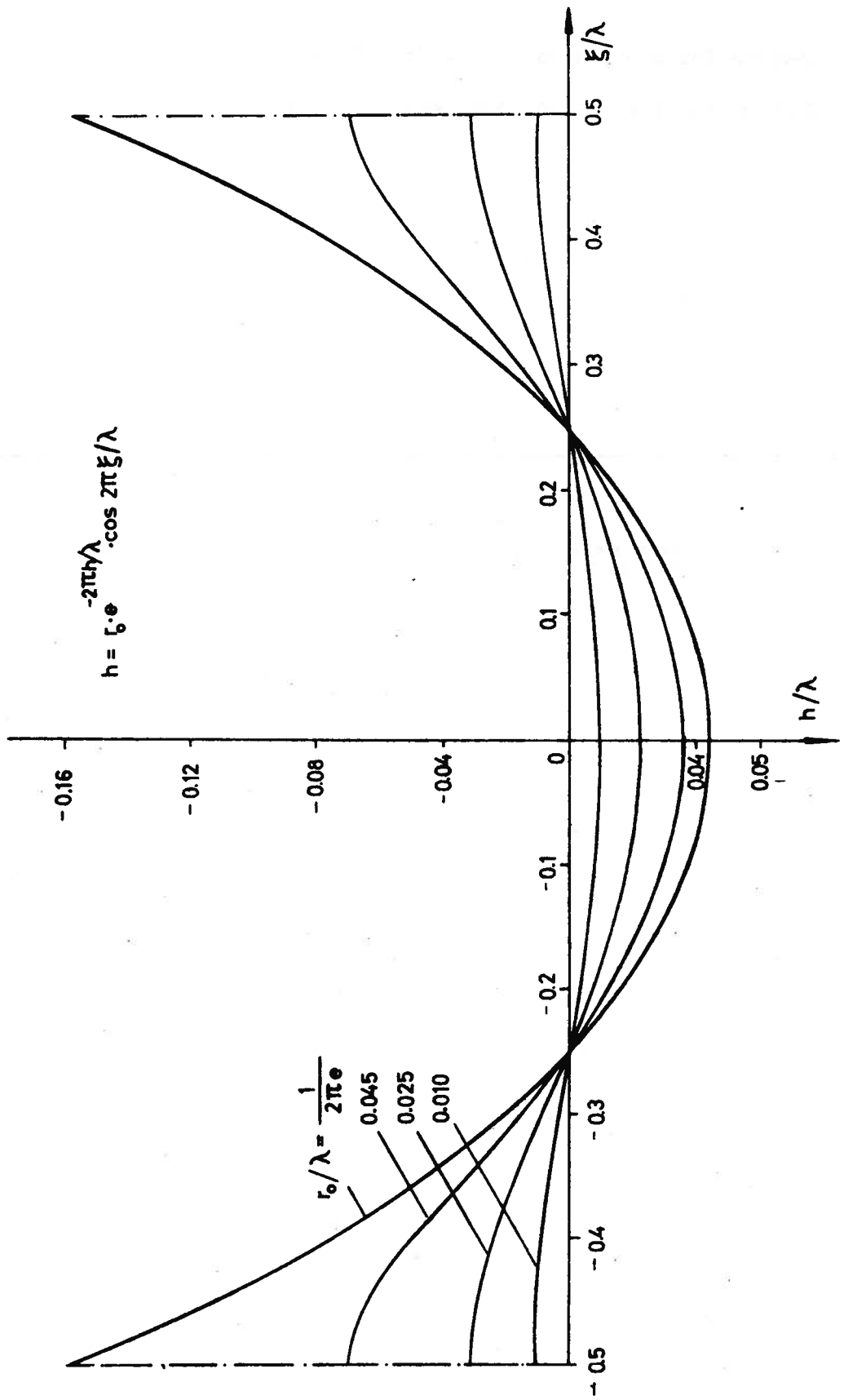
h = r₀·e^{-2πr₀/λ}·cos 2πξ/λ
r₀/λ = 1/2πe
0.045
0.025
0.010
ξ/λ
h/λ
0.5
0.4
0.3
0.2
0.1
0
-0.1
-0.2
-0.3
-0.4
-0.5
-0.16
-0.12
-0.08
-0.04
0.04
0.05

Fig. 1.3.2

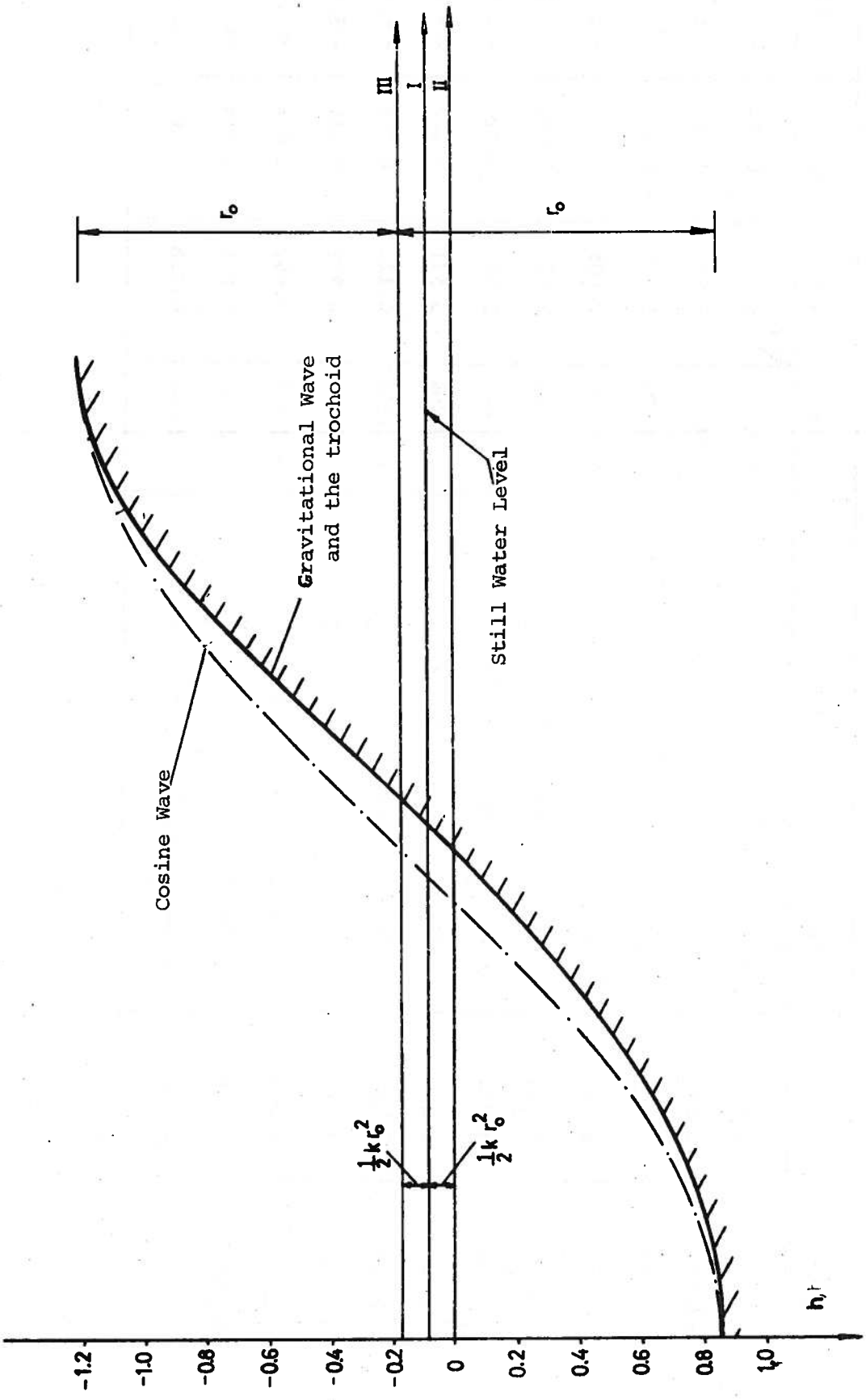
III
I
II
r_o
r_o
Gravitational Wave
and the trochoid
Still Water Level
Cosine Wave
$\frac{1}{2}kr_o^2$
$\frac{1}{2}kr_o^2$
h'
-1.2
-1.0
-0.8
-0.6
-0.4
-0.2
0
0.2
0.4
0.6
0.8
1.0

Fig. 1.3.3

Table 1.3.1 Stocke's Wave

Table of the coordinates ($h/\lambda \cdot 10^2$)

r_o/λ	$x/\lambda = 0$	1/16	1/8	3/16	1/4	5/16	3/8	7/16	1/2
0.010	0.943	0.875	0.678	0.374	0	- 0.392	- 0.741	- 0.983	- 1.070
0.015	1.376	1.279	0.996	0.554	0	- 596	- 1.139	- 1.525	- 1.665
0.020	1.788	1.664	1.303	0.731	0	- 0.805	- 1.560	- 2.110	- 2.313
0.025	2.180	2.033	1.599	0.904	0	- 1.020	- 2.005	- 2.744	- 3.023
0.030	2.555	2.386	1.884	1.073	0	- 1.241	- 2.479	- 3.440	- 3.812
0.035	2.914	2.725	2.161	1.239	0	- 1.469	- 2.986	- 4.214	- 4.703
0.040	3.259	3.051	2.428	1.402	0	- 1.704	- 3.531	- 5.087	- 5.735
0.045	3.591	3.365	2.688	1.561	0	- 1.946	- 4.123	- 6.099	- 6.975
0.050	3.911	3.668	2.939	1.718	0	- 2.197	- 4.772	- 7.314	- 8.563
0.055	4.219	3.962	3.184	1.871	0	- 2.456	- 5.492	- 8.874	-10.930
0.057	4.340	4.076	3.280	1.932	0	- 2.562	- 5.804	- 9.666	-12.510
0.058	4.432	4.164	3.354	1.979	0	- 2.646	- 6.058	-10.390	-15.900

1.3.1.4 Waves in deep water.

The motions of the fluid particles in deeper water with respect to depth are described by equations (1.3.9). For a certain value of ξ (e.g. $\xi = 0$) the equations become:

$$u = - \omega(r_o e^{-k\zeta}) \cos \omega t = - \omega r_\zeta \cos \omega t$$

$$v = - \omega(r_o e^{-k\zeta}) \sin \omega t = - \omega r_\zeta \sin \omega t$$

where (see eqn. (1.3.15)):

$$\omega = k \cdot c = \frac{2\pi}{T} = \sqrt{gk'} \qquad (1.3.16)$$

$$r_\zeta = r_o e^{-k\zeta} \qquad (1.3.17)$$

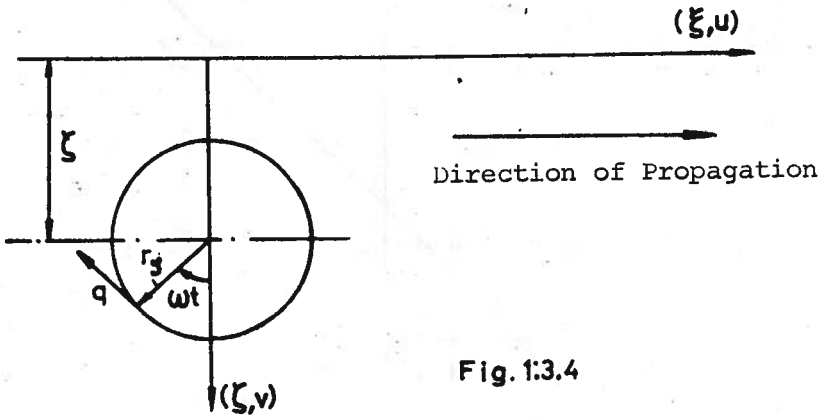

Fig. 1.3.4

A fluid particle which is at a mean position ζ below the free surface, will then move in a circular path whose radius r_ζ is given by equation (1.3.17), (r_o indicates half the wave height at the surface(see fig. 1.3.4).).

The angular velocity ω of the particles is constant and given by equation (1.3.16). From eqn. (1.3.9) it is found that the motion of all particles located at the same ξ-value will be in phase. Particles in the surface move in circular paths of radius (r_o) equal to half the wave length.

The motions in waves decrease exponentially with depth and is described by the formula:

$$h_\zeta(\xi, t) = r_o e^{-k\zeta} \cos k(\xi - ct) = r_\zeta \cos k(\xi - ct) \qquad (1.3.18)$$

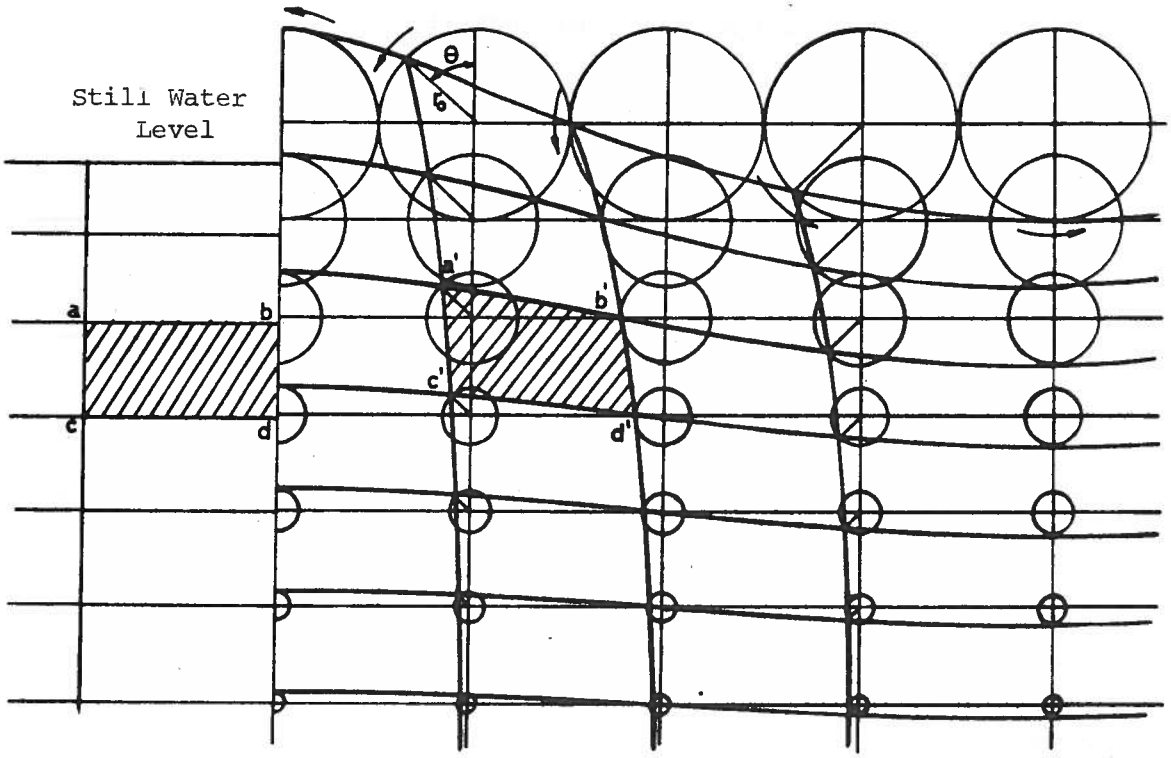

Direction of Wave Propagation

Fig. 1.3.5

Equation (1.3.18) defines the profile of the wave $h(\xi, t)$ in deep water with ζ-values taken from the still water level of the associated wave profile (with same degree of accuracy as in eqn. (1.3.14)).

Figure 1.3.5 shows how the particles rotate at varying depths. The direction of wave propagation is here to the left. On the left hand side of the figure is drawn the still water levels corresponding to all wave surfaces (streamlines). A volume abcd in still water will in the wave be deformed into the volume defined by a'b'c'd' .

The motion decreases rapidly with depth. At a depth equal to $\lambda/2$, for instance:

$$r_\zeta = r_o e^{-\frac{2\pi}{\lambda} \cdot \frac{\lambda}{2}} = r_o e^{-\pi} = 0.043\, r_o$$

1.3.1.5 Pressure relations in waves-Smith's effect.

When calculating the pressures eqn. (1.3.10) is used, but the term $\frac{1}{2} q^2$ is dropped, since it is easily shown to be of higher order effect. This gives:

$$p = \rho\left(\frac{\partial \phi}{\partial t} + g\,\zeta\right) = (\gamma\zeta - k r_o c^2 e^{-k\zeta} \cos k(\xi - ct))$$

$$= \gamma(\zeta - r_o e^{-k\zeta} \cos k(\xi - ct)) = \gamma(\zeta - h_\zeta) \qquad (1.3.19)$$

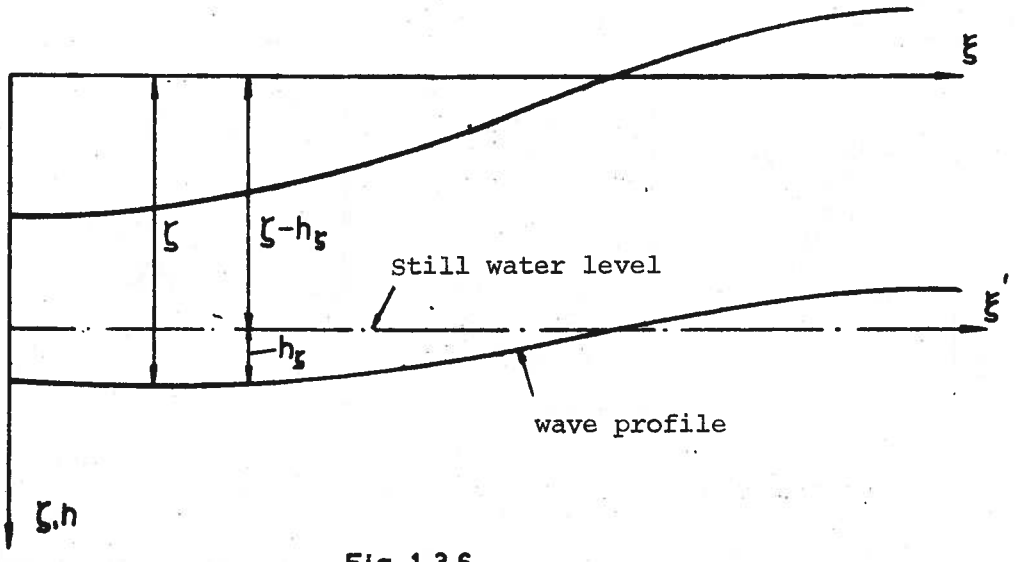

Fig. 1.3.6.

Equation (1.3.19) may be stated as follows (see fig. 1.3.6): The fluid pressure along a wave "profile" is constant and equal to the hydrostatic pressure at the still water level that corresponds to that particular wave profile.

Fig. 1.3.7 shows vertical pressure distributions in the waves at some typical sections. We note that the pressure in a wave trough increases faster with depth than the corresponding hydrostatic pressure. For a wave crest this situation is reversed. One may say that the fluid in the wave trough becomes heavier because of the acceleration of the fluid particles. (Which are added to the acceleration due to gravity.). At wave crests the inertia forces act opposite to the gravitational forces. The significance of the inertia forces due to wave motion decreases with increasing depth since the motion of the fluid particles decreases exponentially.

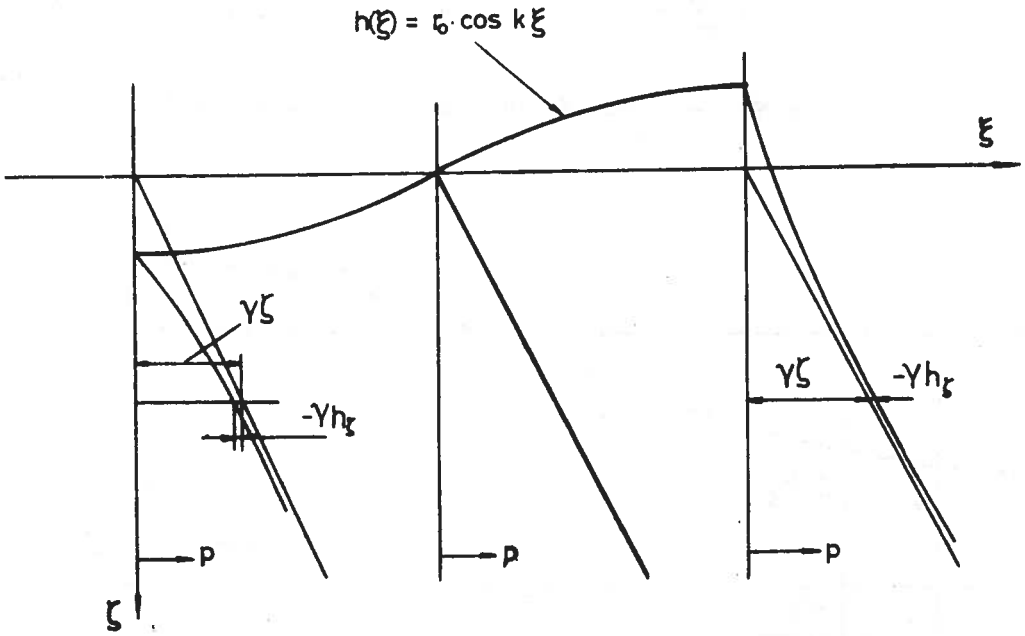

Fig. 1.3.7

When calculating the buoyancy forces acting on a vessel in waves, the hydrodynamic pressure distribution must be taken into consideration. It will be shown in the following that for practical estimates it may be convenient to take these conditions into consideration by introducing an equivalent static wave with reduced height equal to:

$$r_d = K r_o \cos k(\xi - ct) \tag{1.3.20}$$

and then assume that the pressure distribution is hydrostatic. The factor K is usually called the Smith-effect[1].

When a body of breadth B_z and the height d_z is submerged in a fluid as shown in fig. 1.3.8, the buoyancy (dq_z^b) pr. unit length in the x-direction will be equal to:

$$dq_z^b = - B_z \cdot \frac{\partial p}{\partial z} dz = - \frac{\partial p}{\partial z} \cdot dA_z \tag{1.3.21}$$

where

$dA_z = B_z \cdot dz$ = cross-sectional area of the submerged body, and buoyancy is given negative sign as before.

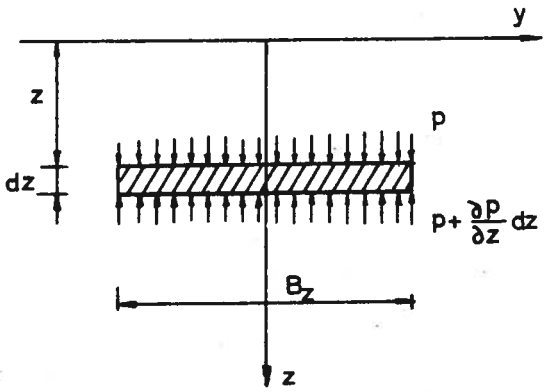

Fig. 1.3.8

Substituting for p from eqn. (1.3.19) with ($\zeta = z$):

$$dq_z^b = - \gamma(1 - \frac{\partial h}{\partial z}) dA_z = - \gamma(1 + kh_z) dA_z \tag{1.3.22}$$

For a submerged body in general:

$$q_z^b = \int_A dp_z^b = - \gamma \int_A (1 - \frac{\partial h_z}{\partial z}) dA_z = - (\gamma A - \int_A \frac{\partial h_z}{\partial z} dA_z) \tag{1.3.23}$$

where A = the area of the hull cross-section.

Example 1.3.1

A box shaped vessel (fig. 1.3.9) of breadth B and length L is located on a wave of length equal to the length of the vessel. The wave profile is

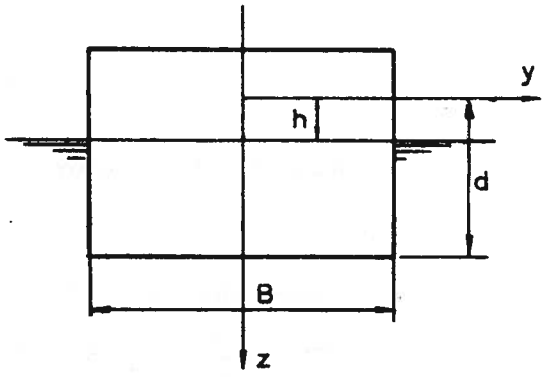

Fig. 1.3.9

given by the formula:

$$h = r_o \, e^{-kh} \cos kx$$

where $k = \frac{2\pi}{L}$ (Stoke's wave)

The vessel's depth relative to the still water level is equal to d. Find the longitudinal buoyancy distribution.

Equation (1.3.23) is used, by substituting $dA_z = B \cdot dz$. This gives:

$$q_z^b = -\gamma B \int_h^d (1 - \frac{\partial h_z}{\partial z}) \, dz$$

$$= -\gamma B \left| z - h_z \right|_h^d$$

$$= -\gamma B (d - h - h_d + h_h) = -\gamma B (d - h_d)$$

since $h_h = r_o \, e^{-kh} \cos kx = h$

The buoyancy including the Smith-effect corresponds to static buoyancy in a wave of height equal to h_d, where:

$$h_d = r_o \, e^{-kd} \cos kx = \kappa h \sim \kappa r_o \cos kx$$

The factor κ is determined from the expression

$$\kappa = e^{-kd} = e^{-2\pi d/\lambda}$$

Assuming now a ratio $d/L = d/\lambda = 0.06$ we obtain:

$$\kappa = e^{-2\pi \cdot 0.06} = e^{-0.377} = 0.686$$

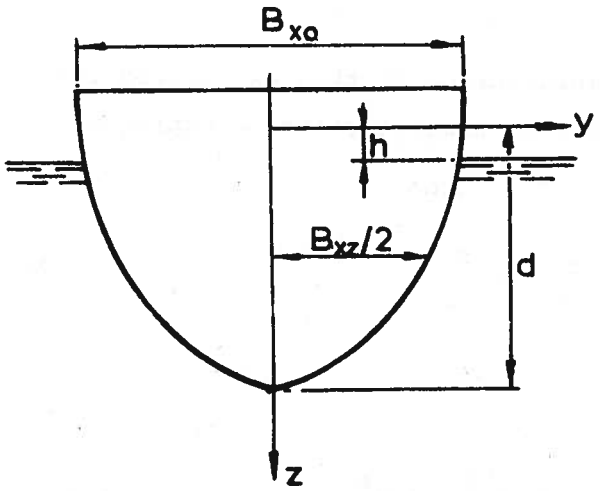

Fig. 1.3.10.

We shall now determine the buoyancy at a section given by the following equation: (Fig. 1.3.10):

$$B_{xz} = B_{xo}\,(1-(\frac{z}{d})^n) \quad \text{for} \quad z > 0$$

$$B_{xz} = B_{xo} \quad \text{for} \quad z < 0$$

The vessel is assumed to be located in a regular cosine-wave such that the local coordinate system in the vessel (x,y,z) coincides with the (ξ,η,ζ)-system.

The sectional area coefficient is calculated from the fomula:

$$C_s = \frac{1}{B_{xo} \cdot d} \int_o^d B_{xo}(1 - (\frac{z}{d})^n)dz = \frac{n}{n+1}$$

From equation (1.3.22) with (ξ= x and ζ= z):

$$q_z^b = -\{\gamma\, B_{xo} \int_o^d (1 - (\frac{z}{d})^n) \cdot (1 + kh_z)\, dz$$

$$-\gamma\, B_{xo} \int_o^h (1 + kh_z)\, dz\}$$

In the last term of this expression we have neglected the variation of the breadth of the water line in the region /z/ < h .

After some mathematical operations we obtain:

$$\frac{q_z^b}{\gamma B_{xo} d} = -\{C_s - \frac{\kappa r_o}{d} \cos k(x - ct)\}$$

where

$$\kappa = \{1 - k \int_o^d (1 - (\frac{z}{d})^n)\, e^{-kz}\, dz\}$$

Following a series of expansion and integration of this expression the Smith factor (κ) may therefore for the above chosen section be expressed by the formula:

$$\kappa = \sum_{m=0}^{\infty} (-1)^m \frac{n}{n+m} \cdot \frac{1}{m!} (kd)^m \qquad (1.3.24)$$

or if n is expressed by C_s:

$$\kappa = \sum_{m=0}^{\infty} (-1)^m \frac{C_s}{C_s + (1-C_s)m} \cdot \frac{1}{m!} (kd)^m \qquad (1.3.25)$$

The Smith-effect estimated from equation (1.3.25) is shown graphically as a function of the ratio d/λ in fig. 1.3.11. The series will converge quite rapidly since $kd = 2\pi \frac{d}{\lambda}$ is usually of magnitude much less than 1.

1.3.1.6 Wave energy .

The kinetic energy in a wave is

$$E_k = \frac{1}{2} \rho \int_v q^2 \, dV \qquad (1.3.26)$$

For the two-dimensional wave $h = r_o \cos k(\xi - ct)$ of unit breadth, $dv = d\xi d\zeta$ and with q as given by equation (1.3.9) we get:

$$E_k = \frac{1}{2} \rho \int_o^{\infty} \int_o^{\lambda} k^2 r_o^2 c^2 e^{-2k\zeta} d\xi d\zeta = \gamma r_o^2 \lambda \qquad (1.3.27)$$

The potential energy of the wave is:

$$E_p = \int_o^{\lambda} \frac{\gamma}{2} h^2 d\xi = \frac{\gamma}{2} r_o^2 \int_o^{\lambda} \cos^2 k \, (\xi - ct) \, d\xi = \frac{1}{4} \gamma r_o^2 \lambda = E_k \qquad (1.3.28)$$

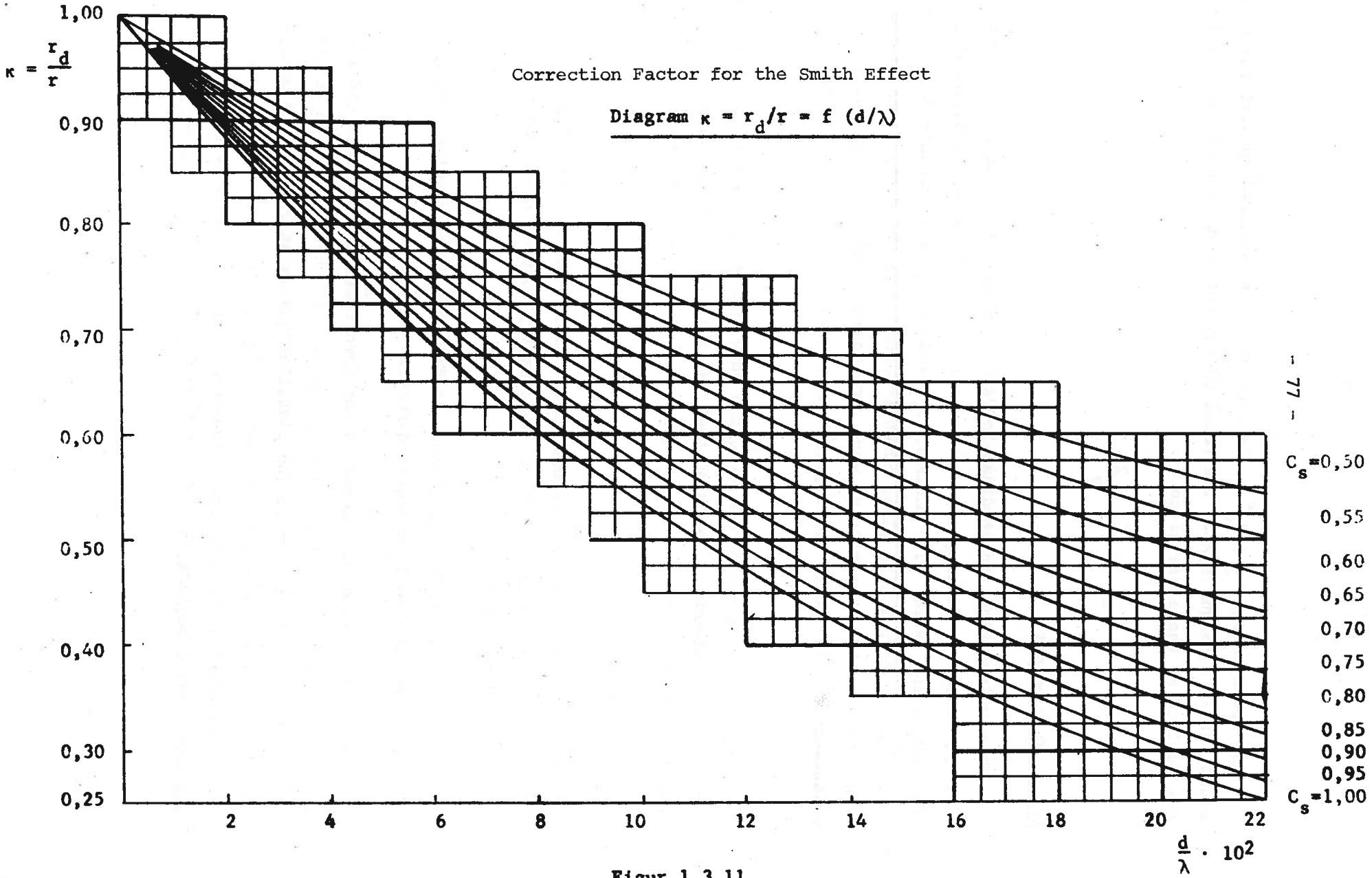
Correction Factor for the Smith Effect
Diagram κ = r_d/r = f (d/λ)
κ = r_d/r
1,00
0,90
0,80
0,70
0,60
0,50
0,40
0,30
0,25
2
4
6
8
10
12
14
16
18
20
22
d/λ · 10²
C_s=0,50
0,55
0,60
0,65
0,70
0,75
0,80
0,85
0,90
0,95
C_s=1,00

Figur 1.3.11

The total energy $\frac{1}{2}\gamma r_o^2 \lambda$ is thus the work required to lift the fluid column $\gamma r_o \lambda$ a height $r_o/2$. The total energy per unit area of the undisturbed free surface is therefore given by:

$$E = \frac{1}{2}\gamma r_o^2 \tag{1.3.29}$$

1.3.2 Wave height.

When calculating longitudinal loads acting on a ship, it is, as mentioned earlier, common to distinguish between still water loads and additional loads produced by the waves. The maximum wave-induced bending moments and shear forces in the center line plane normally occur when the center line of the ship coincides with the direction of wave propagation, and then especially for wave lengths (λ) which are approximately equal to the length of the ship (L).

From the above considerations, the wave induced loads are evaluated by the classical methods by assuming that the ship is in static equilibrium when located in a regular wave of length equal to the length of the ship.

Such an assumption is of course quite unrealistic because:

a) The ship is in continuous motion in the waves, and for an accurate estimate of the loads it is necessary to take into consideration the dynamic forces.

b) The waves in the rough sea are far from being regular, and they also have constantly changing direction of propagation.

How to take into consideration the complications mentioned under a) and b) above will be studied later. However, if these have been considered, it may be useful to return to the classical quasistatic method of analysis but with the calculations being based on an equivalent wave height which as far as possible gives comparable loads to those predicted by the more accurate and complicated methods.

There have been a number of efforts made to find representative wave heights for the evaluation of longitudinal loads. Normal procedure has been to introduce the trocoidal waves[1], often with a correction for the Smith-effect.

From the Frenchman Paris' wave observations (Berlin in TINA from 1873) it seems reasonable to choose $H/\lambda = 1/20$ for $\lambda < 300$ ft. and $H/\lambda = 1/25$ for $\lambda > 300$ ft. Biles[2] suggested that the longitudinal loads should be based on the trochoid-wave with $H = L/20$ and length equal to the length of the ship (L). This standard wave was almost solely used until quite recently. About 1958 Det Norske Veritas and Lloyds Register introduced more representative waves based on the analysis of wave observations. It was found then that the previous standard wave gave a too small wave height for smaller ship lengths, whereas it resulted in unreasonably large wave heights for very large ships, see fig. 1.3.12 and fig. 1.3.13, which also shows some new suggestions.

Det Norske Veritas chose:

$$H_{NV} = 0.45\ L^{0.6} \qquad \text{(meters)}$$

Lloyds chose:

$$H_{LR} \simeq 1.4\ L^{0.5} \qquad \text{(feet)}$$

With a correction for the dynamic wave pressure, the corresponding waves were:

$$H_{NV} = 0.34\ L^{0.6} \qquad \text{(meters)}$$

$$H_{LR} = 1.1\ L^{0.5} \qquad \text{(feet)}$$

---

1) Gestner: "Theorie der Wellen". Abh.d.K. Bohm. Ges. d. Wiss. 1802.

2) Biles: "Standardization of Ships Calculations". TINA 1901. (IESS, 1893).

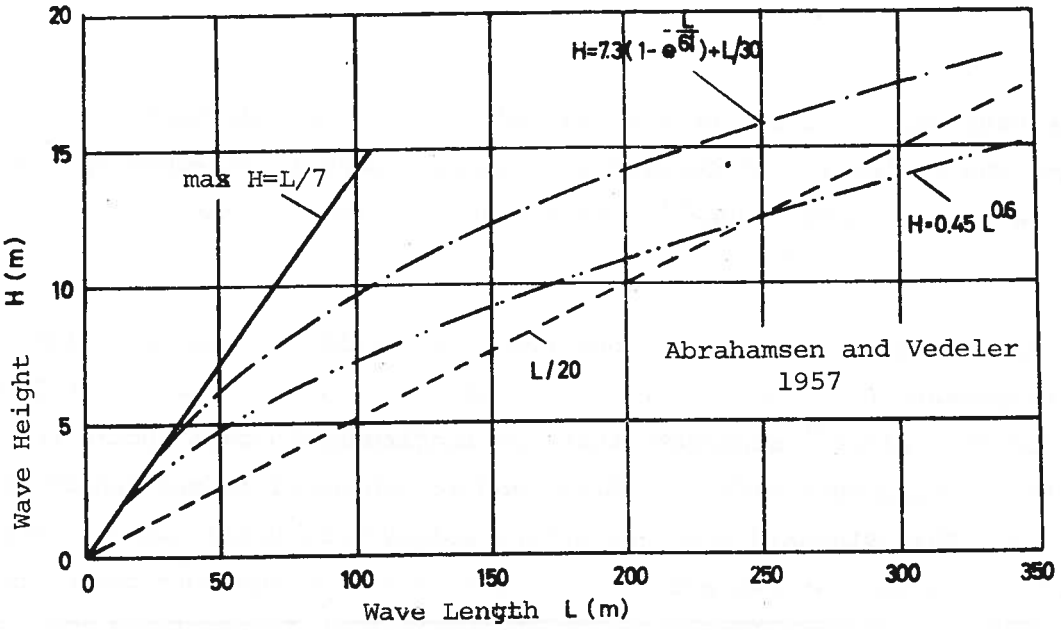

Fig. 1.3.12

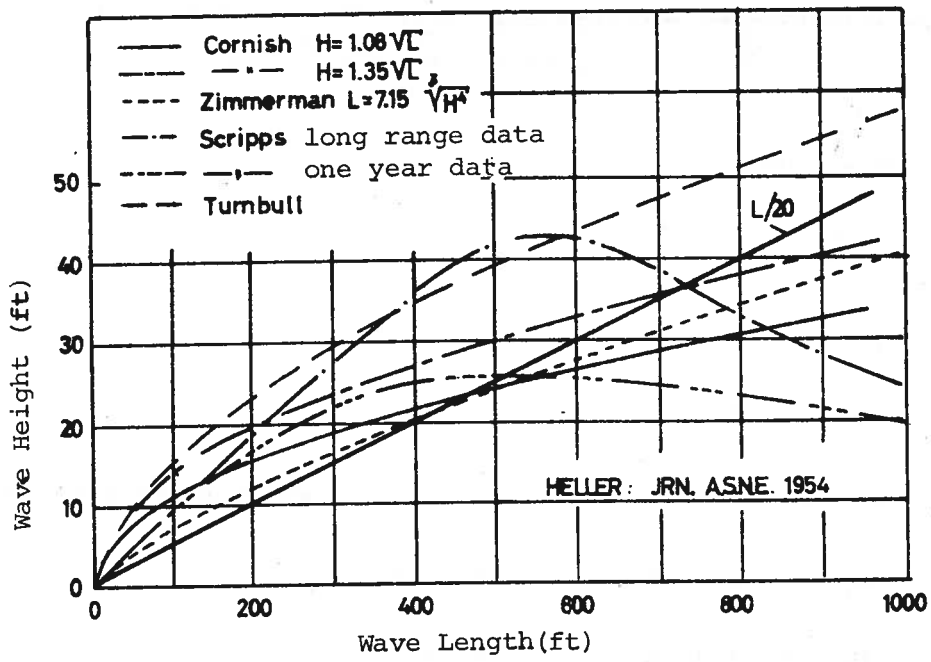

Fig. 1.3.13

The wave slope decreases here with increasing length, for instance:

$$H_{NV}/L = 0.34\ L^{-0.4}$$

Lately, the following relationship has been partially adopted:

$$H = K\ \lambda^{0.3} \qquad (1.3.30)$$

but recent research seems to indicate that the equivalent wave height can be assumed to decrease even more when $L > 300$ m , (fig. 1.3.14). The decision on the height of the standard wave will depend on whether the absolutely largest wave that the ship may encounter is the most critical, or if it is possible that the severest strength problems occur in connection with a somewhat smaller wave which the ship should be expected to meet more often during its life. These problems will be discussed further in chapter I/1.5. Here it should only be noted that there are extensive studies on international basis being conducted to map the wave conditions on the most trafficked ocean routes. Table 1.3.2 gives as an example, the distribution of wave heights and wave periods observed over a long time period, in some regions of the North Atlantic. The number of observations is also given in the table.

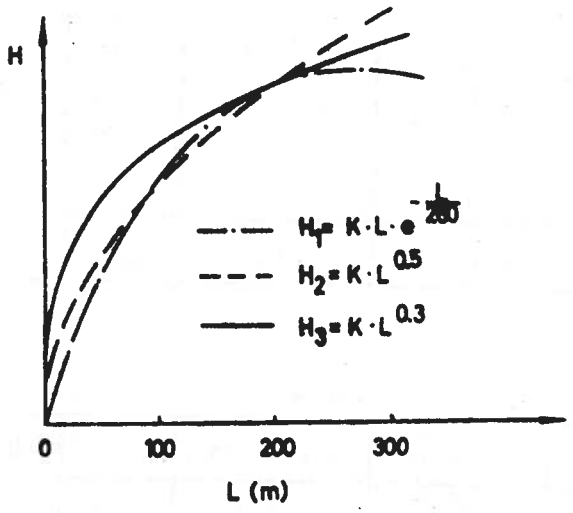

Fig. 1.3.14

Table 1.3.2

The numbers indicate % of all observations; P = observed wave period (sec.)
H = observed wave height (m).

Region 1 a

P \ H	<1 1/2	1 1/2- <3	3- <4 1/2	4 1/2- <6	6- <8	>8	Total
< 7	35.1	25.7	2.5	.3	.1	*	63.7
> 7- 9	2.2	11.3	3.4	.6	.2	.1	17.8
> 9-11	.8	4.5	2.7	.7	.3	.1	9.1
>11-13	.3	1.2	1.4	.7	.2	.1	3.9
>13-15	.1	.4	.5	.2	.1	.1	1.4
>15	1.2	.3	.2	.1	.1	*	2.0
Total	39.7	43.4	10.7	2.6	1.0	.5	97.9

Calm 2.1 * 0.05 per cent No. of. obs. 279,930

Region 1 b

P \ H	<1 1/2	1 1/2- <3	3- <4 1/2	4 1/2- <6	6- <8	>8	Total
< 7	27.4	26.3	3.6	.6	.2	0.1	58.3
> 7- 9	1.4	12.1	4.9	1.2	.5	.2	20.9
> 9-11	.7	4.6	4.1	1.1	.7	.2	11.4
>11-13	.2	1.2	1.7	.7	.5	.2	4.5
>13-15	.1	.4	.6	.3	.2	.1	1.7
>15	.9	.3	.3	.2	.1	.1	1.9
Total	31.2	45.0	15.3	4.1	2.2	.9	98.7

Calm 1.3 No. of obs. 293,557

Region 2

P \ H	<1 1/2	1 1/2- <3	3- <4 1/2	4 1/2- <6	6- <8	>8	Total
< 7	20.6	25.8	5.5	1.1	.5	.1	53.6
> 7- 9	1.5	11.8	6.9	2.0	.9	.4	23.5
> 9-11	.5	4.0	4.5	1.8	1.0	.5	12.3
>11-13	.2	1.1	2.0	.9	.6	.4	5.2
>13-15	.1	.3	.6	.3	.3	.2	1.8
>15	.4	.2	.2	.2	.1	.2	1.3
Total	23.3	43.2	19.7	6.3	3.4	1.8	97.7

Calm 2.3 No. of obs. 67,019

Region 1 a: The Atlantic between 30° and 40° lat. north.
" 1 b: " " " 40° and 50° lat. north
" 2 : " " " 50° and 60° " " , 10°-40° long. west.

1.3.3 Ship in waves.

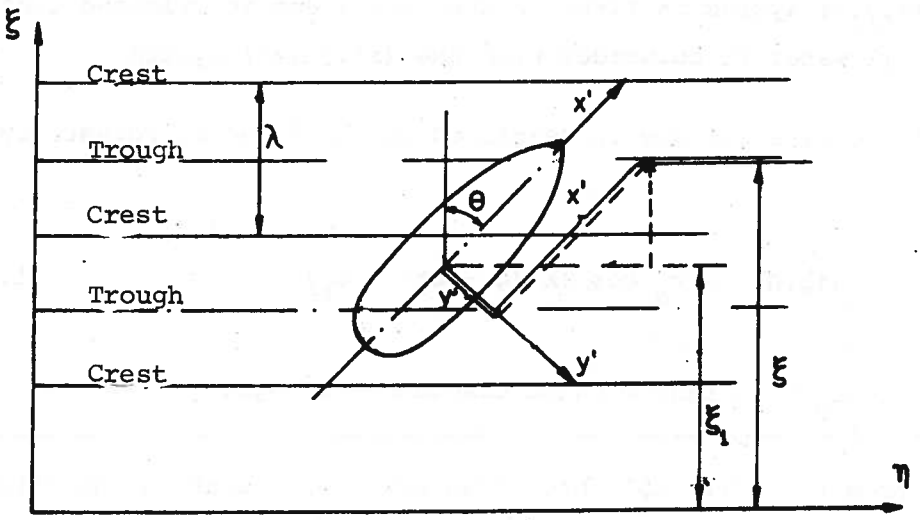

Fig. 1.3.15

In the following we will study the loading conditions when the vessel moves in regular cosine-waves on a course-angle θ relative to the direction of wave propagation. It is assumed that the presence of the vessel does not influence the shape of the wave (which actually is not quite true, see section 1.3.6). Further, an equivalent wave is examined whose height ($2r_d$) has been reduced relatively to that of the real wave, such that hydrostatic pressure conditions in the waves can be used in the calculations.

It is advantageous to use the following coordinate systems:

i) The (ξ,η,ζ) system which is fixed in space with the ξ-axis in the direction of wave propagation and ζ-axis positive vertically downwards. The (ξ,η) plane coincides with the undisturbed water surface.

ii) The (x',y',z') system which is located such that the (x',y') plane coincides with the (ξ,η) plane, but with the z'-axis passing through the center of floatation of the vessel at all times. The x'-axis

is at the CL- of the vessel.

iii) The (x,y,z) system is fixed in the vessel and so oriented that at still water it coincides with the (x',y',z') system.

The form of the wave surface is described in the fixed coordinate system by the equation:

$$h(\xi,\eta) = r_d \cos (k (\xi - ct) - \varepsilon_b) \qquad (1.3.31)$$

where

ε_b = a random phase displacement angle.

It follows from fig. (1.3.15) that at an arbitrary point on the water surface we can set:

$$\xi = \xi_1 + x' \cos\theta - y' \sin\theta \qquad (1.3.32)$$

where

ξ_1 gives the position of the vessel in the ξ-direction

x',y' give the position of the point being examined relative to the vessel.

Substituting now equation (1.3.32) into equation (1.3.31), it is found that the form of the wave surface relative to the vessel can be described by the equation

$$h(x',y') = r_d \cos (k_x x' - k_y y' - (\omega t + \varepsilon)) \qquad (1.3.33)$$

where the following notation is used:

$$\begin{aligned} k_x &= k \cos\theta \\ k_y &= k \sin\theta \\ \omega &= kc \\ \varepsilon &= - k\xi_1 + \varepsilon_b \end{aligned} \qquad (1.3.34)$$

1.3.4 Wave induced loads.

When the vessel is located in waves such as described in the previous section, its position relative to the position in still water may be described by the following quantities:

z'_o = sinkage at original center of floatation.

α = trim angle (positive for increased draft forward).

β = heeling angle (positive for increased draft for positive y).

Relative to the coordinate system (x,y,z) the water surface may now be described by the function (see fig. 1.3.15 and 1.3.16):

$$z_b(x,y) = h(x',y') - (z'_o + \alpha x' + \beta y') = h(x,y) - (z'_o + \alpha x + \beta y) \quad (1.3.35)$$

It is assumed here that the trim angle α and heeling angle β are so small that we can with sufficient accuracy set:

$$\sin\alpha = \alpha \; ; \quad \sin\beta = \beta \; ; \quad \cos\alpha = \cos\beta = 1$$

We may then set $x' = x$ and $y' = y$.

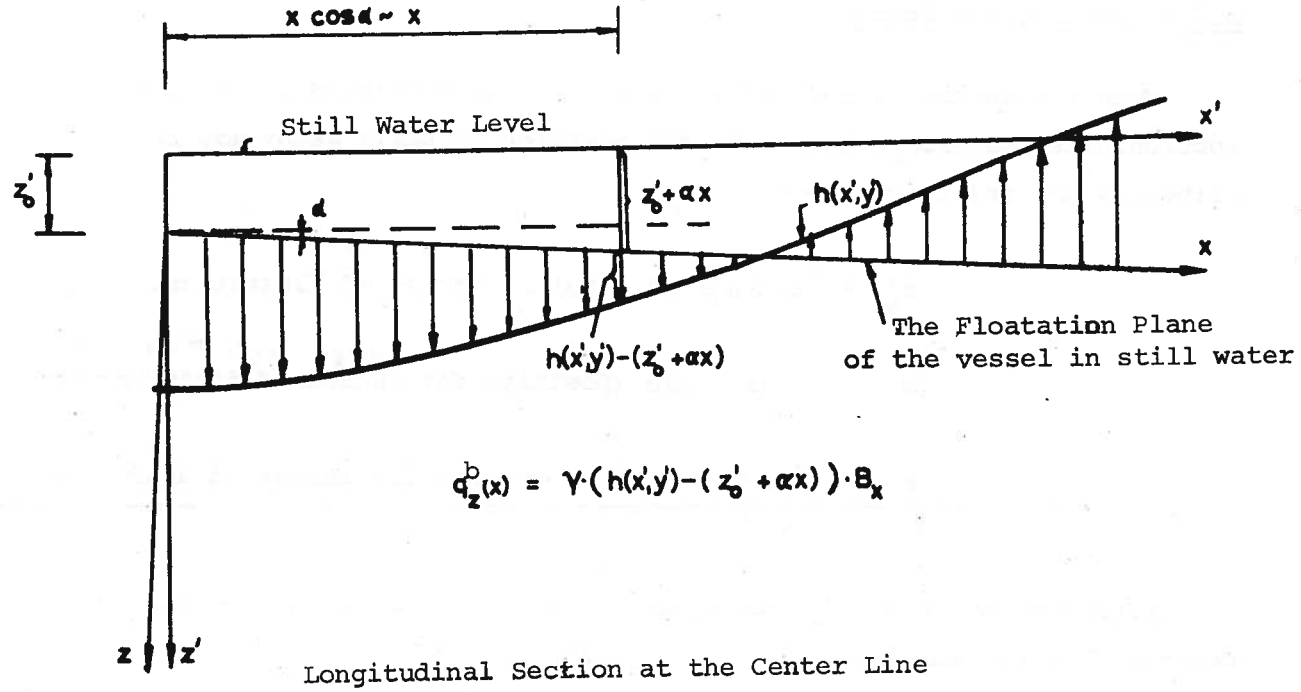

$$q_z^b(x) = \gamma \cdot (h(x',y') - (z_o' + \alpha x)) \cdot B_x$$

Longitudinal Section at the Center Line

Fig. 1.3.16

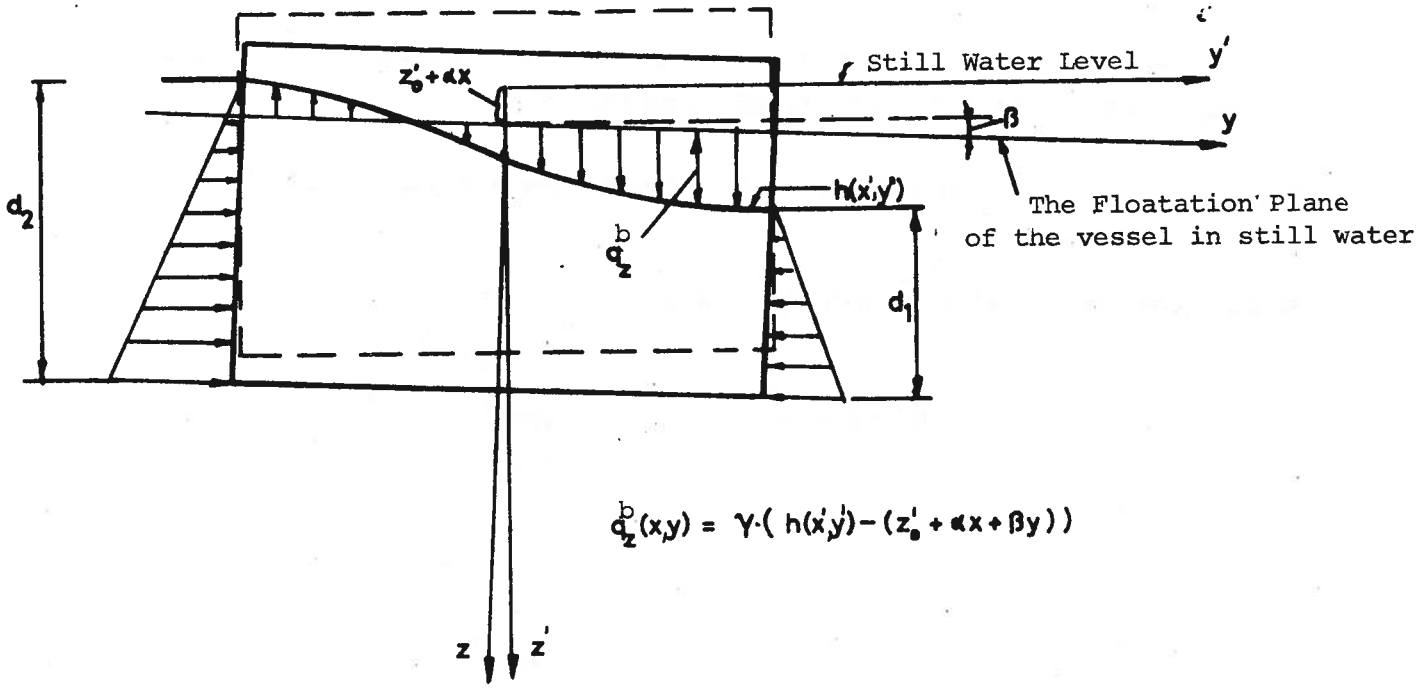

$$q_z^b(x,y) = \gamma \cdot (h(x',y') - (z_o' + \alpha x + \beta y))$$

Section x = constant

Fig. 1.3.17

The wave induced loads consist of:

a) Changes in the buoyancy distribution $q_z^b(x,y)$ calculated per unit area.

b) Changes in the lateral forces on the ship sides.

All together these loads may produce bending moments and shear forces in the center line plane as well as in the lateral plane. Furthermore, they may produce torsion loads.

We have that:

$$q_z^b(x,y) = \gamma \cdot z_b(x,y) = \gamma(h(x,y) - (z_o' + \alpha x + \beta y)) \quad (1.3.36)$$

From fig. 1.3.17 it can be seen that the resulting lateral load per unit length of the hull may be set equal to:

$$q_y(x) = \frac{\gamma}{2}(d_2^2 - d_1^2) \quad (1.3.37)$$

where:

$$d_1 = d - z_b\left(x, \frac{B}{2}\right)$$

$$d_2 = d - z_b\left(x, -\frac{B}{2}\right) \quad (1.3.38)$$

d = draft of the vessel in still water.

The quantities z_o', α and β must be evaluated before the final load-coordinates can be determined. This problem has been discussed earlier. We shall briefly present here a practical method for the approximate estimates of z_o' and α by means of existing diagrams.

If the vessel is kept in the still water position as the wave passes by, a downward force F_z and a pitching-moment F_α will be produced (fig. 1.3.18) which may be estimated by the following expressions:

$$F_z = \iint_{A_{WL}} \gamma h(x,y)\ dxdy$$

$$F_\alpha = \iint_{A_{WL}} \gamma h(x,y) x\ dxdy \qquad (1.3.39)$$

Introducing here the simplification that:

$$h(x,y) = h(x) = r_d \cos\ (k_x x - \varepsilon)$$

we will after some mathematical operations, obtain the following expression, which only applies for vessels with double symmetrical floatation plane.

$$F_z = \gamma \int_L r_d B_x \cos\ (k_x x - \varepsilon) dx = f_z \gamma r_d\ BL \cos\ \varepsilon$$

$$F_\alpha = \gamma \int_L r_d B_x x \cos\ (k_x x - \varepsilon) dx = f_\alpha \gamma r_d\ BL^2 \sin\ \varepsilon \qquad (1.3.40)$$

where

$$f_z = \frac{1}{L} \int_L \frac{B_x}{B} \cos\ k_x x\ dx$$

$$f_\alpha = \frac{1}{L^2} \int_L \frac{B_x}{B} x \sin\ k_x x\ dx \qquad (1.3.41)$$

The extreme values of F_z thus occur when $\varepsilon = i\pi$, $i = 0,1\ ....$, i.e. at wave crest or wave trough at the location of the floatation center. However, the extreme values for F_α are for $\varepsilon = \frac{i\pi}{2}$, $i = 1,3,5,...,$ i.e. at asymmetric wave profile with regard to the y-axis.

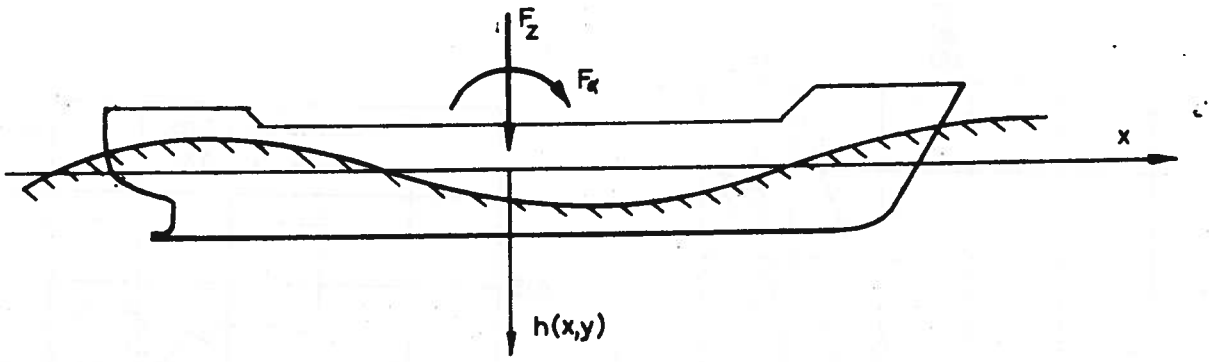

Fig. 1.3.18

The dimensionless parameters f_z and f_α may be determined as functions of the form of the floatation plane, the ratio λ/L and course angle θ. Fig. 1.3.19 a and b shows estimated values for f_z and f_α for various course angles θ. The curves apply only for some special values of the water line coefficient C_{WL} and also actually only when the floatation plane may be described by the function which was used to produce the diagrams, see fig. 1.3.20[1].

When working out the diagrams it is further assumed that the ship has vertical sides and small beam relative to the wave length. Thus the wave profile at the center plane has been used.

---

1) Weinblum & St. Denis: "On the Motions of Ships at Sea". SNAME, Vol. 58, 1950.

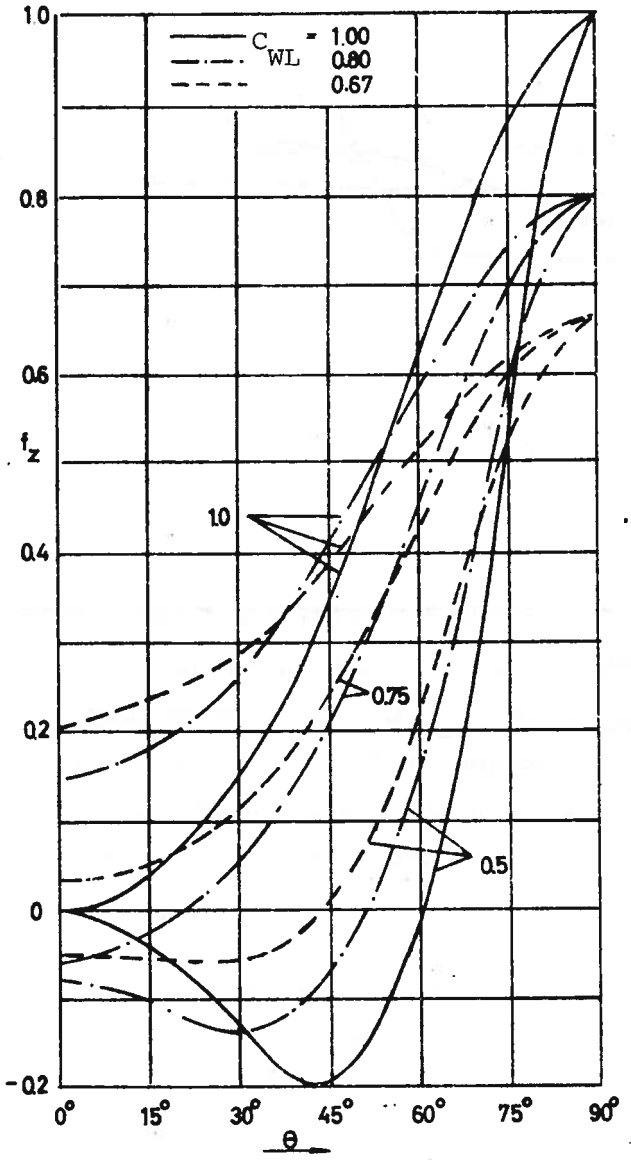

Fig.1.3.19a

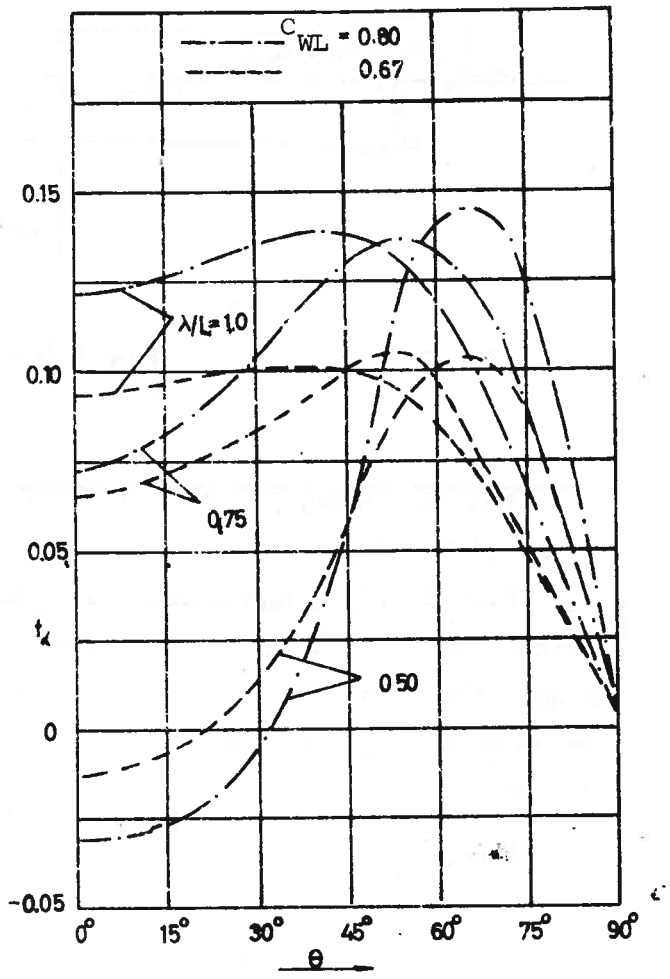

Fig.1.3.19b

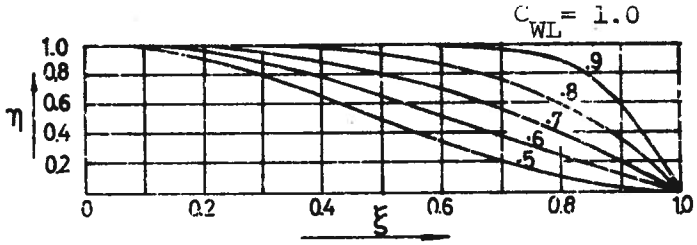

C_{WL}	η
0.50	$1 - 3.0000\,\xi^2 + 2.0000\,\xi^3$
0.60	$1 - 1.5000\,\xi^2 + 0.5000\,\xi^4$
0.70	$1 + 0.5625\,\xi^2 - 0.8750\,\xi^4 + 0.4375\,\xi^6$
0.80	$1 - 1.0000\,\xi^4$
0.90	$1 + 0.9625\,\xi^6 - 2.9250\,\xi^8 + 0.9625\,\xi^{10}$
1.00	1

Fig. 1.3.21 a and b show corresponding values of f_z and f_α for varying ratios of λ/L and C_{WL} for $\theta = 0$[1]. The diagrams apply for vessels of symmetrical floatation plane with regard to transverse axis amidships.

With F_z and F_α determined, we may approximately set:

$$z'_o = \frac{F_z}{\gamma A_{WL}} = \frac{\cos \varepsilon}{C_{WL}} f_z r_d$$

$$\alpha = \frac{F_\alpha}{\gamma I_{WL}} = C_i \sin \varepsilon \, f_\alpha \frac{r_d}{L} \qquad (1.3.42)$$

where

$$C_i = BL^3/I_{WL}$$

The position of the vessel on the wave is thus determined and likewise the quasi-static wave loading. The conditions for heeling have actually been discussed here somewhat superficially. Thus when disregarding heeling, we will have:

$$q_z^b(x) = \gamma r_d B_x \{ \cos (k_x x - \omega t - \varepsilon) - \frac{f_z}{C_{WL}} \cos \varepsilon - \frac{C_i f_\alpha}{L} x \sin \varepsilon \} \qquad (1.3.43)$$

Without loss of generallity one may here set $t = 0$. The vertical wave load may then be estimated for any required combination of λ/L, r_d/L, θ, ε and so forth. ($\varepsilon = 0$ corresponds to a wave trough amidships, $\varepsilon = \pi$ corresponds to wave crest amidships.).

It may be convenient to set:

$$q_z^b(x) = q_{z1}^b \cos \varepsilon + q_{z2}^b \sin \varepsilon \qquad (1.3.44)$$

---

[1] Vossers, G.: "Behaviour of Ships in Waves". ISP, 1962.

which gives:

$$q^b_{z1} = \gamma r_d B_x \left(\cos k_x x - \frac{f_z}{C_{WL}}\right)$$

$$q^b_{z2} = \gamma r_d B_x \left(\sin k_x x - C_i f_\alpha \frac{x}{L}\right) \qquad (1.3.45)$$

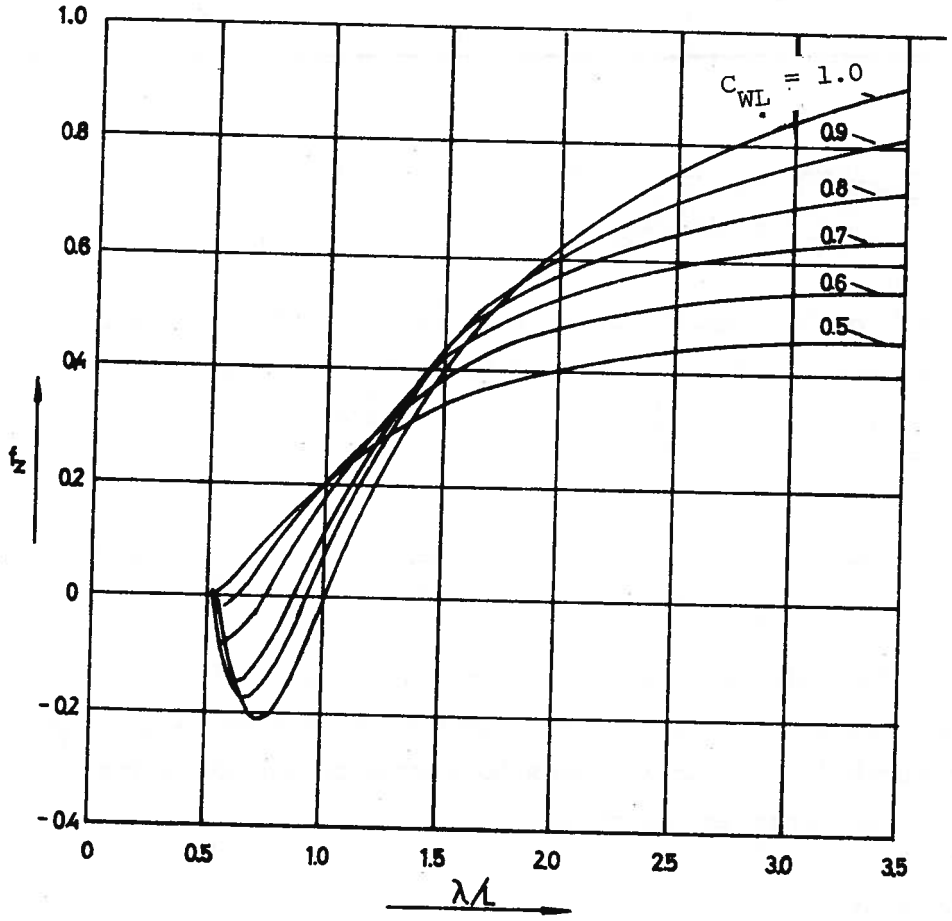

Fig. 1.3.21 a

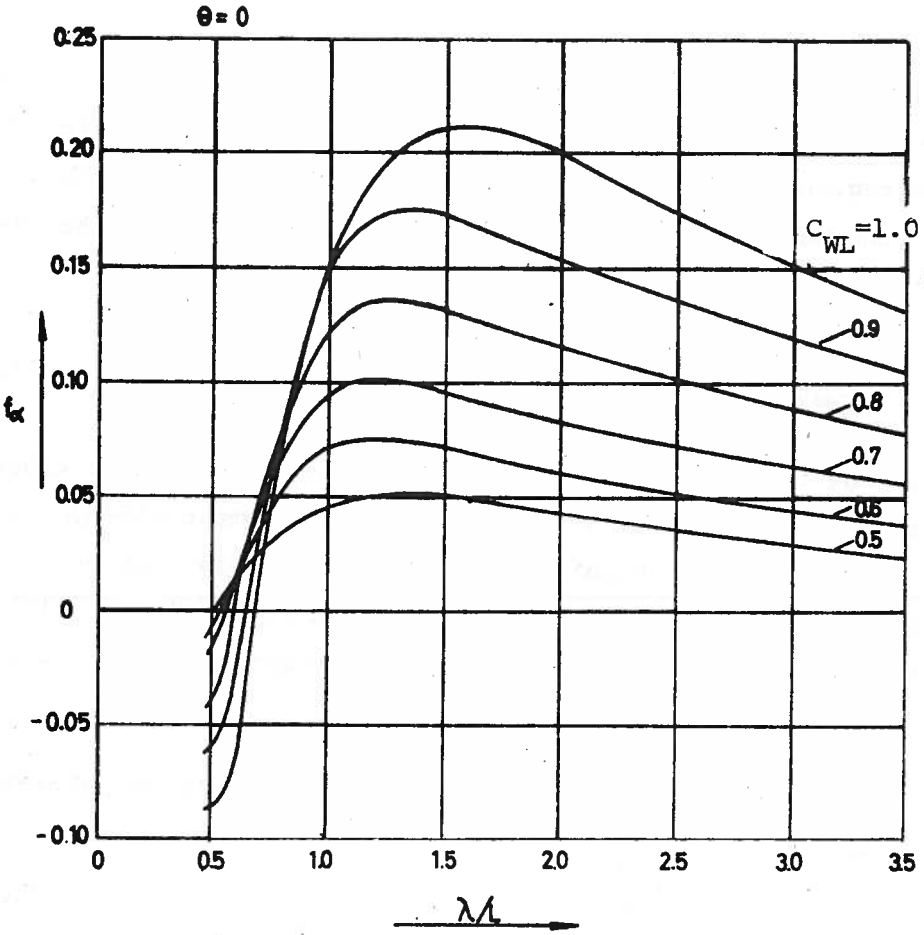

Fig. 1.3.21 b

For a water line plane symmetric with respect to the y-axis, q^b_{z1} is a symmetric function, whereas q^b_{z2} is asymmetric.

Letting $\varepsilon = 0$ or $\varepsilon = \pi$ in equation (1.3.44), the last expression on the right hand side disappears. It follows that:

$$\{q^b_z(x)\}_{\varepsilon=\pi} = -\{q^b_z(x)\}_{\varepsilon=0} \qquad (1.3.46)$$

1.3.5 Wave induced moments and shear forces.

1.3.5.1 Vertical loads.

Wave induced moments and shear forces in the center plane determined by the classical method is calculated, as mentioned earlier, for the vessel

located on a regular wave of length equal to the length of the ship and with a wave crest ($\varepsilon=\pi$) or wave trough ($\varepsilon=0$) amidships. For vessels with vertical sides in the region between the two floatation planes corresponding to the locations of the wave profile ($|z| < |z_w|$) it will be found that (see equation 1.3.46):

$$M_{wy}^{\varepsilon=\pi} = - M_{wy}^{\varepsilon=0} \tag{1.3.47}$$

for any section along the hull girder. Here M_{wy} denotes the wave induced bending moment in the CL-plane. Thus the hogging wave moment midships for $\varepsilon=0$ is numerically of the same magnitude as the sagging wave moment for $\varepsilon=\pi$ when the vessel is moving in cosine-waves. Furthermore it can with sufficient accuracy be assumed that maximum bending moment midships occur when $\lambda \sim L$.

It will be useful to introduce the following non-dimensional parameter:

$$\mu_z = \frac{\overline{M}_{wy}}{\gamma \, r_d \, BL^2} \tag{1.3.48}$$

where $\overline{M}_{wy}$ indicates the wave bending moment amidships. This quantity will then depend on the shape of the floatation plane, the ratio L/λ, and the location of the wave relative to the vessel expressed by ε.

In fig. 1.3.22 is shown the relationships between μ_z and the non-dimensional parameters L/λ and C_{WL} [1]. The curves are determined for vessels with vertical sides in the region near the water line ($|z'| < |z_w|$) and with equations for the floatation planes as given in fig. 1.3.20. The same data are presented in fig. 1.3.23 as functions of C_{WL}. It can be seen here that the bending moment midships is near maximum when $\lambda = L$, but somewhat higher at $\lambda = 1.25\ L$ for normal values of C_{WL}. All curves give the extreme values for μ_z ($\varepsilon = 0$ and $\varepsilon = \pi$).

---

1) Swaan, W.A.: "Amidship bending moments for ships in waves". ISP, Vol. 6, pp. 389-408, 1959.

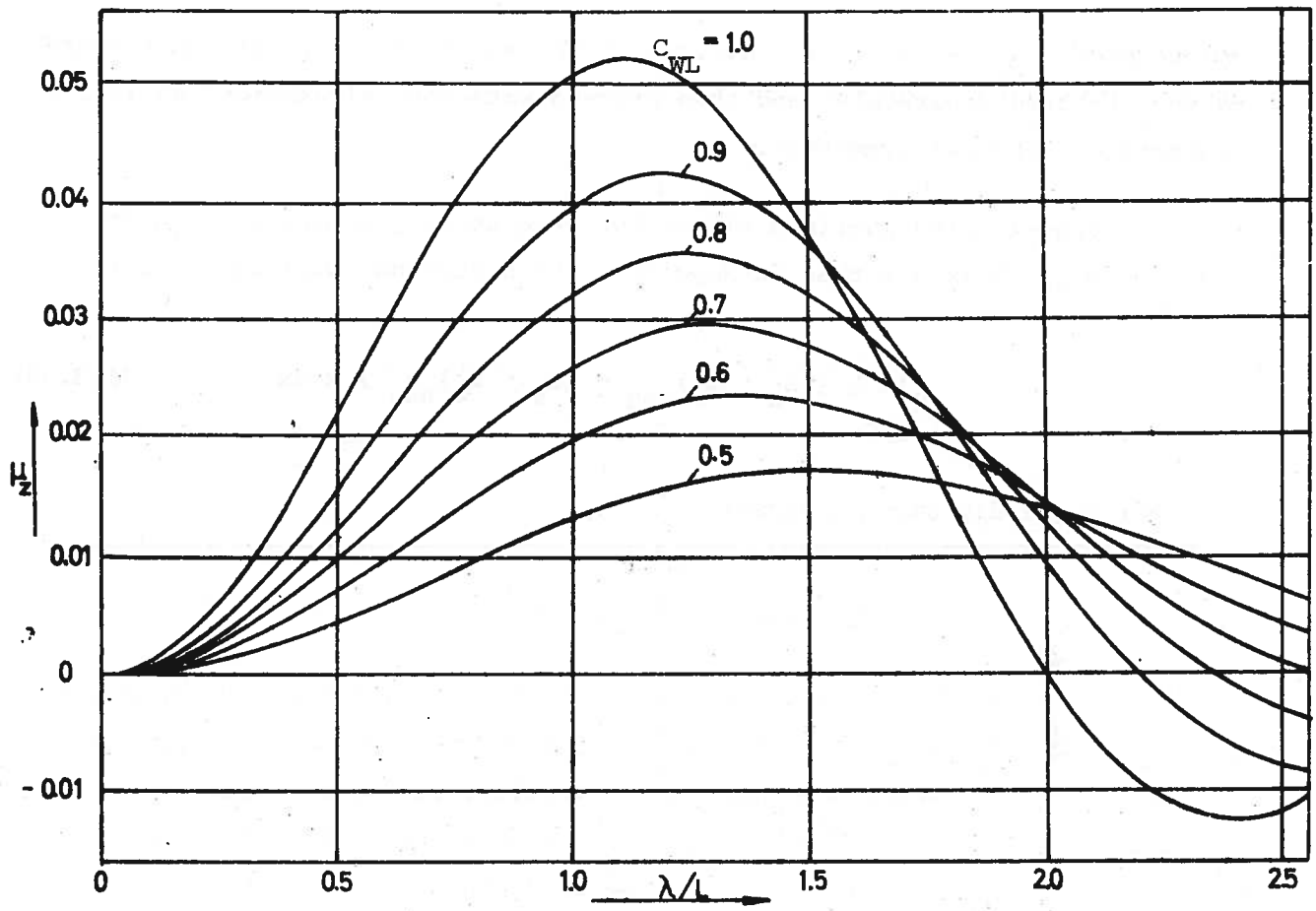

Fig . 1.3.22

From formula (1.3.48) and figure 1.3.23 we note that the wave bending moment in regular quasistatic waves with good approximation can be said to be:

a) Proportional to C_{WL}

b) Proportional to the wave height ($2r_d$).

For unsymmetrical floatation plane, Swaan has shown that good approximation is obtained

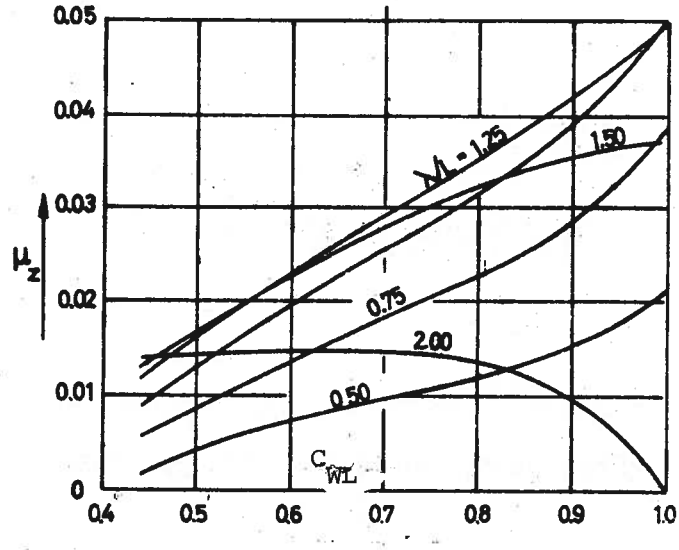

Fig. 1.3.23

by assuming C_{WL} equal to the average of the values for the aft and forward halves, treated separately, and then proceed with the calculations as if the floatation plane was symmetric.

For vessels with inclined sides, the wave bending moment in sagging will normally be larger than in hogging. The difference will be equal to:

$$\int_{-L/2}^{o} \gamma \{(B_x \cdot z_w)_{sag} + (B_x \cdot z_w)_{hog}\} x \, dx \qquad (1.3.49)$$

For outwardly sloping sides:

$$| (B_x z_w)_{sag} | > | (B_x z_w)_{hog} |$$

towards the ends of the ship. The values in these regions are decisive for the magnitude of the moment. Murray[1] did find it convenient to assume that the deviation from moments estimated for vertical sides, is a function of the relation $C_{WL}^{crest} / C_{WL}^{trough}$. C_{WL}^{crest} denotes here the water line coefficient estimated for a plane at the level of the wave crest in hogging. Correspondingly, C_{WL}^{trough} is the water line coefficient for a plane at the level of the wave trough in sagging. Fig. 1.3.24 shows approximately the increase of sagging wave moment (reduction of hogging wave moment) as a function of the relationship defined above.

---

1) Murray, J.M.: "Longitudinal Bending Moments". IESS, Vol. 90, pp. 365-407, 1946/47.

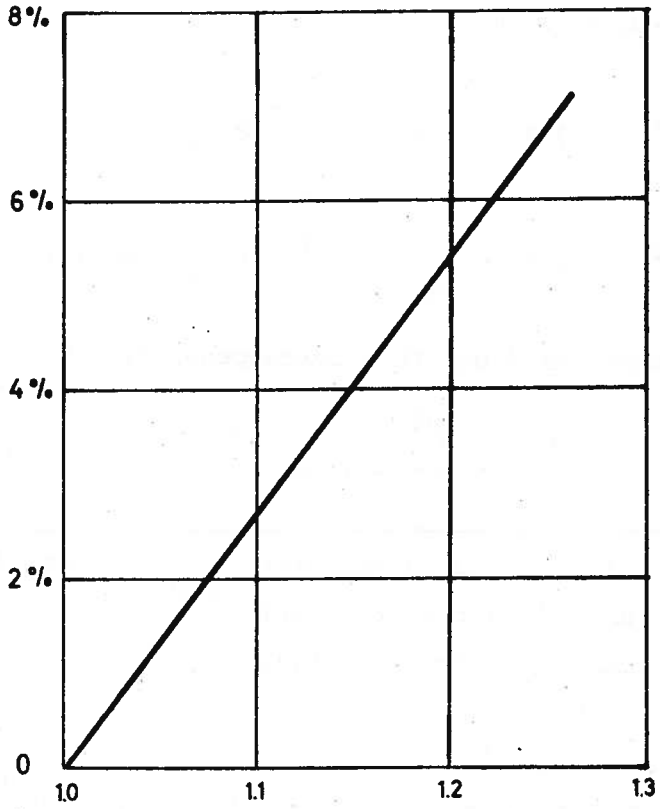

Fig. 1.3.24

Det Norske Veritas' 1964 rules take into consideration the wave bending moments. For dry cargo ships, for instance, the following rule-requirements to the section modulus amidships (Z) apply:

$$Z_{hog} \geq \frac{\bar{M}_{sy}^{hog} + \bar{M}_{wy}^{hog}}{\sigma} = \frac{\bar{M}_{sy}^{hog}}{\sigma} + 0.92L^{2.3}\, B(C_B + 0.7) \quad (cm^3)$$

$$Z_{sag} \geq \frac{\bar{M}_{sy}^{sag} + \bar{M}_{wy}^{sag}}{\sigma} = \frac{\bar{M}_{sy}^{sag}}{\sigma} + 1.02L^{2.3}\, B(C_B + 0.7) \quad (cm^3)$$

where moments and section modulii refer to the section amidships.

Thus it has been assumed that:

$$\bar{M}_{wy}^{hog} = 0.92 \cdot \sigma \cdot L^{2.3} B(C_B + 0.7) \cdot \text{(tons cm.)}^{**}$$

$$\bar{M}_{wy}^{sag} = 1.02 \cdot \sigma \cdot L^{2.3} B(C_B + 0.7) \cdot \text{(tons cm.)}$$

For a vessel with vertical sides this corresponds to:

$$\bar{M}_{wy} = \frac{\bar{M}_{wy}^{hog} + \bar{M}_{wy}^{sag}}{2} = 0.97 \cdot \sigma \cdot L^{2.3} B(C_B + 0.7) \text{(tons cm)}$$

This formula may be interpreted as follows: the wave amplitude reduced for the Smith-effect is made equal to: $r_d = 0.7\, L^{0.3}$. Allowable bending stresses in the hull is made equal to: $\sigma = 1430$ kp/cm^2 $= 1.43 \cdot 10^4$ t/m^2. Thus we find that:

$$\mu_z = \frac{\bar{M}_{wy}}{\gamma \cdot r_d BL^2} = 1.93\ (C_B + 0.7) \cdot 10^{-2}$$

Note that μ_z is here made a function of the block coefficient C_B, whereas it was found earlier that μ_z is a function of C_{WL}.

How is then the agreement between moments and shear forces calculated by the quasistatic method, and measurements taken from model tests in regular waves? The answer must unfortunately be somewhat ambiguous. Even when the reduced effective wave height, due to the hydrodynamic pressure distribution -(the Smith effect)-, is accounted for, will the calculations most frequently indicate larger moments than those found in tests. This also applies to the stationary vessel. Fig. 1.3.25 shows this phenomenon[1]. It can also be seen that the measured moments also depend upon the speed of the vessel, a parameter which we did not include in our discussion.

---

[1] Jacobs, W.R. and Maday, A.: "Comparison of Experimentally Measured and Theoretically Estimated Bending Moments of Three Tanker Models in Regular Head Seas". Davidson Laboratory, Rep. 774 1959. (Stevens Institute of Technology).

** L and B are here given in meters.

a.

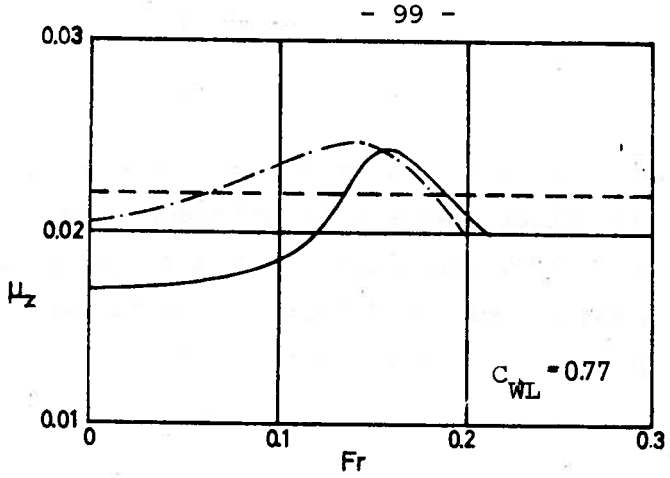

b.

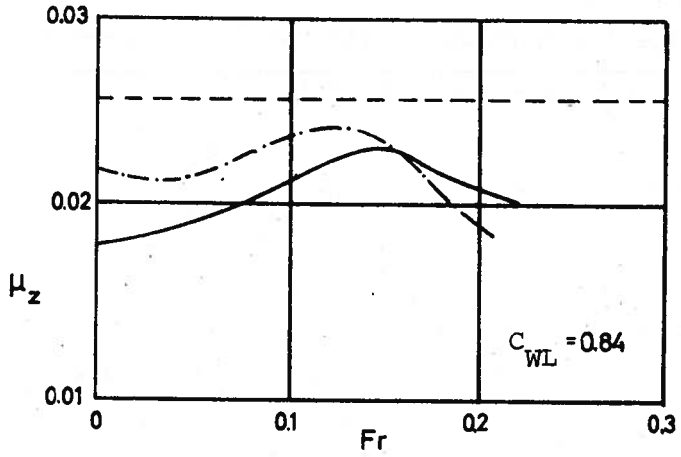

c.

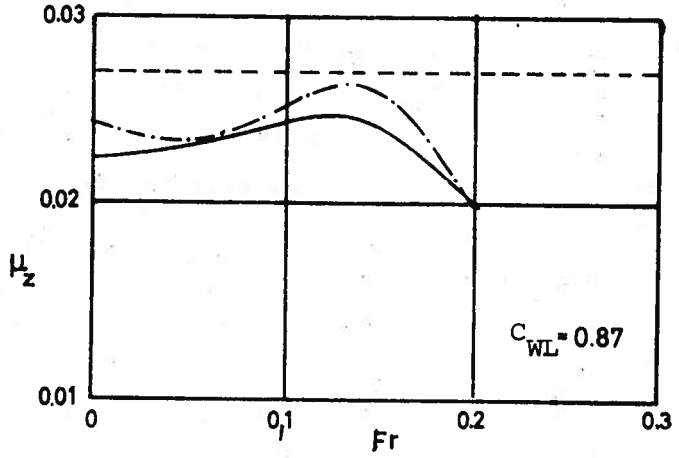

------- Quasi-static analysis, including the Smith effect.

– – – – Dynamic analysis

———— Model tests

Fig. 1.3.25

The primary reason for these discrepancies is that when calculating the moments the inertia forces, which always will be present when the vessel moves in waves, have been totally disregarded. In the next section it will be shown how the loading may be corrected for this condition. The derivations presented above represent a useful starting point.

1.3.5.2 Lateral Loads.

A vessel, close to being upright, is exposed to a lateral load at quasi-static condition and heading θ in regular waves. Fig. 1.3.26 shows measured lateral moments amidships for various heading angles θ and wave lengths (λ/L). The moments are given non-dimensionally by:

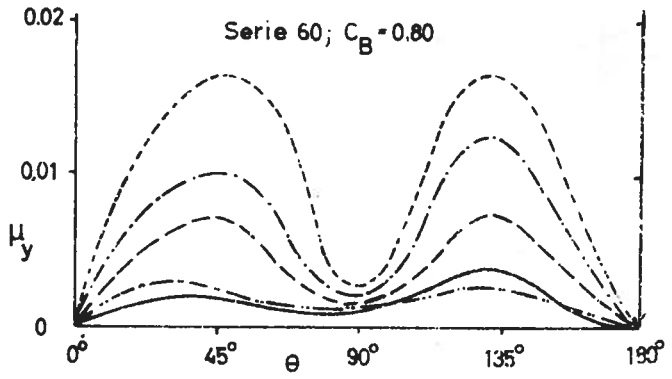

Lateral wave bending moment

Fig.1.3.26

$$\mu_y = \frac{M_{oz}}{\gamma r\, BL^2} \qquad (1.3.50)$$

For wave lengths equal to 0.9 L and 0.6 L the maximum moments in both planes are almost equally large ($\theta = \pi/4$ and $3\pi/4$). If they are in phase at the same time, then the vessel will experience a larger load than the maximum moment in the vertical plane resulting from a wave of length $\lambda/L \simeq 1.2$. Ordinarily, these loads will not be in phase.

1.3.5.3 Torsion.

Torsion moments acting on the hull may be assumed to arise partly because of oblique loading in still water, partly because of waves when the heading angle of the vessel (θ) is different from 0 and π relative to the direction

of wave propagation. Researchers who have determined the magnitude of wave induced torsion moments generally agree they are relatively small. For normal ship types the stresses due to torsion are therefore not assumed to be of any great significance. The situation may be somewhat different for vessel with extremely large or numerous hatch openings.

The torsion moment amidships ($\bar{M}_t$) is usually expressed by non-dimensional parameters such as:

$$\mu_t = \frac{\bar{M}_t}{\gamma \, rB \, L^2} \tag{1.3.51}$$

or

$$C_t = \frac{\bar{M}_t}{\gamma \, B^3 L} \tag{1.3.52}$$

Table 1.3.3 presents some values of C_t [1] taken from the literature dealing with the subject of torsion of ships. As can be seen, the spread in the suggested values is quite large. The torsion moments should be assumed to increase with increasing fullness of the water plane. This is illustrated in fig. 1.3.27 [2].

Fig. 1.3.28 is interesting because it shows the relative magnitudes of vertical and lateral bending moments plus torsion moments measured from model test [3] at a heading angle $\theta = 120°$.

---

1) Abrahamsen, E.: "Torsion of Ships". ISSC, Glasgow 1961.

2) Abrahamsen, E.: "The Strength of Dry Cargo Ships". Det Norske Veritas, Meddelelse nr. 7, 1958.

3) Numata: "Longitudinal Bending and Torsional Moments Acting on a Ship Model at Oblique Headings to Waves". Journal of Ship Research, April. 1963.

Table 1.3.3 Wave induced torsion moments

Author	Year	C_{WL}	H	θ	$C_t \cdot 10^3$	Remark
Vedeler	1924	0,8	λ/20	45°	2,39	
					3,26	incl. dyn. effect
Inokuty	1929		λ/20 ?	45°	3,34	
Davydov	1955	0,8	$\lambda/9=(\lambda/30+2)^n$	70°	5,80	L = 75,0 m
Abrahamsen	1958	0,6			1,80	
		0,7	λ/10	≈ arctg L/B	2,42	
		0,8			3,80	
		0,9			5,33	
Webster	1959	0,6			2,04	
		0,7	$1,1\sqrt{\lambda}$	60°=70°	2,82	B = 70'
		0,8			3,80	
		0,9			5,00	

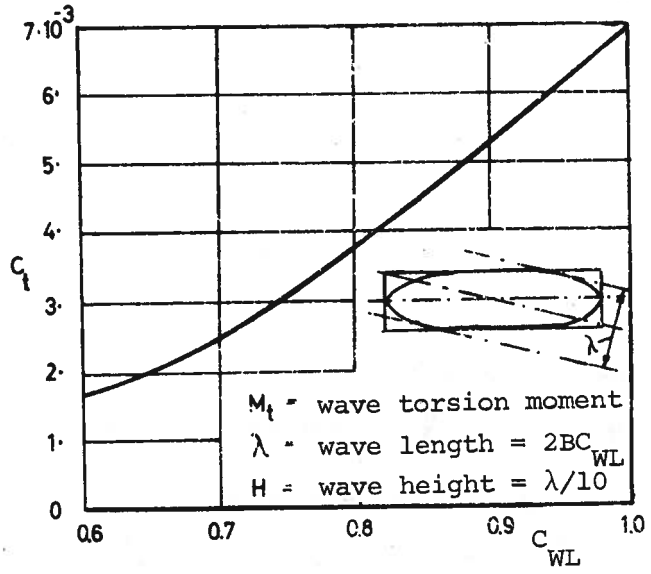

Fig. 1.3.27

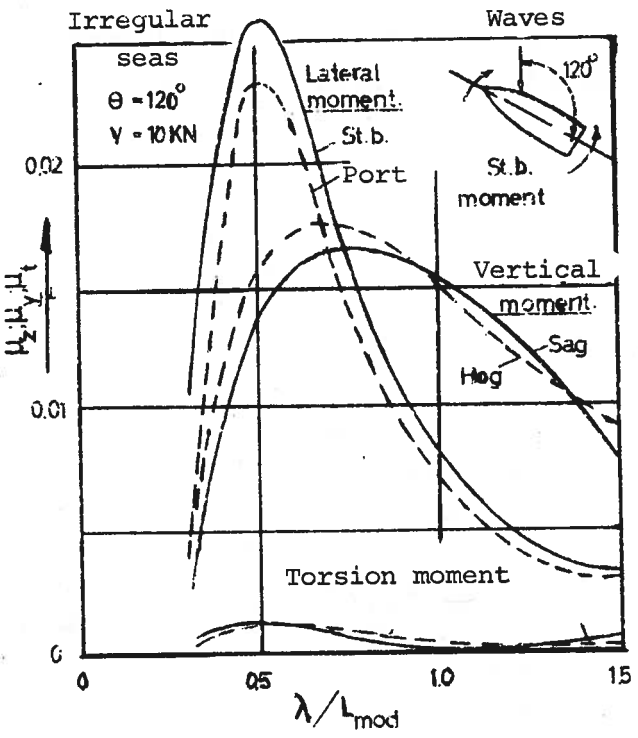

Fig. 1.3.28

1.3.6 Waves created by the ship when operating in still water.

A ship proceeding at a velocity V m/s in still water, creates pressure and velocity fields. At the very moment the vessel starts to move, a pressure increase $+\Delta p$ occurs at the bow and stern and a pressure drop $-\Delta p$ similarly occurs amidships. The water surface along the vessel assumes then a wave shape determined by the Bernoulli pressure equation. This Bernoulli-wave travels with the vessel without any change in shape (at constant speed). The pressure disturvances which this advancing pressure field transfer to the surrounding media are the source of the travelling waves, Velox-waves[x], see fig. 1.3.29.

The Bernoulli-wave produces trim and parallel sinkage with corresponding change in the load distribution, the Velox-wave produces ordinary wave loading. The waves are gravitational waves.

We can approximately set:

$$h_x = \text{constant} \quad \frac{V^2}{2g} = \text{constant } (Fr)^2 \qquad (1.3.53)$$

where

h_x = the wave height

Fr = Froude number

Bending moments and shear forces then become functions of Fr . The non-dimensional coefficient μ_s^v for the additional moment amidships caused by the speed when moving in still water:

$$\mu_s^v = \frac{\overline{M}_s^v}{\gamma B L^3} \qquad (1.3.54)$$

has been determined by model tests at NSMB, Holland[1], see fig. 1.3.30.

---

x) The waves are roughly approximated here. See Saunders: "Hydrodynamics in Ship Design". Vol. I, II, 1957.

1) Vossers, G. et. al.: "Vertical and Lateral Bending Moment Measurements on Series 60 Models". ISP, Vol. 8, No. 83, July 1961.

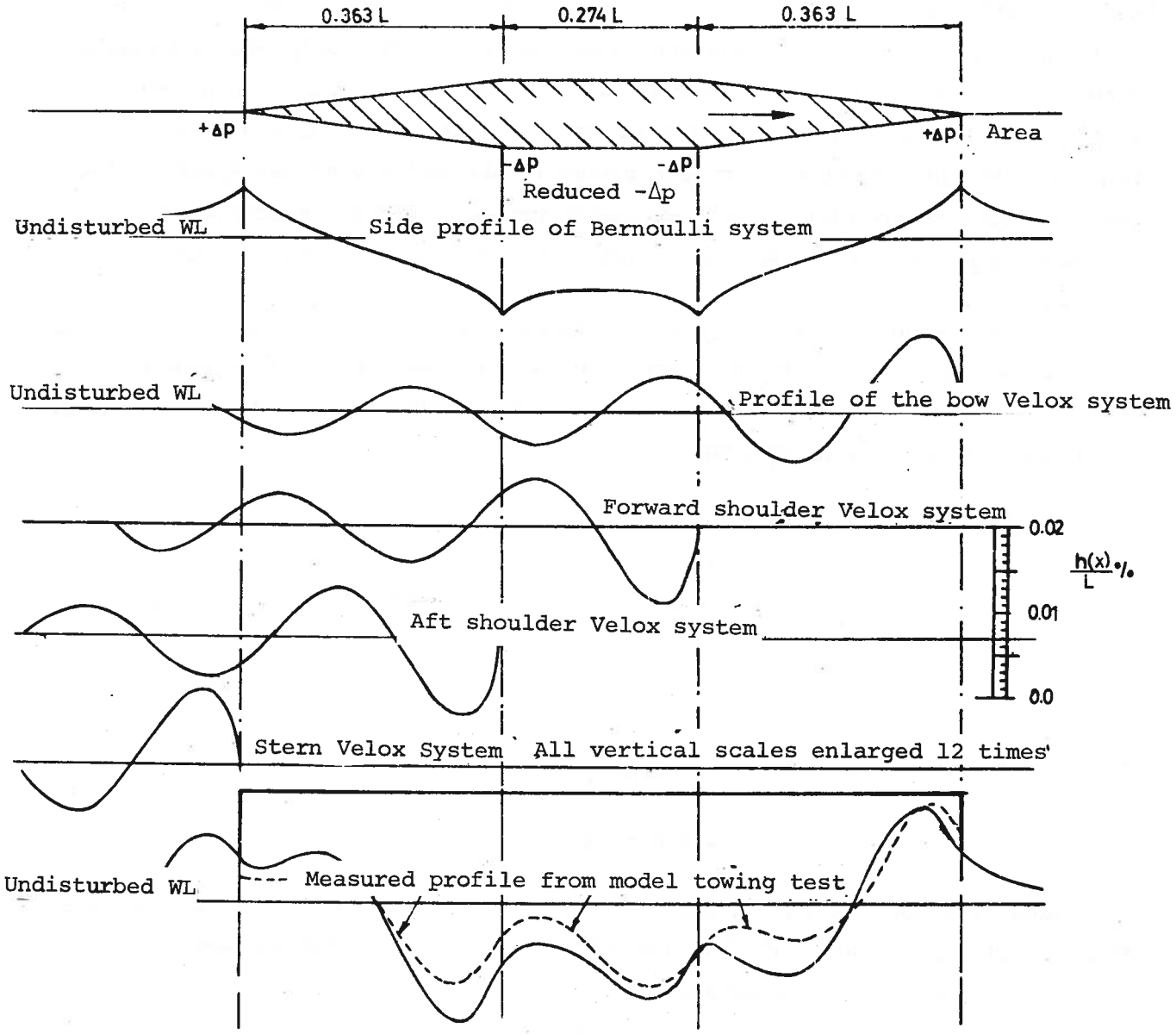

Estimated profile equal to the algebraic coordinate sum of five Bernoulli - and Velox - components

Fig. 1.3.29 (from Saunders)

It appears that μ_s^v depends upon C_B and Fr , but is almost independent of the L/d and L/B ratios. The total bending moment in motion in still water becomes $M_s + M_s^v$.

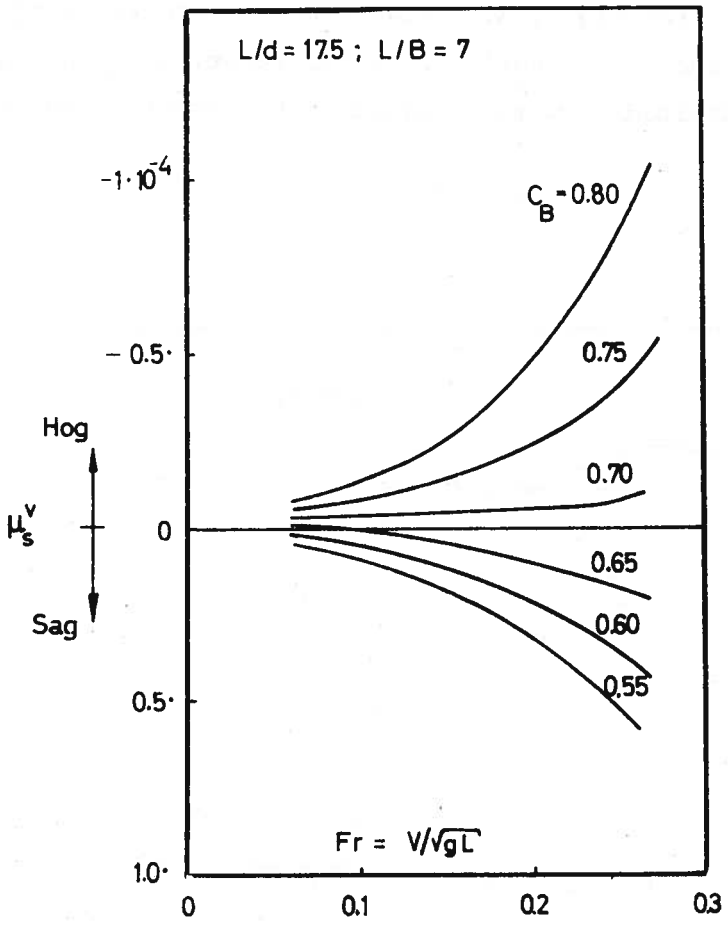

Fig. 1.3.30

Example 1.3.2

In Saunder's "Hydrodynamic Design", pp. 247, is shown the wave contours along the ship side for Fr = 0.253 for series 57, Model 4202 W-1 (further described in SNAME, 1951, pp. 642-691). With this wave as starting point, fig. 1.3.31 gives the loading, shear force, and bending moment curves. The

midship bending moment is approximately 5 times larger than corresponding values found from fig. 1.3.30, which apply to series 60 hulls. Some of the difference is likely caused by not taking into consideration the Smith-effect in the estimates, but relatively speaking the disagreement is still large. It can, however, be seen from fig. 1.3.31 that the absolute value of the moment midships is very small. In motion in still water, the bending moment peak will usually be distorted forward relative to the static condition, see fig. 1.3.31.

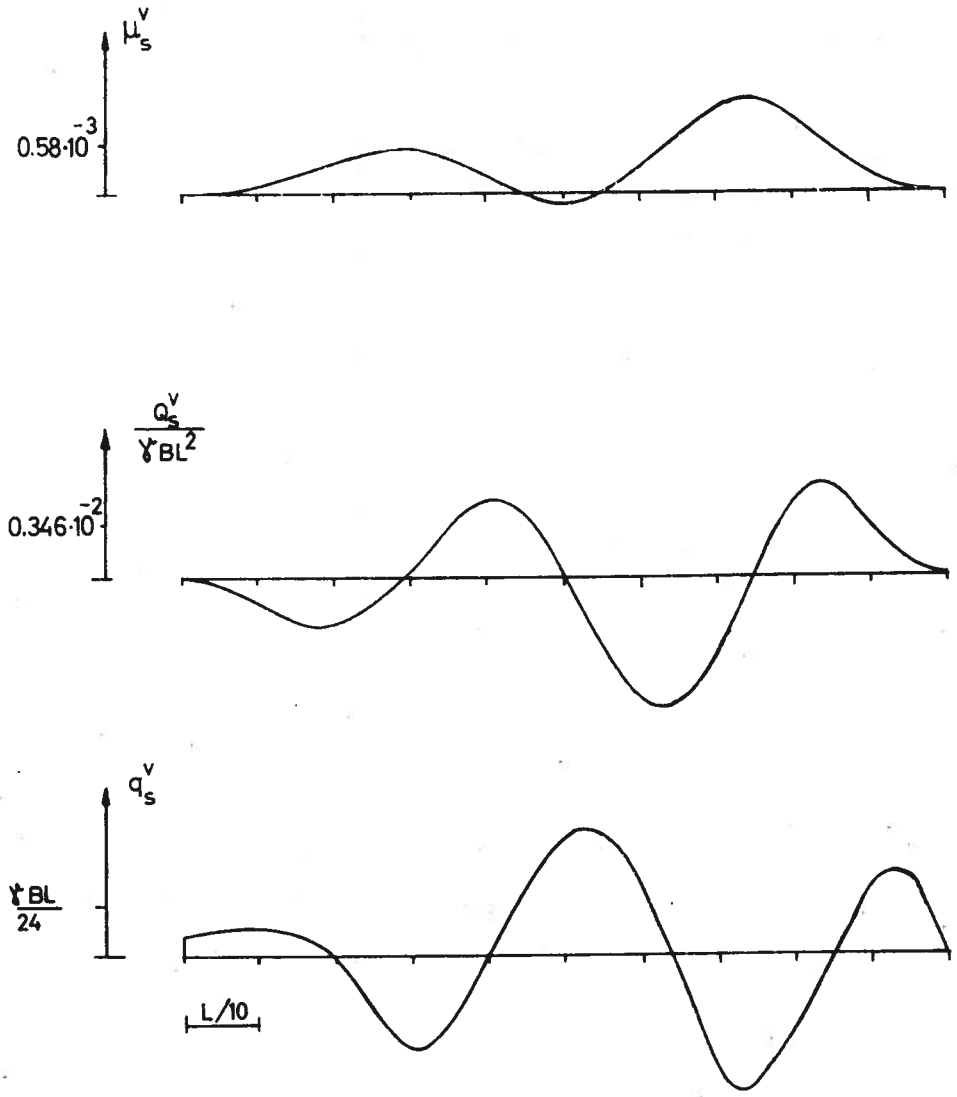

Fig. 1.3.31

1.4 Dynamic loading in regular waves.

1.4.1 Introduction

In this chapter the discussion will be limited to analyzing the ship at zero speed on a heading parallel to the direction of wave propagation. Also it will be assumed that the vessel moves as a system with two degrees of freedom, i.e., coupled heaving and pitching motions. It is also assumed that the vessel has vertical ship sides in the region between upper and lower floatation planes during the motions.

The vessel is responding to the impulses that are supplied by regular waves of the form:

$$\begin{aligned} h(x) &= r_d \cos(kx - \omega t) \\ &= r_d (\cos kx \cos \omega t + \sin kx \sin \omega t) \end{aligned} \tag{1.4.1}$$

where x as before is measured positive forward from the floatation center in the vessel. The resulting motion is harmonic.

A hydrostatic pressure distribution in the wave is assumed and the reduced wave amplitude r_d is therefore introduced. The oscillating motions and the consequential dynamic forces are required.

In the following treatment of the problem the general theory of harmonic oscillations is assumed known.

1.4.2 Loads.

The wave induced impulses bring the vessel to perform forced oscillations of frequency equal to the frequency of wave encounter, but normally with a certain phase difference between impulse and oscillation. We may therefore write:

$$\begin{aligned} \zeta_o &= \zeta_1 \cos \omega t + \zeta_2 \sin \omega t \\ \alpha &= \alpha_1 \cos \omega t + \alpha_2 \sin \omega t \end{aligned} \tag{1.4.2}$$

where

ζ_o = the heaving motion of the center of gravity of the vessel,

α = the pitching motion in the center plane.

(Alternatively the motions may be expressed by equations (1.4.10), where the relationships between ε_ζ, ζ_∞, ζ_1, ζ_2, etc. are given by equations (1.4.11)).

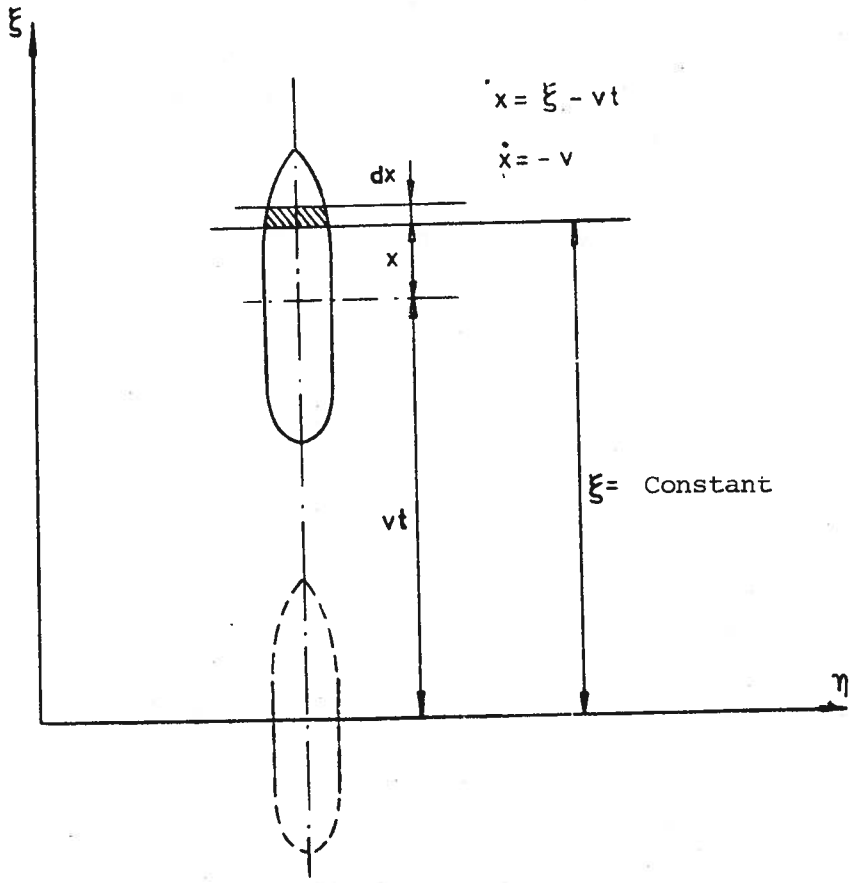

Fig. 1.4.1

The quantities ζ_1, ζ_2, α_1, and α_2 are regarded, for the time being, as known. It will appear from the next section how these may be determined.

Considering now two vertical sections perpendicular to the center line of the ship located at distances x and x + dx from the center of floatation,

respectively, an expression for the wave induced loads on that part of the hull located between these two sections will be derived, taking into consideration the dynamic forces.

According to eqn. (1.3.35) the location of the floatation plane for the ship in a wave, relative to the water line plane at static equilibrium in still water, will be given by the expression ($\beta = 0$):

$$z = -(\zeta_o + \alpha x - h(x)) \tag{1.4.3}$$

The relative speed ($\dot{z}$) and acceleration ($\ddot{z}$) of the hull section relative to the liquid is given by the expressions

$$\begin{aligned} \dot{z} &= -(\dot{\zeta}_o + \dot{\alpha} x - \dot{h}(x)) \\ \ddot{z} &= -(\ddot{\zeta}_o + \ddot{\alpha} x - \ddot{h}(x)) \end{aligned} \tag{1.4.4}$$

where the speed of the vessel $v = -\dot{x} = 0$ (see fig. 1.4.1).

The absolute velocity and acceleration of the hull section are respectively

$$\dot{\zeta}_o + \dot{\alpha} x$$

and

$$\ddot{\zeta}_o + \ddot{\alpha} x \tag{1.4.5}$$

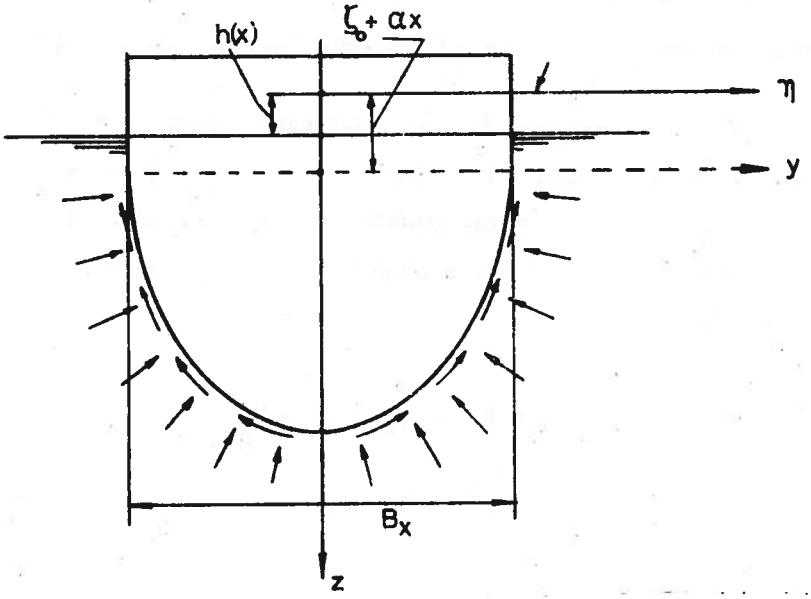

When the hull section in fig. 1.4.2 moves relative to the surrounding liquid, the following two types of forces between hull and liquid are present in addition to the hydrostatic pressure (including the Smith-effect).

a) An additional pressure which is used to accelerate the fluid between the two planes at x and $x + dx$.
This pressure is assumed to be proportional to the acceleration of the hull and is directed 180° out of phase with respect to the acceleration similar to the inertia forces that arise from the mass of the ship. In section 1.4.6 it is shown that it is convenient to replace this pressure from the surrounding liquid with an assumed hydrodynamic mass which oscillates with the vessel. The quantity of the mass is adjusted such that it exerts the same effect on the hull as the acceleration pressure. The hydrodynamic mass for the hull section of unit length will be denoted m_{zh} for vertical oscillations. The hydrodynamic mass is a function of hull shape and frequency, see section 1.4.6.

b) A damping force assumed to be produced by friction between hull, fluid and waves generated by the motion. The friction in a viscous liquid is normally assumed to be proportional to the relative velocity between the oscillating body and the fluid. The damping force on the hull section for vertical oscillations are set equal to:

$$\dot{z}\, N_z(x)\, dx$$

The magnitude of $N_z(x)$ is discussed further in section 1.4.5.

Table 1.4.1 gives expressions for all <u>dynamic</u> loads acting on the hull section, including here the total effect of the waves. Introducing the expressions for $h(x)$, ζ_o, and α from equations (1.4.1) and (1.4.2) we now sum all the loading expressions. The dynamic load $\tilde{q}_z$ may after a few operations be written in the form:

$$\tilde{q}_z = q_{z1} \cos \omega t + q_{z2} \sin \omega t \qquad (1.4.6)$$

Table 1.4.1 Dynamic forces on the hull section.

TYPE	FORMULA
Quasistatic buoyancy	$-\gamma B_x \{\zeta_o + \alpha x - h(x)\}\, dx$
Mass inertia force (vessel)	$-\{\ddot{\zeta}_o + \ddot{\alpha} x\}\, m\, dx$
Mass inertia force (fluid)	$-\{\ddot{\zeta}_o + \ddot{\alpha} x - \ddot{h}(x)\}\, m_{zh}\, dx$
Damping force	$-\{\dot{\zeta}_o + \dot{\alpha} x - \dot{h}(x)\}\, N_z(x)\, dx$

$m\, dx$ = mass of the vessel section

where

$$q_{z1} = \{\omega^2 (m + m_{zh}) - \gamma B_x\}\zeta_1 - \omega N_z(x)\,\zeta_2 + \{\omega^2 (m + m_{zh}) - \gamma B_x\} x_{\alpha 1} - \omega N_z(x) \cdot x_{\alpha 2} - \{\omega^2 m_{zh} - \gamma B_x\} r_d \cos kx + \omega N_z(x)\, r_d \sin kx \qquad (1.4.7)$$

$$q_{z2} = \{\omega^2 (m + m_{zh}) - \gamma B_x\}\zeta_2 + \omega N_z(x)\,\zeta_1 + \{\omega^2 (m + m_{zh}) - \gamma B_x\} x_{\alpha 2} + \omega N_z(x)\, x_{\alpha 1} - \omega N_z(x)\, r_d \cos kx - \{\omega^2 m_{zh} - \gamma B_x\} r_d \sin kx$$

In principle, the problem is now solved provided ζ_1, ζ_2, and α_1, and α_2 are known. Moments and shear forces are found in the usual manner by integrating the loading function (1.4.6) once and twice respectively. This will be repeated in section 1.4.8. We shall first show, however, how ζ_1, ζ_2, and α_1 and α_2 may be found.

1.4.3 Determination of the motions

The forces and moments that act on the vessel must be in equilibrium at any time, such that:

$$\int_L \tilde{q}_z dx = \int_L \{q_{z1} \cos \omega t + q_{z2} \sin \omega t\} dx = 0$$
$$\int_L \tilde{q}_z x dx = \int_L \{q_{z1} \cos \omega t + q_{z2} \sin \omega t\} x dx = 0 \qquad (1.4.8)$$

Furthermore, since the equations (1.4.8) must be satisfied at all times,

$$\int_L q_{z1} dx = \int_L q_{z2} dx = 0$$
$$\int_L q_{z1} x dx = \int_L q_{z2} x dx = 0 \qquad (1.4.9)$$

After substituting the expressions (1.4.7), these equations give a linear system of equations where the four coefficients ζ_1, ζ_2, α_1, and α_2 can be determined. Table 1.4.2 gives the equations for the general case, as well as for two special cases. Table 1.4.3 gives a survey of the physical significance and definitions of a number of notations that are used.

In table 1.4.2 it appears that heave and pitch motions in the general case are coupled - all four quantities ζ_1, ζ_2, α_1, and α_2 must be determined at the same time by solving four linear equations. For vessels symmetric with respect to the cross-section at $x = 0$, the system of equations in table 1.4.2 is reduced to two independent set of equations, each with two unknowns. Then the heave and pitch motions may be determined separately, and the motions are said to be uncoupled.

It may be convenient to write the formulas (1.4.2) in the following form:

$$\zeta_o = \zeta_{oo} \cos (\omega t - \varepsilon_\zeta)$$
$$\alpha = \alpha_o \cos (\omega t - \varepsilon_\alpha) \qquad (1.4.10)$$

Here, the following relations apply:

$$\zeta_{oo} = \sqrt{\zeta_1^2 + \zeta_2^2} \quad , \quad \text{tg } \varepsilon_\zeta = \frac{\zeta_2}{\zeta_1}$$

$$\alpha_o = \sqrt{\alpha_1^2 + \alpha_2^2} \quad , \quad \text{tg } \varepsilon_\alpha = \frac{\alpha_2}{\alpha_1} \qquad (1.4.11)$$

Fig. 1.4.3 shows schematically how heave and pitch motions are phased relative to the wave crest midships. The whole vector group rotates with an angular velocity ω .

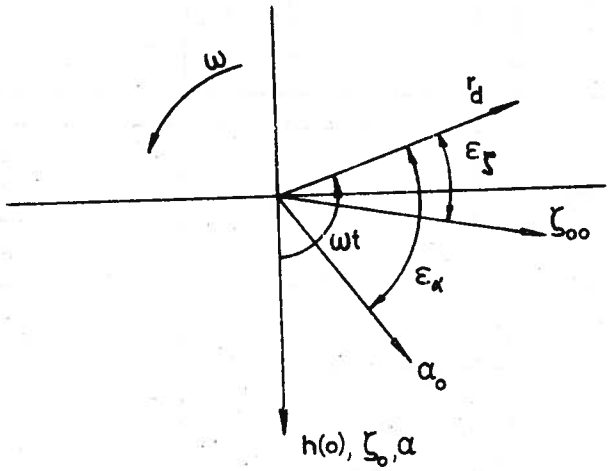

Fig. 1.4.3

Table 1.4.2 Systems of equations for determination of ship motions in harmonic waves

($\theta = 0$)

Case	ζ_1	ζ_2	α_1	α_2	=
Generally when $v = 0$	$\omega^2(a + \bar{m}) - c$ $\omega\, b$ $\omega^2(d + S_m) - f$ $\omega\, e$	$-\omega\, b$ $\omega^2(a + \bar{m}) - c$ $-\omega\, e$ $\omega^2(d + S_m) - f$	$\omega^2(d + S_m) - f$ $\omega\, e$ $\omega^2(A + I_m) - C$ $\omega\, B'$	$-\omega\, e$ $\omega^2(d + S_m) - f$ $-\omega\, B'$ $\omega^2(A + I_m) - C$	$-r_d(\gamma BLf_z - \omega^2 K + \omega \bar{L})$ $-r_d(\gamma BLf'_z - \omega^2 K' - \omega L')$ $-r_d(\gamma BL^2 f_\alpha - \omega^2 M + \omega N)$ $-r_d(\gamma BL^2 f'_\alpha - \omega^2 M' - \omega N')$
Vessels Symmetric w.r.t. $x = 0$	$\omega^2(a - \bar{m}) - c$ $-\omega\, b$	$-\omega\, b$ $\omega^2(a + \bar{m}) - c$	$\omega^2(A + I_m) - C$ $\omega\, B'$	$-\omega\, B'$ $\omega^2(A + I_m) - C$	$-r_d(\gamma BLf_z - \omega^2 K)$ $+r_d\, \omega\, L'$ $-r_d\, \omega\, N$ $-r_d(\gamma BL^2 f'_\alpha - \omega^2 M')$
Symmetric vessels in still water $B_z(x) = 0$	$\omega^2(a + \bar{m}) - c$	$\omega^2(a + \bar{m}) - c$	$\omega^2(A + I_m) - C$	$\omega^2(A + I_m) - C$	0 0 0 0

Table 1.4.3 List of constants in table 1.4.2.(All integrals are taken over the whole ship length)

Constant (1)		Generally when v = 0 (2)	Symmetric vessel w.r.t. x = 0 (3)	Remarks (4)
Mass Distribution	$\bar{m}$	$\int m\,dx$	As column 2 (as col.2)	The vessels' mass
	S_m	$\int mx\,dx$	0	
	I_m	$\int mx^2\,dx$	(as col. 2)	The vessels' mass moment of inertia
Floatation plane coeffs.	c	$\gamma \int B_x\,dx = \gamma A_{WL}$	(as col. 2)	A_{WL} = area of the floatation plane
	f	$\gamma \int B_x x\,dx = \gamma S_{WL}$	0	S_{WL} = static mom. of fl. pl.
	C	$\gamma \int B_x x^2\,dx = \gamma J_{WL}$	(as col. 2)	I_{WL} = moment of inertia of the fl. pl.
Hydrodynamic mass	a	$\int m_{zh}\,dx$	(as col 2)	Hydrodyn. mass
	d	$\int m_{zh} x\,dx$	0	Static mom. of hydrodyn. mass
	A	$\int m_{zh} x^2\,dx$	(as col. 2)	Inertia mom. of hydrodyn. mass
Damping term	b	$\int N_z(x)\,dx$	(as col. 2)	
	e	$\int N_z(x) x\,dx$	0	
	B'	$\int N_z(x) x^2\,dx$	(as col.2)	
Heaving force coeffi-cients	f_z	$\frac{1}{L}\int \frac{B_x}{B} \cos kx\,dx$	(as col. 2)	(See eqn. 1.3.41 and fig. 1.3.18)
	K	$\int m_{zh} \cos kx\,dx$	(as col. 2)	
	$\bar{L}$	$\int N_z(x) \sin kx\,dx$	0	
	f'_z	$\frac{1}{L}\int \frac{B_x}{B} \sin kx\,dx$	0	
	K'	$\int m_{zh} \sin kx\,dx$	0	
	L'	$\int N_z(x) \cos kx\,dx$	(as col. 2)	
Trim moment coeffi-cients	f_σ	$\frac{1}{L^2}\int \frac{B_x}{B} x \cos kx\,dx$	0	(See eqn. 1.3.41 and fig. 1.3.18)
	M	$\int m_{zh} x \cos kx\,dx$	0	
	N	$\int N_z(x) x \sin kx\,dx$	(as col. 2)	
	f'_α	$\frac{1}{L^2}\int \frac{B_x}{B} x \sin kx\,dx$	(as col. 2)	
	M'	$\int m_{zh} x \sin kx\,dx$	(as col. 2)	
	N'	$\int N_z(x) x \cos kx\,dx$	0	

1.4.4 Oscillations in still water

The equations at the bottom of table 1.4.2 describe those oscillations that result if a symmetric vessel is displaced from the equilibrium position in still water and then released. The equations are valid only for undamped oscillations (ideal liquid and no waves). The assumed harmonic oscillations (1.4.2) are not valid for free dampened motions.

The natural frequencies for heave and pitch motions are found from the equations at the bottom of table 1.4.2.

$$\omega_{c\zeta} = \sqrt{\frac{c}{a + m}} = \sqrt{\frac{\gamma A_{WL}}{m\ (1 + k_z)}}$$

$$\omega_{c\alpha} = \sqrt{\frac{C}{A + I_m}} = \sqrt{\frac{\gamma I_{WL}}{I_m (1 + k_\alpha)}} \qquad (1.4.12)$$

where

$$k_z = \frac{1}{m} \int_L m_{zh}\, dx$$

$$k_\alpha = \frac{1}{I_m} \int_L m_{zh} x^2 dx \qquad (1.4.13)$$

1.4.5 Damping.

Considering now a vessel heaving according to equation (1.4.10a). Since the camping forces always resist the motion these will over a unit length of the vessel produce a work (A_1) which during one full period is equal to:

$$A_1 = \int_0^{T_\zeta} N_z(x) \cdot \dot{\zeta}_o\, d\,\zeta_o = N_z(x) \cdot \zeta_{oo}^2 \omega^2 \int_0^{T_\zeta} \sin^2(\omega t - \varepsilon_\zeta) dt =$$

(1.4.14)

$$= N_z(x)\ \zeta_{oo}^2 \omega^2 \frac{T_\zeta}{2} = \pi\ \omega\ N_z(x)\ \zeta_{oo}^2$$

where we have used the following relationship:

$$T_\zeta = \frac{2\pi}{\omega} \quad \text{and} \quad d\zeta_o = -\zeta_{oo}\,\omega \sin(\omega t - \varepsilon_\zeta)\,dt$$

The work (A_1) is used to produce a wave system which propagates away from the vessel in all directions (Velox-wave). Assuming that the height of the Velox-wave (h_v) is proportional to ζ_{oo} we set:

$$H_v = A_z \cdot \zeta_{oo} \tag{1.4.15}$$

where the quantity A_z is unknown at this time.

The amount of energy per unit length of vessel (A_2) which is transported by the Velox-waves on both sides of the vessel during one oscillation is equal to (see equation (1.3.29)):

$$A_2 = 2 \cdot \frac{1}{2}\,\gamma(A_z\,\zeta_{oo})^2\,\lambda = \gamma A_z^2\,\zeta_{oo}^2\,\frac{2\pi g}{\omega^2} \tag{1.4.16}$$

Making $A_1 = A_2$, the following relationship between the damping coefficient $(N_z(x))$ and the specific height (A_z) of the Velox wave is obtained[x]:

$$N_z(x) = 2\,\rho\,g^2\,\omega^{-3}\,A_z^2 \tag{1.4.17}$$

Values for A_z found from two-dimensional hydrodynamic analyses are published by Tasai.[1] Similar diagrams are also worked out by Grim.[2] Gerritsma[3] has shown by model tests that a good agreement exists between theory and experiment in the case of the zero forward speed.

---

x) Internal viscous dissipation of energy of the fluid is disregarded.

1) Tasai: "Damping Force and Added Mass of Ships Heaving and Pitching". Report of Res. Inst. for Appl. Mech., Kyushu University, Japan, Vol.VII,No.26, 1959.

2) Grim, O.: "A Method for a More Precise Computation of Heaving and Pitching Motions Both in Smooth Water and in Waves". Third Symp. on Naval Hydrodynamics, Scheveningen 1960.

3) Gerritsma, J. & v.d.Bosch, JJ.: "Ship Motions and Roll Stabilization". Institutt for Skipsbygging II, Meddelelse SKB II/MI, Trondheim 1965.

1.4.6 Hydrodynamic mass.

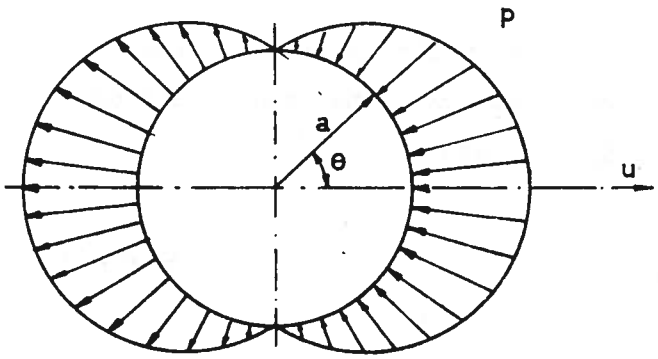

Fig. 1.4.4

A vertical infinitely long cylinder of circular cross-section and radius a is assumed moving with velocity u in an ideal fluid along a straight line perpendicular to the axis of the cylinder. If the cylinder is given an acceleration $(\partial u/\partial t)$, a pressure component will arise which is acceleration dependent. The pressure can be found [1] to be equal to (see fig. 1.4.4):

$$p = \rho\, a \cos\theta \cdot \frac{\partial u}{\partial t} \qquad (1.4.18)$$

where ρ = density of the liquid.

In order to give the cylinder this acceleration, a force (K) per unit length of the cylinder must be applied, where:

$$K = m \cdot \frac{\partial u}{\partial t} + \int_0^{2\pi} p \cos\theta \cdot a\,d\theta = (m + \pi\rho a^2)\,\frac{\partial u}{\partial t} \qquad (1.4.19)$$

The acceleration pressure due to the liquid may thus be substituted by an assumed mas (m_h) which has to be accelerated to a velocity equal to that of the cylinder. In the literature this fictive liquid mass is frequently denoted "virtual added mass". Here the notation hydrodynamic mass (m_h) will be used. In the chosen example then:

$$m_h = \pi\,\rho\,a^2 \qquad (1.4.20)$$

which corresponds here to the mass of the amount of liquid displaced by the cylinder. The determination of the hydrodynamic mass for bodies of cross-

---

[1] Wendel, K.: "Hydrodynamische Massen und Hydrodynamische Massenträgheitsmomente". JSTG, 44, 1950.

sections similar to those of ships has been studied by a number of researchers. The reader is referred to the special literature, e.g. works by Tasai, Grim and Gerritsma which were mentioned in the previous section.

1.4.7 The velocity of the vessel.

In this whole section it has so far been assumed that the velocity of the ship is zero $v = 0$. If $v \neq 0$, then the frequency of encounter (ω_e) must be substituted for ω. The solution then obtained may be regarded as a first approximation. More accurate solutions are discussed in the work by Gerritsma referred to above.

1.4.8 Moments and shear forces.

An analysis as the one outlined above is fairly complex and time consuming. It is performed most conveniently by means of computers. Moments and shear forces are found by integrating equations (1.4.7). The still water loads are additive.

The dynamic load (eqn. 1.4.6) may be written:

$$\tilde{q}_z = q_{zo} \cos(\omega t - \varepsilon_q) \tag{1.4.21}$$

where

$$q_{zo} = \sqrt{q_{z1}^2 + q_{z2}^2} \tag{1.4.22a}$$

and

$$\operatorname{tg} \varepsilon_q = q_{z2}/q_{z1} \tag{1.4.22b}$$

Note that q_{zo} as well as ε_q are here functions of x. The maximum value of $\tilde{q}_z$ does not therefore necessarily occur simultaneously in all places.

The shear forces must be determined by integration of equation (1.4.6). This yields:

$$\tilde{Q}_z = -\int_{-L_a}^{x} \tilde{q}_z dx = -\cos \omega t \int_{-L_a}^{x} q_{z1}\, dx - \sin \omega t \int_{-L_a}^{x} q_{z2}\, dx$$

$$= Q_{z1} \cos \omega t + Q_{z2} \sin \omega t \qquad (1.4.23)$$

$$\tilde{M}_y = \int_{-L_a}^{x} \tilde{Q}_z dx = \cos \omega t \int_{-L_a}^{x} Q_{z1} dx + \sin \omega t \int_{-L_a}^{x} Q_{z2} dx =$$

$$= M_{y1} \cos \omega t + M_{y2} \sin \omega t \qquad (1.4.24)$$

Here one may again set:

$$\tilde{Q}_z = Q_{zo} \cos (\omega t - \varepsilon_Q)$$

$$\tilde{M}_y = M_{yo} \cos (\omega t - \varepsilon_M) \qquad (1.4.25)$$

where

$$M_{yo} = \sqrt{M_{y1}^2 + M_{y2}^2}$$

$$\operatorname{tg} \varepsilon_M = M_{y2}/M_{y1} \qquad (1.4.26)$$

and similarly for Q_{yo} and $\operatorname{tg} \varepsilon_Q$.

It should again be noted that the quantities M_{yo}, ε_M, Q_{yo} and ε_Q are functions of x .

The magnitude of the hydrodynamic loads will depend on the weight distribution on board. This is partly due to the influence of the weight distribution on the mass moment of inertia I_m and consequently on the natural frequency of the pitching motion. But even by keeping I_m constant and varying the cargo distribution, it will be found that there is a dependency between the cargo distribution and dynamic loads. Fig. 1.4.5 shows measured shear forces and moments together with associated cargo distributions[1].

---

[1] Lotveit, M., Murer, Chr., Vedeler, B. and Chirstensen, Hj.: "Wave Loads on a T-2 Tanker Model". DNV Meddelelse nr. 18, 1961.

All cargo distributions gave the same mass moment of inertia.

Normally it may be expected that vessels loaded in sagging in still water, will be exposed to dynamic forces that cause an increase of the wave induced moments admiships both in a sagging and hogging wave. Vice versa, hogging still water moment will normally cause dynamic forces that reduce the quasistatically calculated wave moments. Fig. 1.4.6 shows this relationship schematically. The figures a) and b) show how the conditions will be for a vessel loaded to produce a sagging still water moment, whereas figures c) and d) refer to the same vessel loaded to produce hogging. In the figure the following notations are used:

T = mass inertia forces for forward and aft halves of the vessel considered separately. T is assumed to include hydrodynamic mass.

O = dynamic correction of the buoyancy forces.

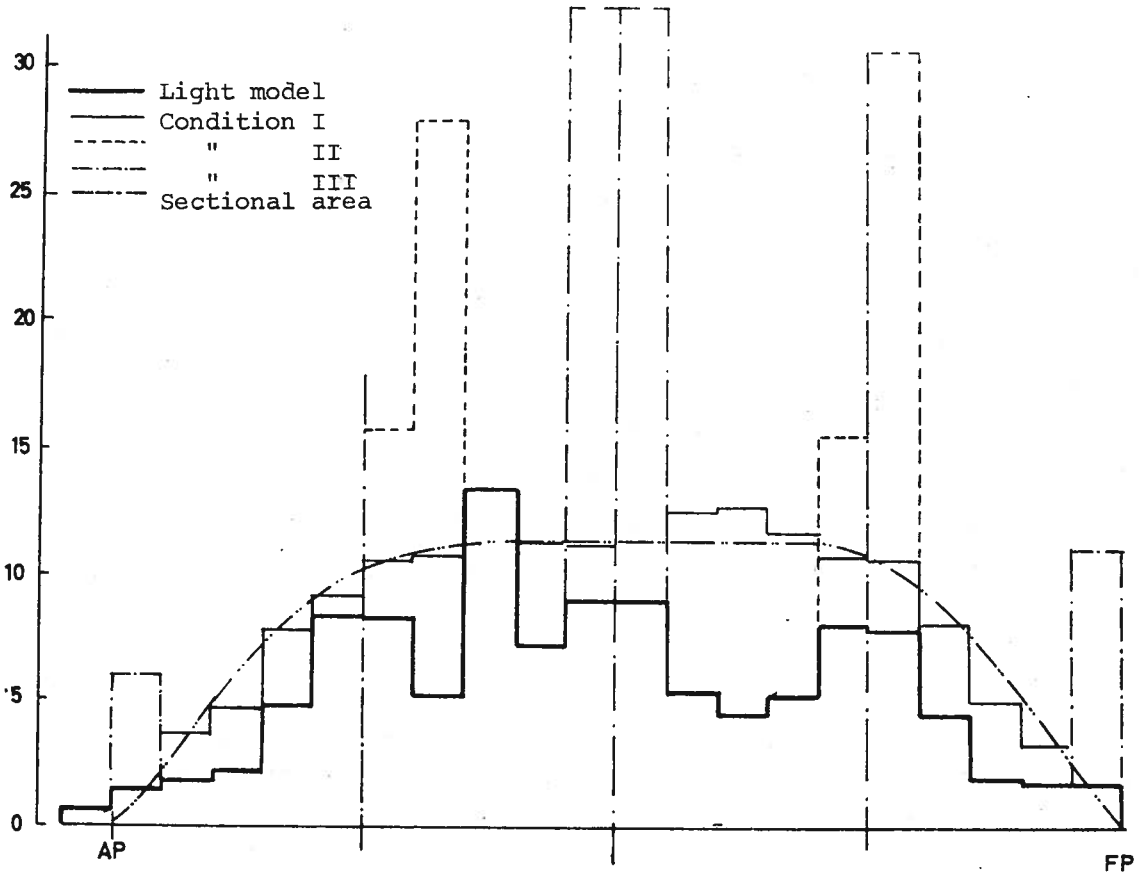

M 428 Weight Distribution. Constant Mass Moment of Inertia.

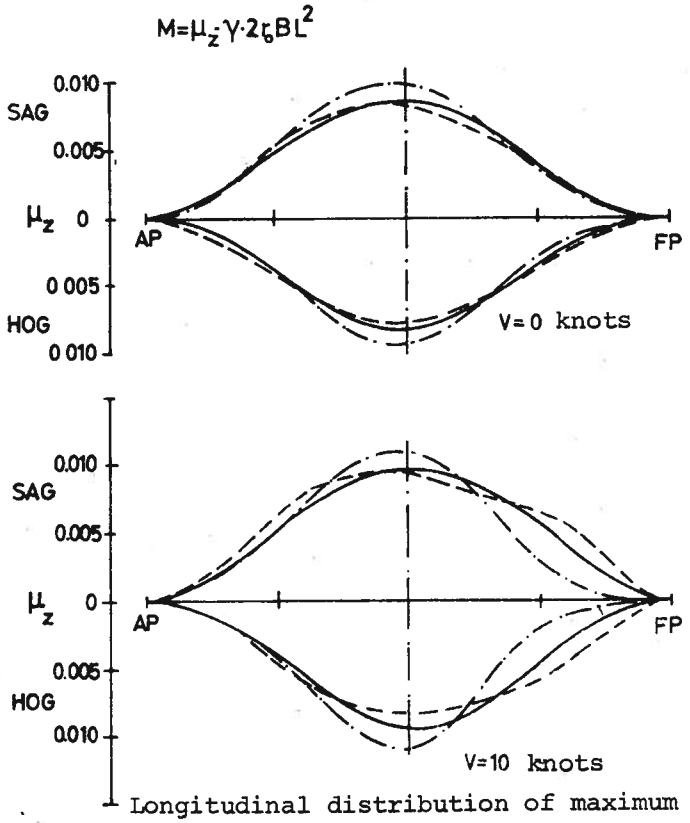

Longitudinal distribution of maximum bending moment.

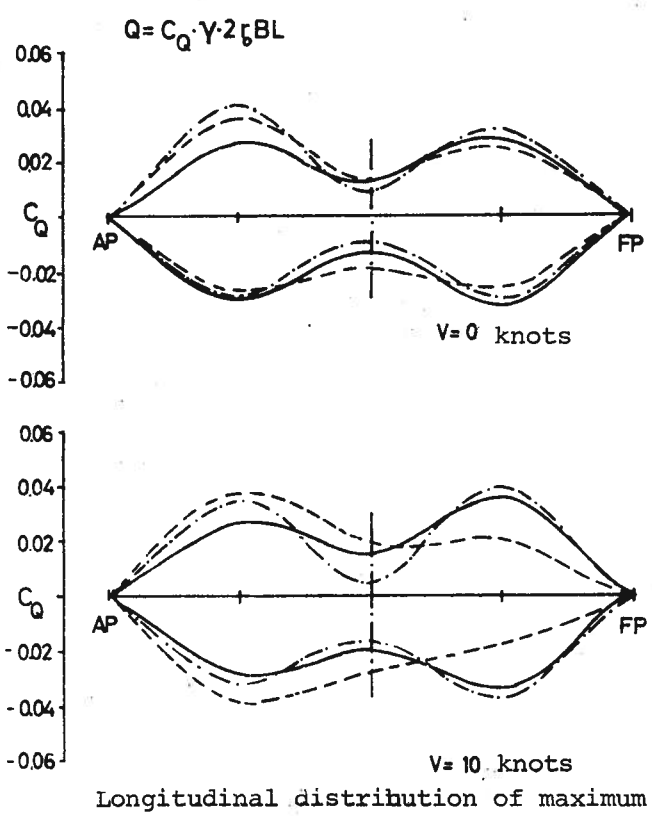

Longitudinal distribution of maximum shear forces.

Fig. 1.4.5

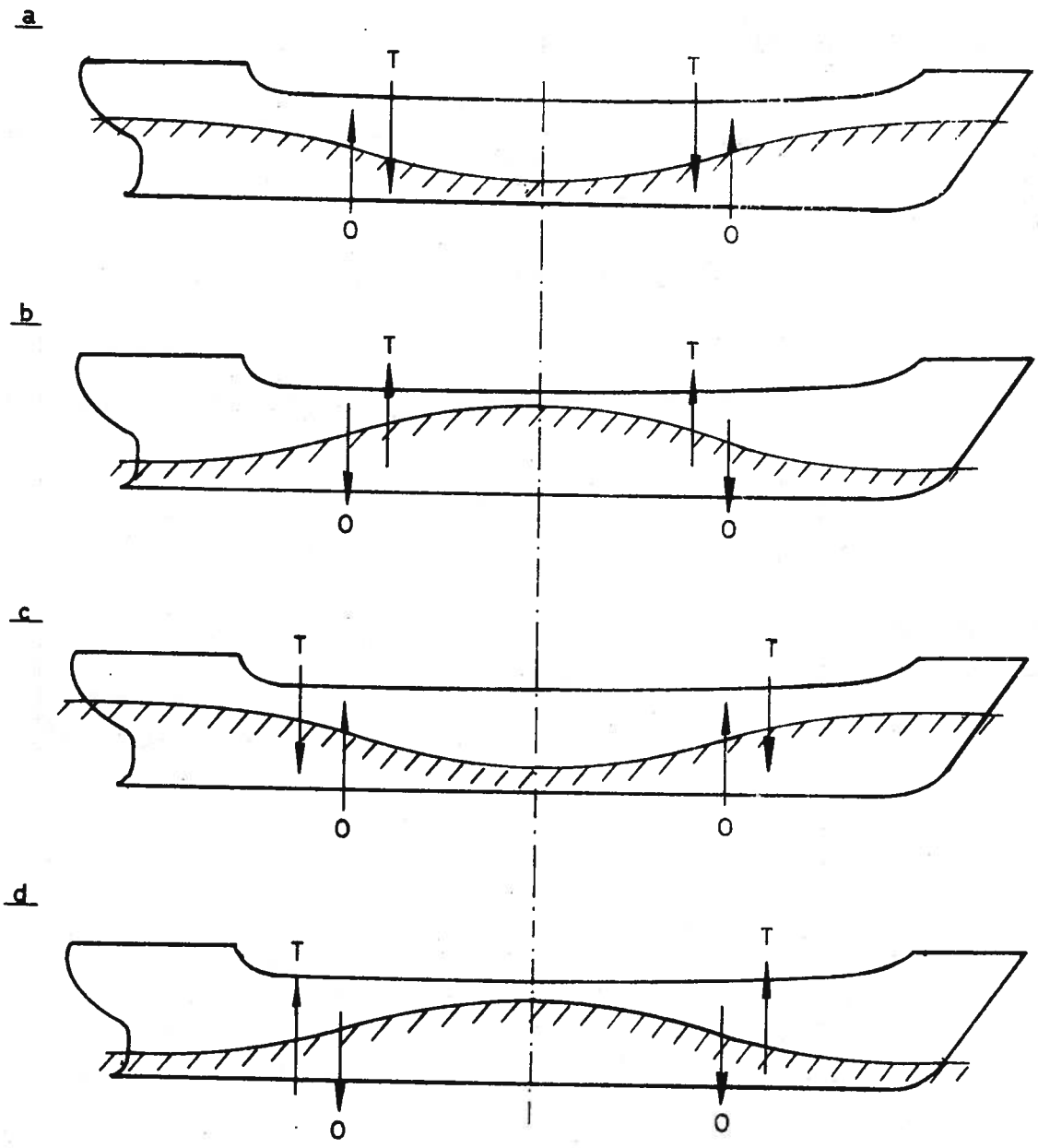

Fig. 1.4.6

In figures a) and c) the vessel floats deeper than corresponding to a quasistatic condition, whereas the opposite is true for figures b) and d).

Jacobs[1,2] has made a comparison between measured and estimated bending moments for a model of a tanker of the type T-2-Se-A1 in regular waves (L_{mod} = 4.8 ft.). The calculations were performed using the Korvin-Kroukovsky's method of analysis[3] which includes the effect of forward velocity. Damping constants are those given by Grim.

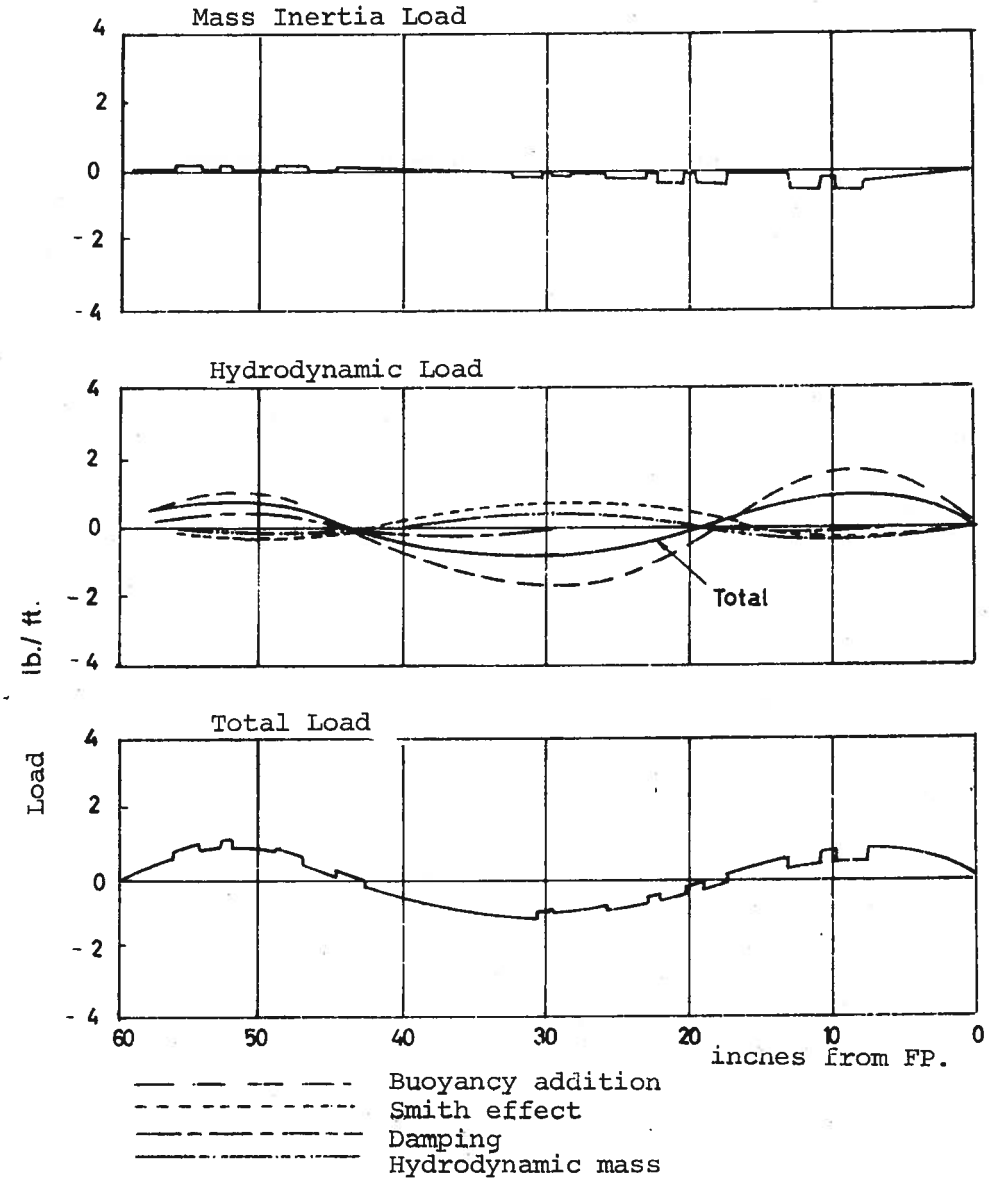

Dynamic load curves for tanker model at v_{mod} = 0, t = 0

Fig. 1.4.7

---

1) Jacobs, W.R.: "The Analytical Calculation of Ship Bending Moments in Regular Waves". Journal of Ship Research, Vol. 2, pp. 20-29, June 1958.

2) Jacobs, W.R. & Dalzell, J.F.: "Theory and Experiment in the Evaluation of Bending Moments Acting on a Ship in Waves". ISP, Vol.7, No 73, Sept. 1960.

3) Korvin-Droukovsky, B.V.: "Theory of Seakeeping". Ship Structure Committee SNAME, New York, 1961.

The load curves for $V_{mod} = 0$ and $V_{mod} = 2.4$ ft./sec. are shown in fig. 1.4.7 and 1.4.8 for the time $t = 0$, which here corresponds to a wave trough midships. The wave length is equal to the length of the vessel and the wave height is equal to L/40. The dynamic bending moment midships calculated from the loads, is seen in fig. 1.4.9, together with experimental values. The agreement at $V_{mod} = 0$ is very good, whereas the results for $V_{mod} = 2.4$ ft./sec. show a somewhat larger discrepancy. For static estimates it will be found that the wave bending moment (L/40 - wave) becomes 36 in-lb. Including the Smith-effect, it becomes 28 in-lb. Both of those values are larger than the dynamic moments.

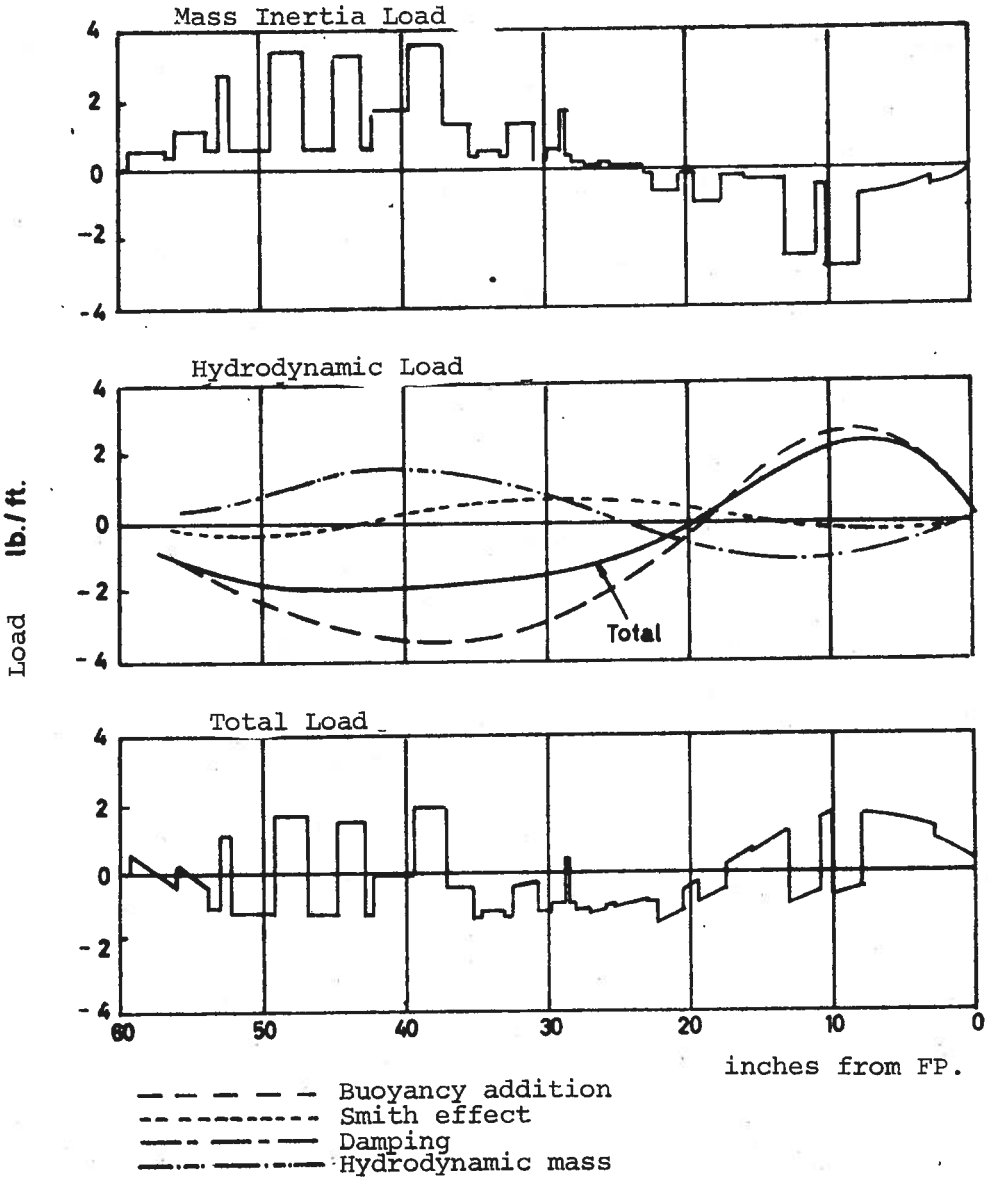

Dynamic load curves for tanker model at $V_{mod} = 2.4$ ft./sec; t = 0.

Fig. 1.4.8

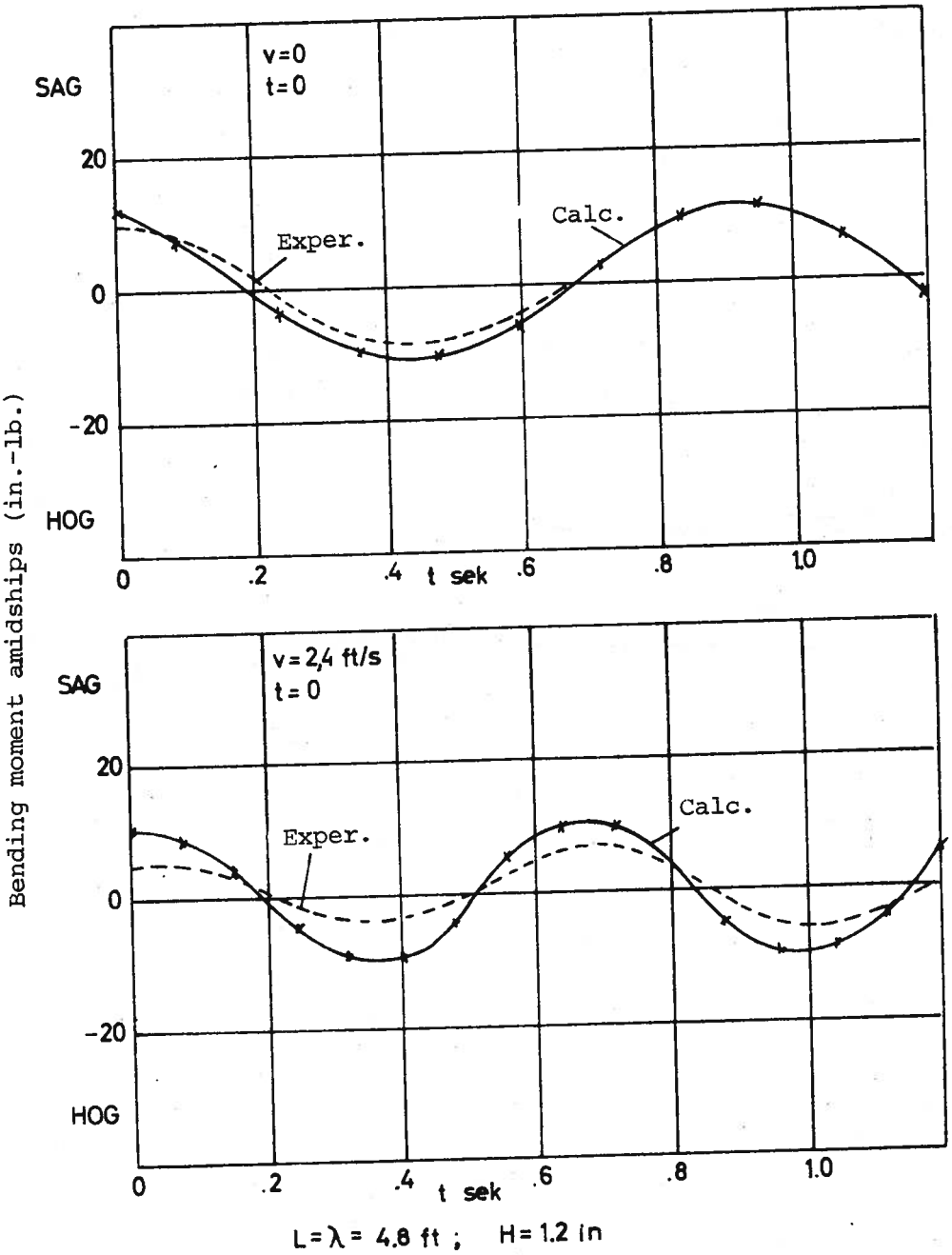

Fig.1.4.9

The relative motion between wave and ship causes, in addition to the Smith-effect, a dynamic reduction which often is of the comparative magnitude.

Vossers, Swaan, Fijken[1] investigated the magnitude of the dynamic reduction of bending moment realized in following and head-seas. Their results are reproduced in fig. 1.4.10 a and b as functions of d/λ . The curves represent mean values found for Series-60 models with C_B ranging from 0.55 to 0.80. Tests were conducted in regular waves at speeds corresponding to Fr = 0.18-0.28. (The $\frac{\tilde{M}_O}{M_O}$ = the relation between the measured moment and statically calculated (without Smith correction)). C_V = the vertical prismatic coefficient.

The wave induced loads in following seas are small. In head seas the wave induced loads give larger loads, but still the mean wave bending moment midships is considerably lower than the corresponding moment calculated by quasi-static methods.

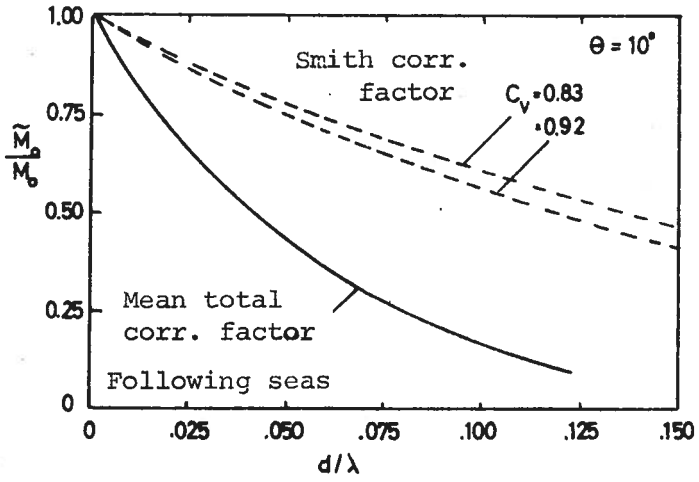

Fig.1.4.10a

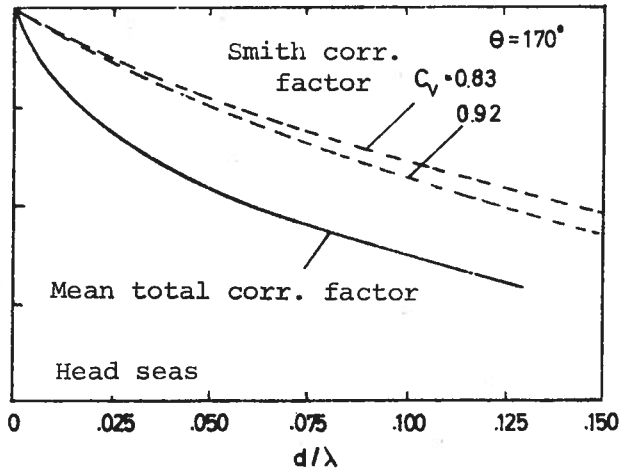

Fig.1.4.10b

Further discussions of the influence of the cargo distribution on the distribution of dynamic moment and shear force along the hull girder are published by Murer and Lotveit[2]. In regions of larger concentrated weights

---

1) Vossers, G., Swaan,W.A. & Rijken, H.: "Vertical and Lateral Bending Moment Measured on Series 60 Models". ISP, Vol. 8, July 1961.

2) Murer, Chr. and Lotveit, M.: "Further Model Tests to Determine Wave Loads on a T-2 Tanker". European Shipbuilding, No. 3, 1964.

the inertia forces become large as well as the resulting dynamic moments and shear forces. Heesch[1] shows examples on how to do practical estimates based on the above theory.

---

[1] Heesch, F.G.: "Ytre Langskipspakjenninger". Institutt for Skipsbygging II, Trondheim, 1964.

1.5 Static analysis of stresses in irregular waves.

1.5.1 Introduction.

The hull girder must be designed to satisfactorily sustain the loads it is exposed to in a seaway. It is very important that the design is based in sound fundamentals. On the one hand a significant part of the required hull material is determined by selecting the scantlings of the longitudinal structural elements. Heavy and expensive hulls will be the result in the case of over-design. On the other hand, and under-design in this area may result in loss at sea.

The absolutely largest loads that an arbitrary ship may experience is not known, and even if it was it would be unreasonable to require all ships to survive this load. Most ships would then be overdimensioned, since during their life they would never experience this extreme value. On the other hand it would be very useful if during the design stage a probable load spectrum could be established for the ship, as indicated in fig. 1.5.1. Such a spectrum would show the probable maximum value of loading during the life of the ship, as well as a probable number of load reversals up to the various lower load levels. A diagram of the type indicated in fig. 1.5.1 will normally only apply for a certain ship on a certain route, as will be shown in the following.

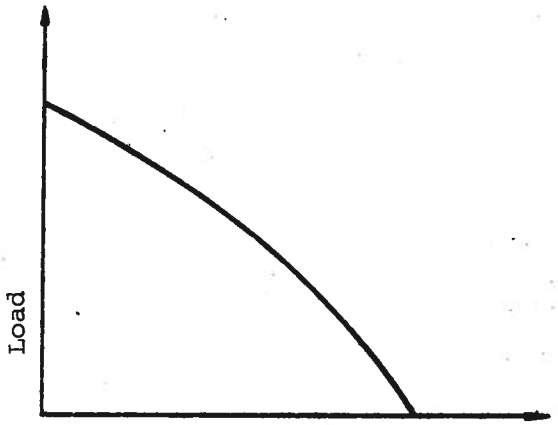

Fig.1.5.1

The above somewhat vague formulation indicates the necessity of analyzing the whole loading problem from a statistical point of view. The motions in a storm sea as well as the loads they produce in the ship's hull, are highly irregular in character and can, therefore,not be described in a

deterministic sense. However, by using a statistical approach, it is possible to bring the apparently indescriptive into order. For the discussion of the statistical characteristics of waves below we shall simplify the problem by assuming a one-dimensional sea, i.e., waves are parallel waves and perpendicular to the direction of wave propagation. This simplification is not strictly necessary since waves of arbitrary direction may be similarly treated.

1.5.2 Harmonic analysis of irregular one dimensional waves.

From the Fourier-analysis it is known that any curve which is sectionally continuous (e.g. see fig. 1.5.4), may be developed as a Fourier series. The series may with an increasing number of terms fit the given curve outline with an increasing degree of accuracy.

Similarly, the surface of the irregular sea, represented by observed wave heights at a certain location over a certain time, may be described by the function:

$$h(t) = \sum_{n=1}^{\infty} (r_{\omega n}) \cos (\omega_n t + \varepsilon_n) \qquad (1.5.1)$$

that is, as a sum of harmonic waves.

Here are:

$h(t)$ = height of the surface above the still water level.

ω_n = angular frequency of the n'th harmonic term.

$r_{\omega n}$ = amplitude of the n'th term.

ε_n = phase angle of the n'th term.

Before continuing the discussion of equation (1.5.1), it may be convenient to repeat some important properties of the harmonic waves.

Introducing the notations:

T(sec) = wave period.

λ(m) = wave length.

H(m) = wave height.

c(m/sec) = wave velocity of propagation.

r(m) = wave amplitude (= $H/2$).

ω(rad/sec) = angular frequency.

E(kgm/m^2) = wave energy.

ρ = water density.

g = gravitational constant.

we may write the following relationships:

$$\omega = 2\pi/T$$

$$c = \lambda/T = g/\omega = \sqrt{g\lambda/2\pi}$$

$$\lambda = \frac{2\pi c^2}{g} = \frac{2\pi g}{\omega^2} = \frac{gT^2}{2\pi} \qquad (1.5.2a\text{-}d)$$

$$E = \frac{1}{8}\rho g H^2 = \frac{1}{2}\rho g r^2$$

It should be noted in particular that the wave is singly determined by just two of the parameters above, e.g. ω and E .

To every harmonic term in the series (1.5.1) of amplitude $r_{\omega n}$ there corresponds an amount of energy $E_{\omega n}$ given by the formula (1.5.2d). The total amount of energy (E) in a seaway is then equal to:

$$E = \sum_{n=1}^{\infty} E_{\omega n} = \frac{1}{2}\rho g \sum_{n=1}^{\infty} (r_{\omega n})^2 \qquad (1.5.3)$$

The constant term $\frac{1}{2}$ g in the above formula is often ommited in the literature and the reduced expression

$$E' = \sum_{n=1}^{\infty} (r_{\omega n})^2 \qquad (1.5.4)$$

is taken instead as representative of the energy in the waves. This convention will be adhered to here. Fig. 1.5.2a shows the energy content so defined of a wave system consisting of four harmonic components of angular-frequencies ω_1, ω_2, ω_3, and ω_4 .

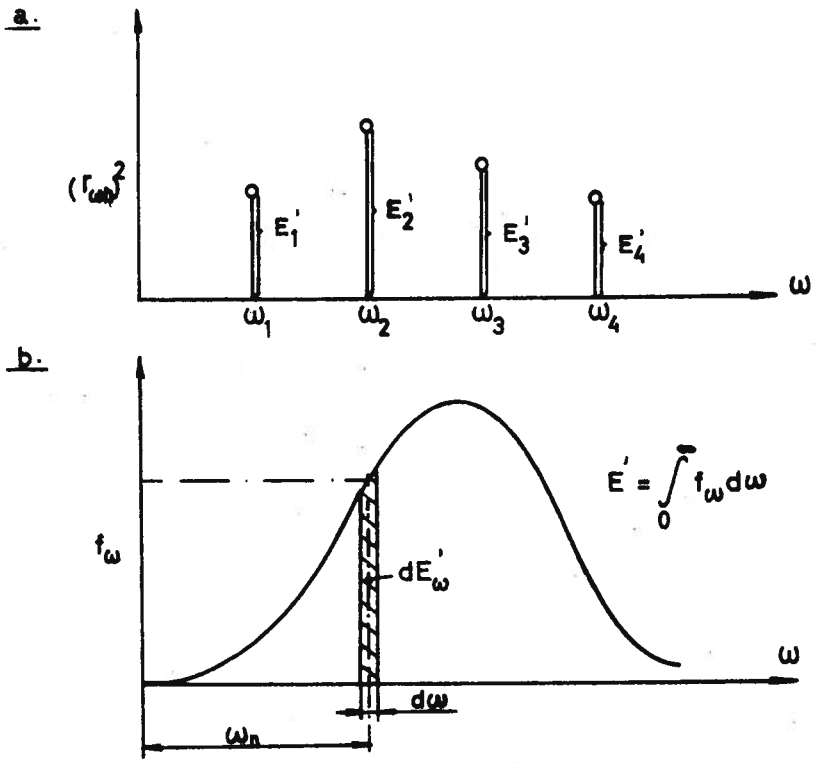

Fig. 1.5.2

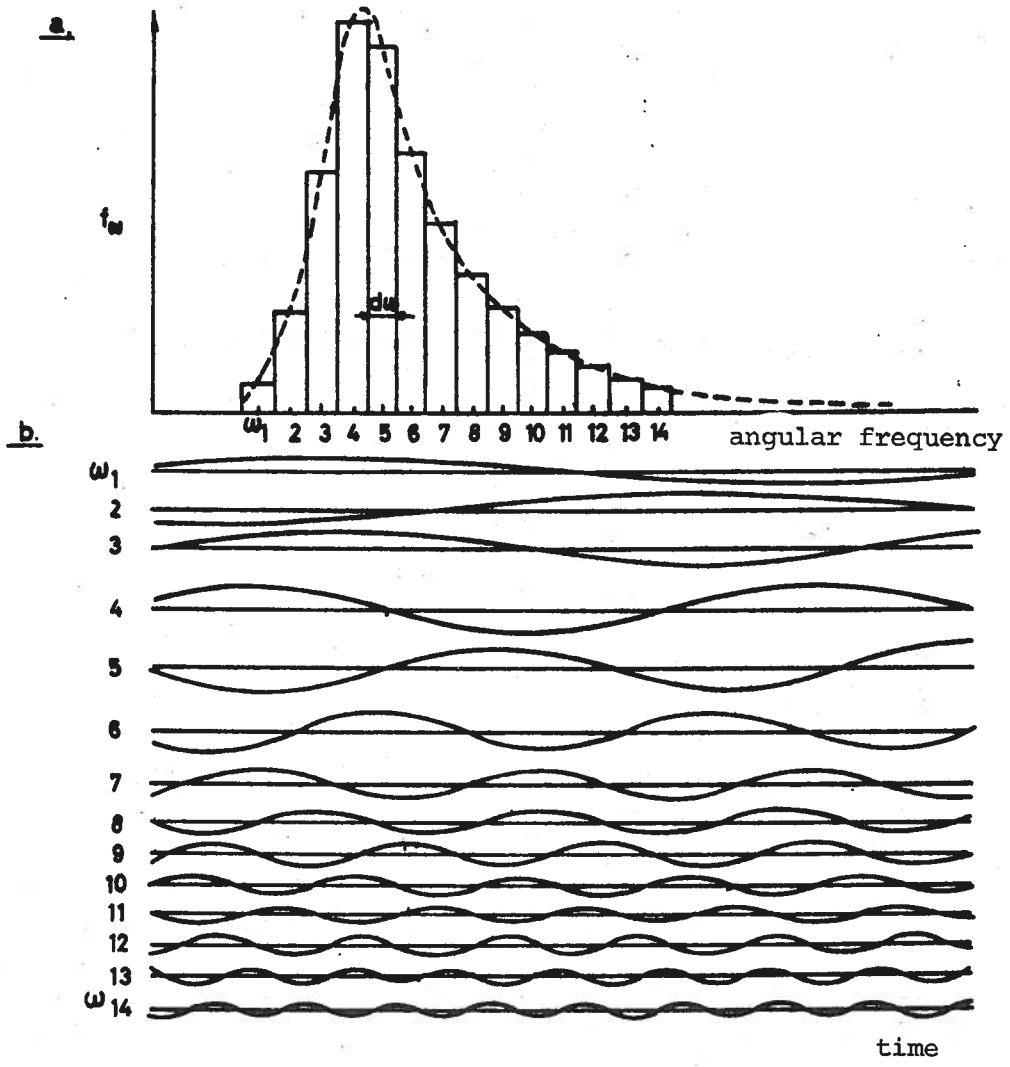

Typical wave spectrum and corresponding harmonic components.

Fig. 1.5.3

There is no reason to believe that the energy spectrum is discontinuous, which would correspond to some wave components missing within the actual region of interest. It should instead be assumed that the waves would be built up by an infinite number of harmonic terms, such that there is a continuous energy spectrum as shown in fig. 1.5.2b.

We then have that:

$$E' = \int_0^\infty f_\omega \, d\omega \qquad (1.5.4a)$$

where f_ω is the coordinate in a so-called energy spectrum.

The energy content (dE') of all waves of frequency (ω) within the region:

$$\omega_n - \frac{1}{2} d\omega < \omega < \omega_n + \frac{1}{2} d\omega$$

is according to fig. 1.5.2b approximately equal to:

$$dE'_\omega \sim f_{\omega n} \, d\omega \qquad (1.5.5)$$

Even though the seaway is defined by a continous wave spectrum it may be convenient to assume that it consists of a finite number of harmonic components. Fig. 1.5.3a shows how the energy spectrum may be assumed divided into rectangles of frequency width $d\omega$. The energy corresponding to such a band may then be assumed concentrated in a single harmonic wave which is called the elementary wave. The height of the elementary wave ($r_{\omega n}$) will then be given by the expression:

$$(r_{\omega n})^2 = dE'_\omega = f_{\omega n} \, d\omega \qquad (1.5.6)$$

Note that f_ω has the dimensions $(\text{length})^2$ sec. corresponding to the expression $(r_\omega)^2/d\omega$.

Fig. 1.5.3b shows schematically the elementary waves corresponding to the energy spectrum above. The amplitudes are given by the formula (1.5.6). Substituting from equation (1.5.6) into equation (1.5.1), the following expression is obtained for the resulting wave.

$$h(t) = \sum_{1}^{n} \sqrt{f_{\omega n} d\omega} \cos (\omega_n t + \varepsilon_n) \qquad (1.5.7)$$

Even if the shape of the elementary waves for a given energy spectrum is known (see fig. 1.5.3b), equation (1.5.7) does not give any definite information on what the resulting wave looks like at a given instance. The phase-angle ε_n between the different elementary waves at the time $t = 0$ could have been anything between 0 and 2π. Any value is just as probable as any other. The phase angle between the elementary waves will in addition change continuously. Two elementary waves with frequency ω_m and ω_n which were in phase at the time $t = t_1$, will at the time $t = t_2$ have a phase difference of an angle $(\omega_m - \omega_n)(t_2 - t_1)$. It is said that the fomula (1.5.7) produces a "stocastic" process.

By using formula (1.5.7) it is possible to produce a totally irregular sea with a given energy spectrum.

Note the following relationships:

1) From an observed wave profile (see fig. 1.5.4) it is possible by using harmonic analysis to come up with the amplitudes and frequencies of the elementary wave. Consequently the corresponding energy spectrum can be determined.

2) If an energy spectrum is known, it is on the other hand not possible to work backwards to the wave profile that was used for obtaining the energy spectrum. This sould be clear from what was said above about the properties of the wave functions.

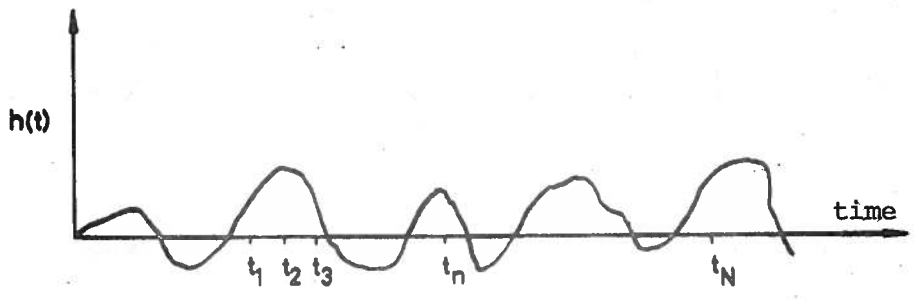

Fig. 1.5.4

1.5.3 Wave statistics.

Even though the formula (1.5.7) does not singularly describe the shape of the water surface at any given time, it is possible by using statistical methods to draw far reaching conclusions concerning the wave conditions that are described by such a continuous wave spectrum.

Thus it is possible to show that all wave coordinates (h) at a certain point on the sea surface measured at arbitrary times t_1 ----- t_n (fig. 1.5.4), will be normally distributed, such that:

$$P(h_1 < h(t_n) < h_2) = \frac{1}{s\sqrt{2\pi}} \int_{h_1}^{h_2} \exp.(-h^2/2s^2)\, dh \qquad (1.5.8a)$$

The left hand side of this equation is read as follows:"The probability that the wave coordinate $h(t_n)$ at a certain time $t = t_n$ is between the values h_1 and h_2, is equal to..."

Equation (1.5.8a) is valid with good approximation as long as the energy spectrum for the waves is relatively narrow.

"Standard deviation" (s) is determined as usual by taking a large number of observations of the wave-coordinate, which gives:

$$s^2 = \frac{\sum_{i=1}^{N} h_i^2}{N} \qquad (1.5.9)$$

The value for s may also be determined by integration, by setting:

$$s^2 = \frac{1}{\tau} \int_0^{\tau} h^2(t)dt = \frac{1}{\tau} \int_0^{\tau} \{\sum_1^n r_{\omega n} \cos(\omega_n t + \varepsilon_n)\}^2 dt$$

where the region of integration is large.

Here

$$\int_0^{\tau} \cos(\omega_n t + \varepsilon_n) \cos(\omega_m t + \varepsilon_m)\, dt = \begin{cases} \tau/2 & \text{for } m = n \\ 0 & \text{for } m \neq n \end{cases}$$

which gives:

$$s^2 = \frac{1}{2}(r_{\omega 1}^2 + r_{\omega 2}^2 \text{ --- } + r_{\omega n}^2) = \frac{1}{2}\sum_1^n r_{\omega n}^2$$

Substituting now from equation (1.5.4), the following very important relation is obtained:

$$s^2 = E'/2 \qquad (1.5.10)$$

a) Gaussian distribution function

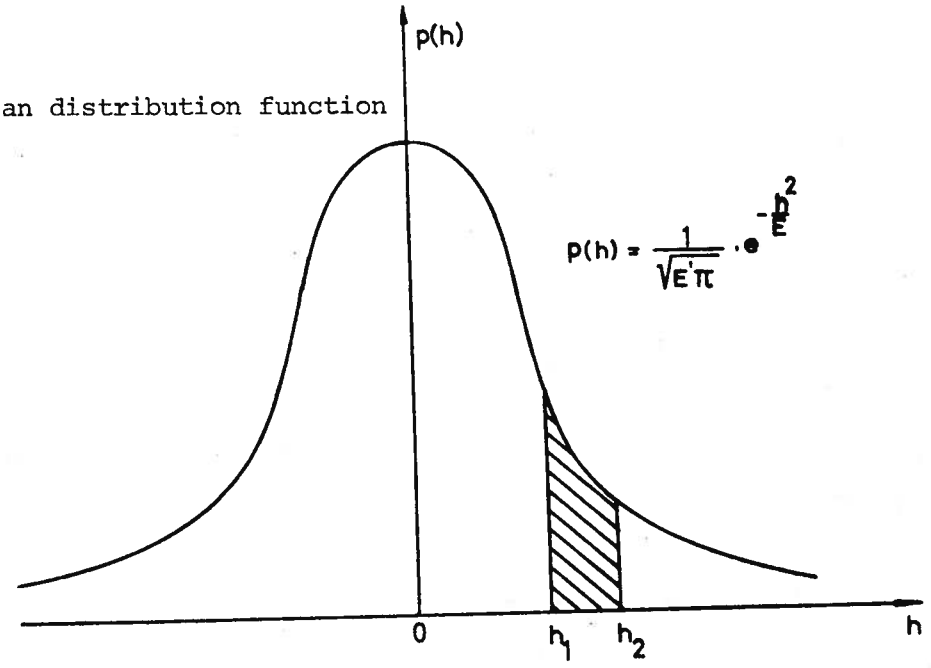

b) Rayleigh's distribution function.

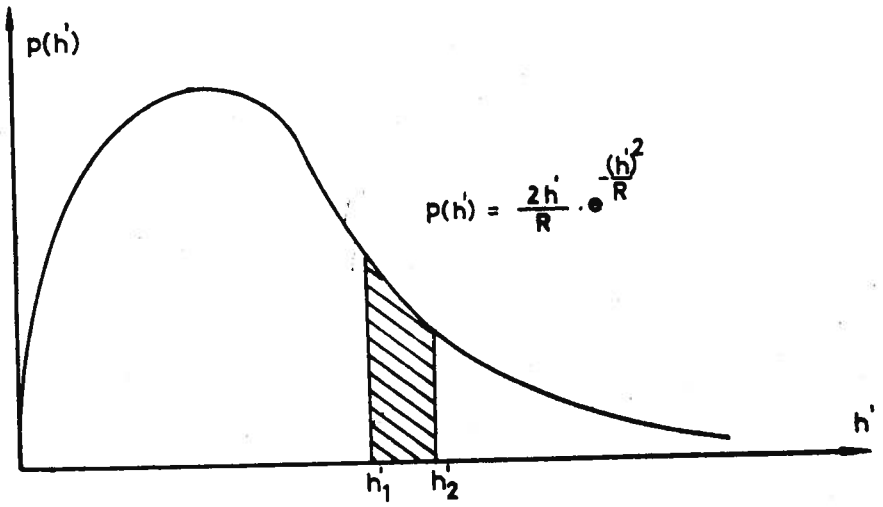

Fig. 1.5.5

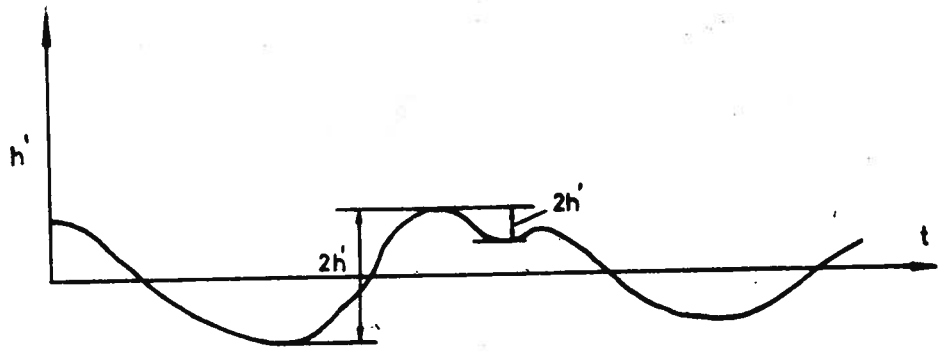

Fig. 1.5.6

Such that:

$$P(h_1 < h(t_n) < h_2) = \frac{1}{\sqrt{\pi E'}} \int_{h_1}^{h_2} e^{-h^2/E'} \, dh \qquad (1.5.8b)$$

The Gaussian normal distribution function is graphically represented in fig. 1.5.5a where the hatched area represents $P(h_1 < h(t_n) < h_2)$. The area under the curve integrated from $-\infty$ to $+\infty$ is equal to 1 .

The probability that $h(t_n) > h_3$ is correspondingly given by the expression:

$$P(h(t_n) > h_3) = \frac{1}{\sqrt{\pi E'}} \int_{h_3}^{\infty} e^{-h^2/E'} \, dh \qquad (1.5.8c)$$

In other words, when the area under the energy spectrum (E') is known, it can, by means of equation (1.5.8c) be used to define the probability that wave coordinate exceeds a certain value.

If instead of observing the wave heights <u>at a certain place</u> over a certain length of time we take a picture of a <u>larger area of the seaway</u> and group all the wave coordinates over the area according to magnitude, it will be found that these also are normally distributed and that the function (1.5.8b) applies.

Instead of observing the wave coordinate (h) , the attention is now directed on the apparent wave amplitudes (h') represented by half the vertical distance between wave crest and adjacent wave trough (and vice versa) (see fig. 1.5.6). It has been found that h' over a longer period of time will be ditributed according to "Rayleigh's distribution function" which is given by the expression[1]: (1.5.11)

$$P(h_1' < h' < h_2') = \int_{h_1'}^{h_2'} \frac{2h'}{R} \quad \text{exp.} -(h')^2/R) dh'$$

---

1) Cartwright, D.E. and Lounget-Higgins, M.S.: "The statistical distribution of the maxima of a random functions". PRS A 237, 1956.

Fig. 1.5.5b shows this distribution function. Here also the hatched area represents the probability that an arbitrarily observed value of h' is within the area between h'_1 and h'_2. Rayleigh's distribution function must also together with the horizontal coordinate, enclose an area equal to 1.0, which leads to

$$\frac{1}{\sqrt{\pi E'}} \int_{-\infty}^{+\infty} \text{exp.} -(h^2/E')\ dh = \int_{0}^{+\infty} \frac{2h'}{R} \text{exp.} -(h'^2/R)dh' = 1$$

In a group of numbers which are normally distributed it can then theoretically be found numbers of any magnitude between $-\infty$ and $+\infty$, whereas for the Rayleigh distribution all values must be positive.

The Rayleigh-factor R is here directly related to the energy content in the waves by the relation:

$$R = E' \tag{1.5.12}$$

Equation (1.5.11) applies strictly for waves with small energy spectrum, but is applied anyway for the normal wave spectrum,and apparently with good results.

1.5.4 Extreme wave heights

We are of course especially interested in the largest wave heights that with a certain degree of probability will be met.

The probability of meeting a wave with $h' > h'_m$ is according to the equations (1.5.11) and (1.5.12) given by the expression:

$$P(h' \geq h'_m) = \int_{h_m}^{\infty} \frac{2h'}{E'} \text{exp.} -(h'^2/E')\ dh' = \text{exp.} -(h'^2_m/E') \tag{1.5.13a}$$

Realizing, on the other hand, that if h'_m is the largest value found for a large number (N) of observations, we can say that:

$$P(h' \geq h'_m) = \frac{1}{N} \qquad (1.5.13b)$$

The above two equations then give:

$$\frac{1}{N} = \exp. -(h'^2_m/E')$$

by which

$$h'_m = \sqrt{E' \ln N} \qquad (1.5.14)$$

Equation (1.5.14) expresses the following:

If we, for a given sea state of energy content E', undertake N observations of the height difference (2h') between adjacent waves, it is probable that the largest observed value of h' is given by the formula (1.5.14). Equation (1.5.14) will give the correct value for the average of the registered values of h'_m if the observation series mentioned above is repeated a large number of times.

Table 1.5.1 shows the relation between h'_m and N according to equation (1.5.14)

Table 1.5.1

N	10	100	1000	10000	100000
$h'_m/\sqrt{E'}$	1.518	2.146	2.628	3.035	3.393

It can be seen that the longer the observations are continued, the larger will probably the largest observed wave height be, even though, as here, the sea state is assumed to remain unchanged, (unchanged energy content E').

The probable value for the largest wave height (H_m) can with adequate accuracy be set equal to $2h'_m$.

1.5.5 Energy spectrum of the seaway

If reliable values for the energy content (E') in seas can be found, it is possible by the above derivations to make some important statements about the probable maximum wave heights.

Considerable research work has been done in the last years in order to obtain a reliable basis for wave forecasts. Very significant in this context is the work that the norwegians Svendrup and Munk have done and which during the last world war was used to predict the sea state on the french coast during the invasion.

Of the fomulas that have been proposed for the energy spectrum, that due to Neumann is one of the better known[1].

When the wind starts blowing over a calm water surface, small ripples are first formed on the surface, i.e., waves of high frequency. As the wind acts on the water over a longer period of time, there appear wave components of increasing lengths and consequent decreasing frequency. Neumann has suggested the following formula for a fully developed sea-spectrum

$$f_\omega = \frac{dE'}{d\omega} = C \cdot \omega^{-6} \quad \text{exp.} -(2g^2/u^2\omega^2) \qquad (1.5.15)$$

where C is an empirical constant which is usually made equal to $3.05\ m^2 sec^{-5}$.

---

1) Neumann, G.: "On Ocean Wave Spectra and a New Method of Forecasting Wind Generator Sea". Beach Erosion Board, Techn. News. No. 43, 1953.

g = gravitational acceleration (m/sec^2)

u = wind velocity (m/sec).

Fully developed sea-spectrum is obtained when the wind has blown sufficiently long with constant velocity and over long enough fetch, so that the sea state becomes stationary.

Fig. 1.5.7 shows fully developed Neumann-spectrum for some wind velocities, and fig. 1.5.8 shows schematically how a spectrum may be assumed to develop in time from right to left.

Table 1.5.2 gives some values for smallest free-ocean area and shortest duration of constant weather condition in order to obtain a fully developed Neumann spectrum. It can be seen that it is very unlikely that the weather conditions any time can be assumed to be such that the spectra corresponding to the very largest wind velocities in the table at any time will be able to fully develop.

If the ship velocity is zero and the waves come head on, the frequency of encounter (ω_e) is equal to the wave frequency (ω).

For other velocities and headings the frequency of encounter will be different from ω , and given by the expression:

$$\omega_e = \omega(1 - \frac{\omega \cdot v}{g} \cos \theta) \qquad (1.5.16)$$

Here

v = the ship velocity

θ = the angle between the ships' heading and the direction of wave propagation, see fig. 1.5.9.

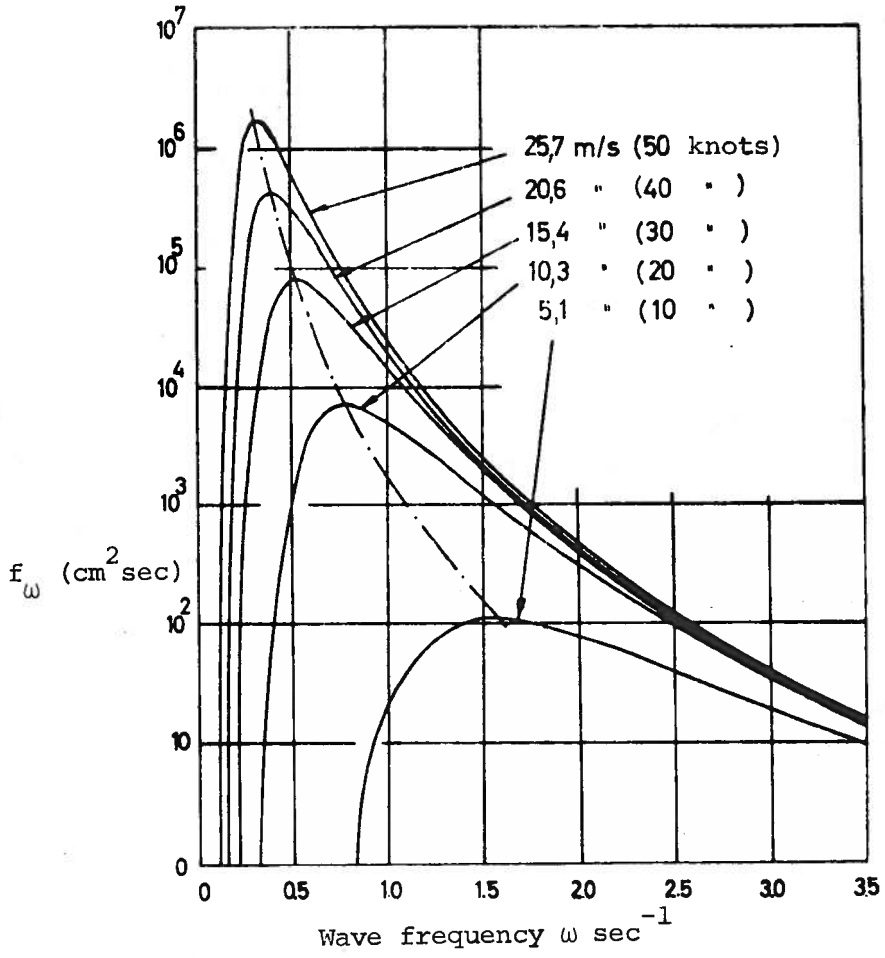

Fig.1.5.7

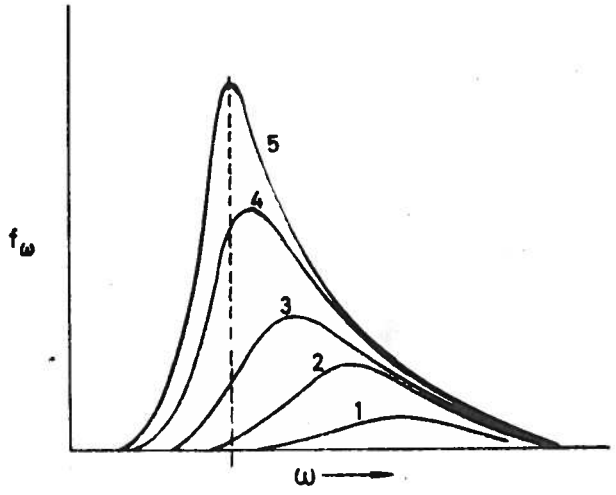

Fig.1.5.8

Table 1.5.2

Wind Velocity		Min. Fetch	Least Duration
m/sec.	Beaufort	km.	hours
1,0	1	0,1	0,07
4,4	3	11	2,3
9,8	5	120	9,2
15,7	7	540	24
22,6	9	1780	52
30	11	4600	101

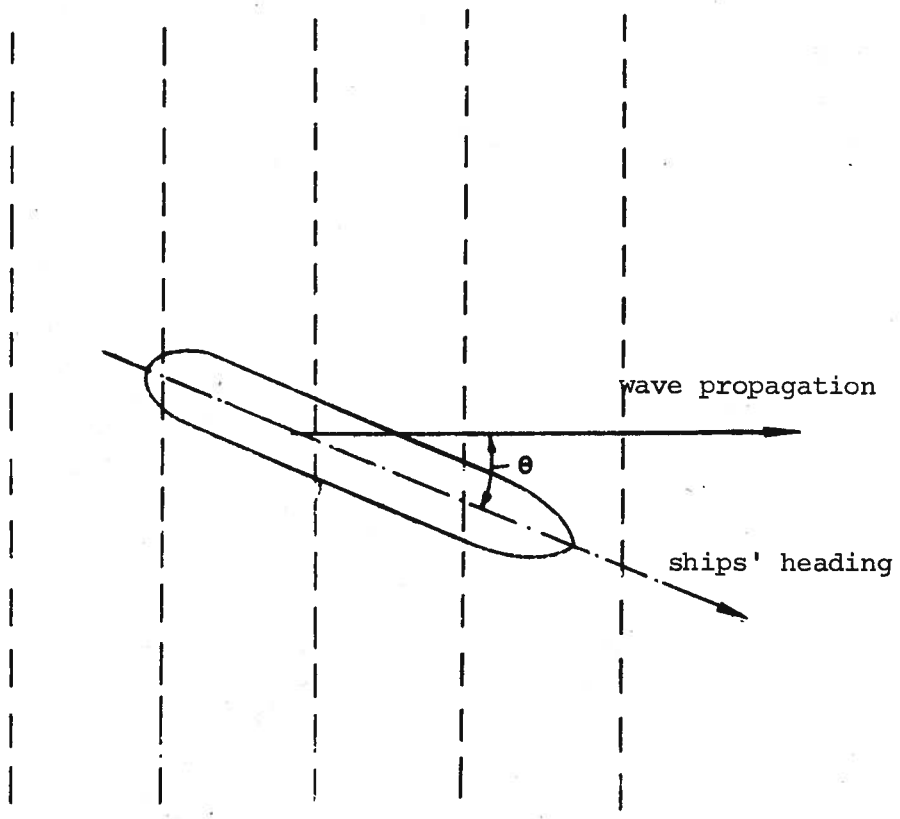

Fig.1.5.9

Fig. 1.5.10 shows how an energy spectrum (Neumann) changes when the ship's course and velocity varies. The total energy content is of course the same for all the curves shown, but the energy concentrates in a narrow frequency band for following seas. In head seas the energy content will be shifted towards higher frequencies.

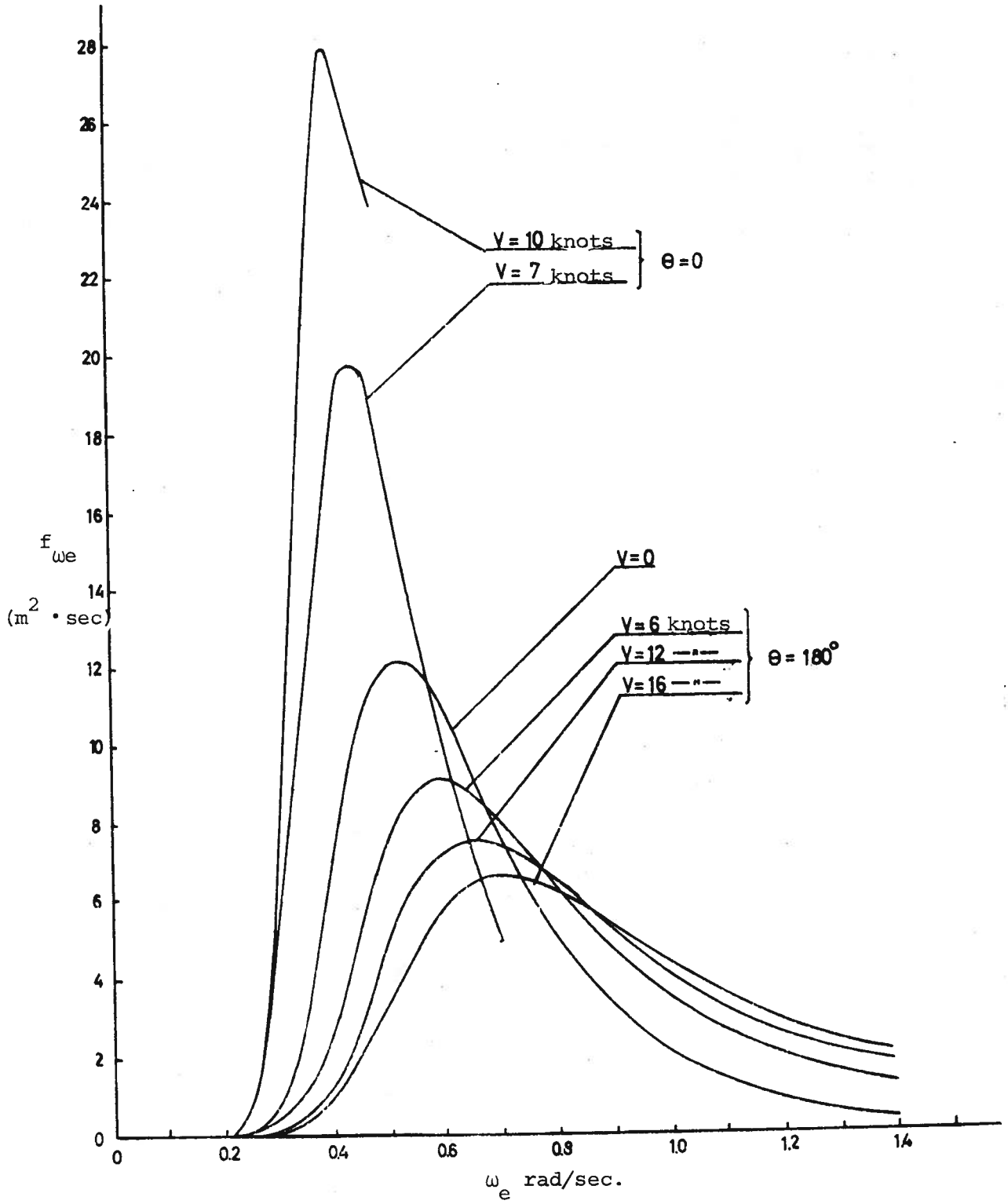

Fig. 1.5.10

Concentrated research efforts are now made to obtain representative expressions for wave spectrum. A committee established by the International Ship Structure Congress suggested at the meetings in Delft during the summer of 1964 the following equation:

$$E'(f) = 0.22\, H_v^2\, T_v\, (T_v f)^{-5}\, e^{-0.44/(T_v f)^4} \qquad (1.5.17)$$

Here the energy spectrum is given as a function of:

$$f = \frac{\omega}{2\pi}$$

Also the sea state is characterized by the quanitites H_v and T_v where

H_v = a characteristic wave height (in meters), usually defined as the average height of the highest one third of all waves ("significant wave height").

T_v = a wave period that approximately corresponds to average apparent period T_t(sec.).

H_v and T_v are usually observed by weather ships etc. and table 1.3.2 indicates the results of such observations in the North Atlantic. When the energy spectrum is known, H_v may be estimated directly. It is found that:

$$H_v = 2\sqrt{2E'} \qquad (1.5.18)$$

or, in other words, that $E' = H_v^2/8$.

1.5.6 Loads on ships in a seaway.

Static calculations and model tests show that it is fairly accurate to assume that the wave moment acting on a ship's hull is proportional to the wave height (see section 1.3). In a simple sine-wave (elementary wave) that meets the ship with the frequency ω_e and wave height $2r_{\omega e}$, the wave moment ($M_{\omega e}$) may be set equal to:

$$M_{\omega e} = A_{\omega e} \cdot r_{\omega e} \tag{1.5.19}$$

where $A_{\omega e}$ is an "influence function" that gives the bending moment for a sine wave with frequency ω_e and with $r_{\omega e} = 1$.

$$A_{\omega e} = \mu_{z\omega e} \gamma \, BL^2 = \left(\frac{M_{by}}{r_{\omega e}} \right) \tag{1.5.20}$$

When determining the total load that is caused by a number of elementary waves of various frequencies, the super position principle is assumed to apply. The following formula for the variation of the total wave bending moment with time, may then be written: (see equation 1.5.7)

$$M(t) = \sum_{1}^{n} \sqrt{A^2_{\omega en} \, f_{\omega en} \, d_{\omega e}} \cos(\omega_n t + \varepsilon_n) \tag{1.5.21}$$

This equation represents a wave moment spectrum that has exactly the same stocastic character as the energy spectrum for the wave height. Fig. 1.5.11 shows how, by using the wave spectrum plus the influence function $A^2_{\omega e}$ (fig.a) it is possible to calculate the coordinates $(m^2_{\omega e})$ of the moment spectrum (fig. b). We have that:

$$m^2_{\omega e} = A^2_{\omega e} \cdot f_{\omega e} \tag{1.5.22}$$

The area under the moment spectrum is equal

$$E_M = \int_0^{\infty} m^2_{\omega e} \, d_{\omega e} \tag{1.5.23}$$

where

$$\omega_e = \omega - \frac{\omega^2}{g} v \cos\theta$$

$$\frac{d_{\omega e}}{d_{\omega}} = 1 - \frac{2\omega}{g} v \cos\theta \tag{1.5.24}$$

and

$f_{\omega e}$ = the coordinate in the wave spectrum

$A^2_{\omega e}$ = the coordinate for the influence function,

the index e indicates that the values are given as functions of the frequency of encounter.

The curves in fig. 1.5.11 were determined from model tests by Lewis[1]. The wave spectrum is observed in the tank and curve 1 in fig. 1.5.11 b shows corresponding observed moment spectrum on the model. The curve for $A^2_{\omega e}$ is found experimentally by testing the model in regular waves with varying frequencies of encounter. Curve 2 in fig. 1.5.11 b is calculated by using equation 1.5.22. The correlation between the curves 1 and 2 is, as can be seen, very good. Lewis is of the opinion that the drop in $A^2_{\omega e}$ at $\omega_e \sim 10$ is not real, but is caused by complications in the measuring technique. Without this drop the greement would perhaps be even better.

When the area under the moment spectrum is known, it is possible by using the previously given properties of the Rayleigh distribution, to find the probable maximum bending moments, by setting R equal the area under the spectral curve (E_M).

The values for $A_{\omega e}$ for various values of ω_e may be found either by using model tests or by means of calculations. In $A_{\omega e}$ must be included dynamic effects. This quanitity will, therfore, depend on the hull shape, cargo distribution, ratios of frequencies of encounter to natural frequencies of pitching and heaving, etc. (see section 1.4).

---

1) Lewis, E.V.: "A study of midship bending moments in irregular head seas, T2-Se-AL tanker model". Journ. Ship Res. Vol. 1, 1955, No. 1, pp. 43-54.

The moment spectrum may be determined more directly by using measurements at sea. That determines for instance the moment coordinates directly and it can be shown that the area under the spectrum is given by the formula (compare equation (1.5.10) and (1.5.9)):

$$E_M = 2 \frac{\sum x_i^2}{N} \qquad (1.5.25)$$

where

x_i = observed coordinates of moment at random time intervals

N = number of observations

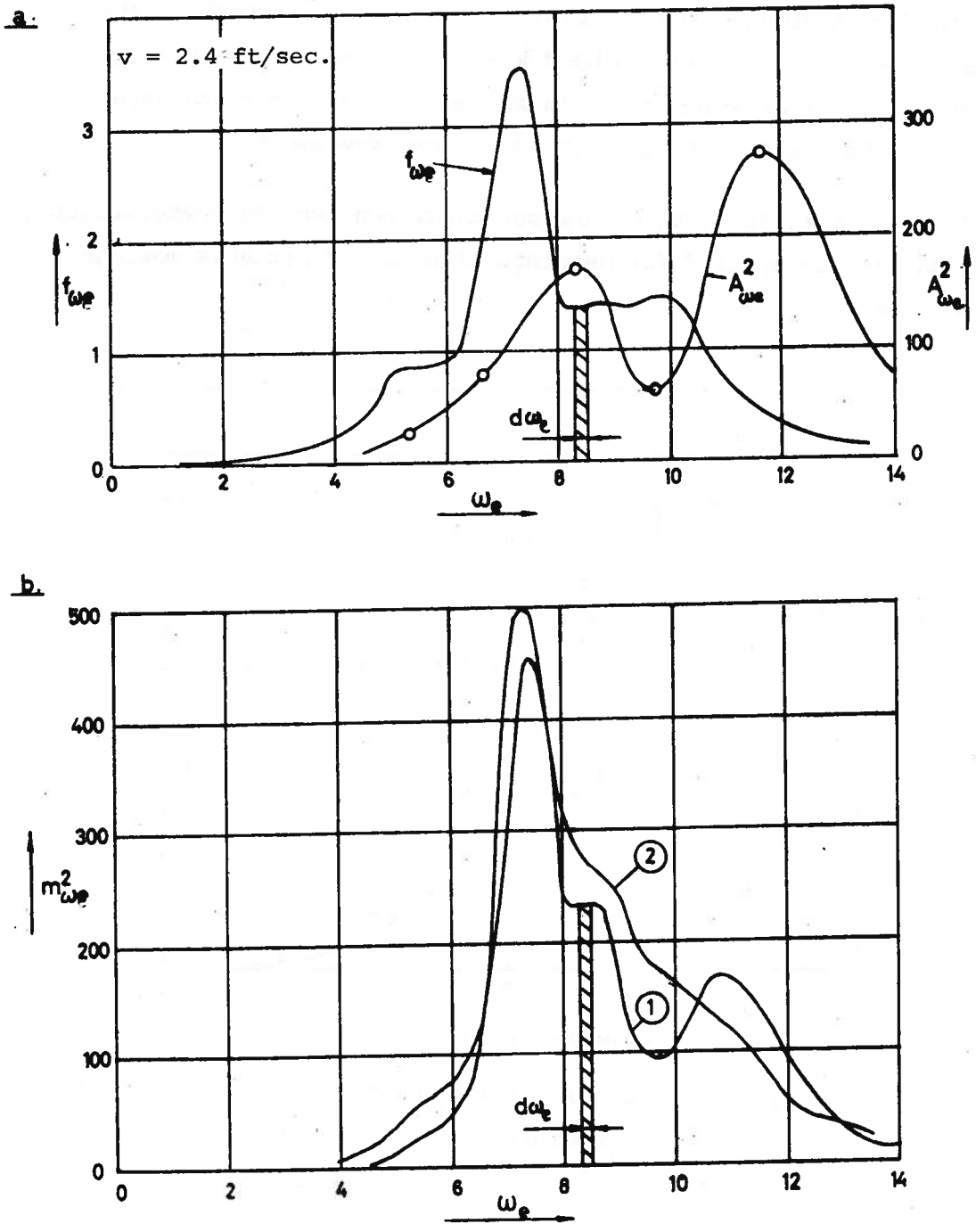
a.
v = 2.4 ft/sec.
f_{ω_e}
$A^2_{\omega_e}$
$d\omega_e$
ω_e
b.
$m^2_{\omega_e}$
2
1
$d\omega_e$
ω_e

Fig. 1.5.11

Fig. 1.5.12 shows a frequency diagram for the observed values of longitudinal stresses in the main deck on a ship in a seaway, and corresponding Rayleigh distribution. The correlation is seen to be good[1)]. The results in the figure were obtained in head seas with a speed of about 6 knots. Significant wave height was approx. 16 ft. and the measurements were done in approx. 1/2 hour with all together 230 stress reversals.

A method corresponding to the one described here for determination of loads can also be applied for determination of the probable motions of the ship in seas.

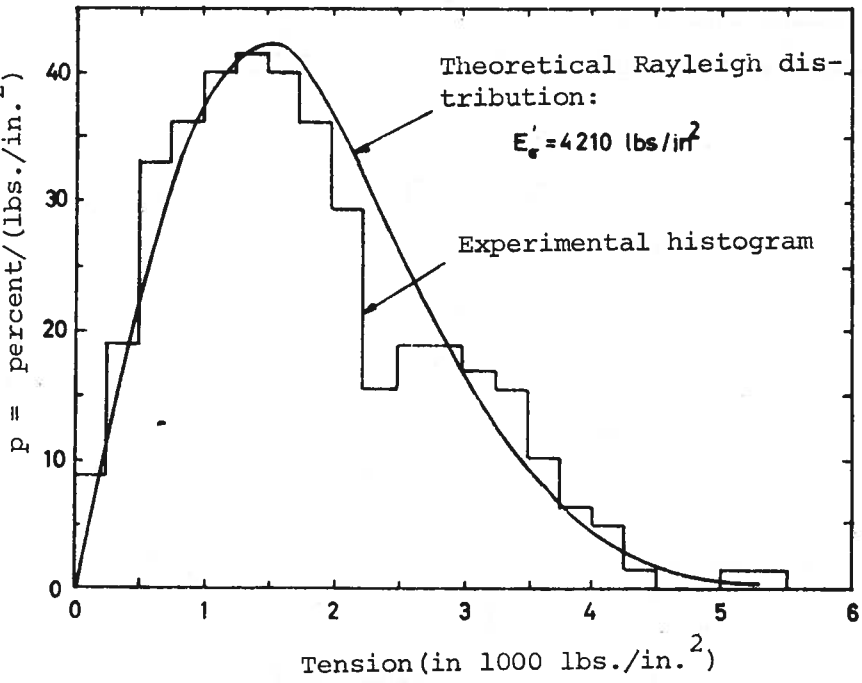

Fig. 1.5.12 Distribution of tension variations longitudinally in main deck midships.

1) Jasper, N.H.: "Statistical Distribution Patterns of Ocean Waves and of Wave-Induced Ship Stresses and Motions, with Engineering Applications". David Taylor Model Basin, Rep. 921. Oct. 1957.

1.5.7 Distribution functions for stresses over longer time periods.

The discussions above have all the time been based on a tacit assumption that the sea within the time period considered did not alter its character. In other words, it has been assumed unaltered energy content in the sea.

In reality the sea will constantly alter it character and it is really not permissible to draw conclusions that are valid for any time period much longer than 1/2 hour.

Before the distribution of the loads over a longer time period can be estimated, it must be known how the conditions over the particular region of the ocean changes from time to time. This information can only be obtained from observations made at sea. The seas may then either be determined directly expressed by E , or its influence on the ship can be determined, expressed , e.g. by E_M (= area under the moment spectrum).

Observations show that the values of (log E) and (log E_M) be assumed, with good approximation, to be normally distributed, such that:

$$p(\log E_M) = \frac{1}{s\sqrt{2\pi}} \exp. - ((\log E_M - \mu)^2/2s^2) \qquad (1.5.26)$$

where

s = standard deviation for (log E)

μ = mean value for (log E_M)

These values are assumed determined either by theoretical estimates or, more likely, by observations made at sea.

From equation (1.5.26) the probability that E_M exceeds a certain limit value E_{M1} , can be determined

(1.5.27)

$$P\{\log E_M > \log E_{M1}\} = \frac{1}{s\sqrt{2\pi}} \int_{\log E_{M1}}^{\infty} \exp. -((\log E_M - \mu)^2/2s^2) d\{\log E_M\}$$

Corresponding formulas can be set up for the stresses at certain points in the hull expressed by E_σ . Usually it is then the stress reversals that are measured as the ship moves through a wave, thus only wave induced stresses are recorded, and then as the difference between sagging and subsequent hogging.

Fig. 1.5.13 shows on logarithmic probability paper how for some vessels, the hull stresses expressed by the amidships have varied, where the observation were made over a longer period of time. The stresses are here expressed by the Rayleigh factor E_σ . Note that straight lines in fig. 1.5.13 correspond to so-called log-normal distribution according to equation (1.5.26). The location and slope of the lines in the figure depend upon the spread s and mean value μ , which again varies from route to route, from ship to ship, from one loading condition to another.

From fig. 1.5.13 it is found, for example that for "Minnesota" $\sqrt{E_\sigma}$ will with 99.8% probability be <480 kp/cm^2. From table 1.5.1 it is further seen that on the average there is only 1 wave out of 100.000 that gives a stress that is $\geq 3.393 \cdot \sqrt{E_\sigma}$. It can thus be concluded that stresses reversals $> 3.393 \cdot 480$ kp/cm^2 $= 1630$ kp/cm^2 will rarely occur.

During a sailing period of 30 years (time at sea) the ship will probably be in a seaway with $\sqrt{E_\sigma} > 480$ kp/cm^2 over a period of all together $30 \cdot 365 \cdot 24 \cdot 0.002 = 525$ hours. If the ship meets on the average n waves per hour, the stress will probably exceed 1630 kp/cm^2 $525 \cdot n \cdot 10^{-5} =$ $= 5.25n \cdot 10^{-3}$ times.

There is of course a certain chance that just this stress occurs in, say, a seaway of less intensity. This more moderate sea will occur more often but the percentage probability that the stresses will be brought up to $\sqrt{E_\sigma} =$ $= 480$ kp/cm^2 in the moderate sea is on the other hand lower, see fig. 1.5.14 where the hatched areas represent the probability that the stresses will be between the values that correspond to the lines a and b.

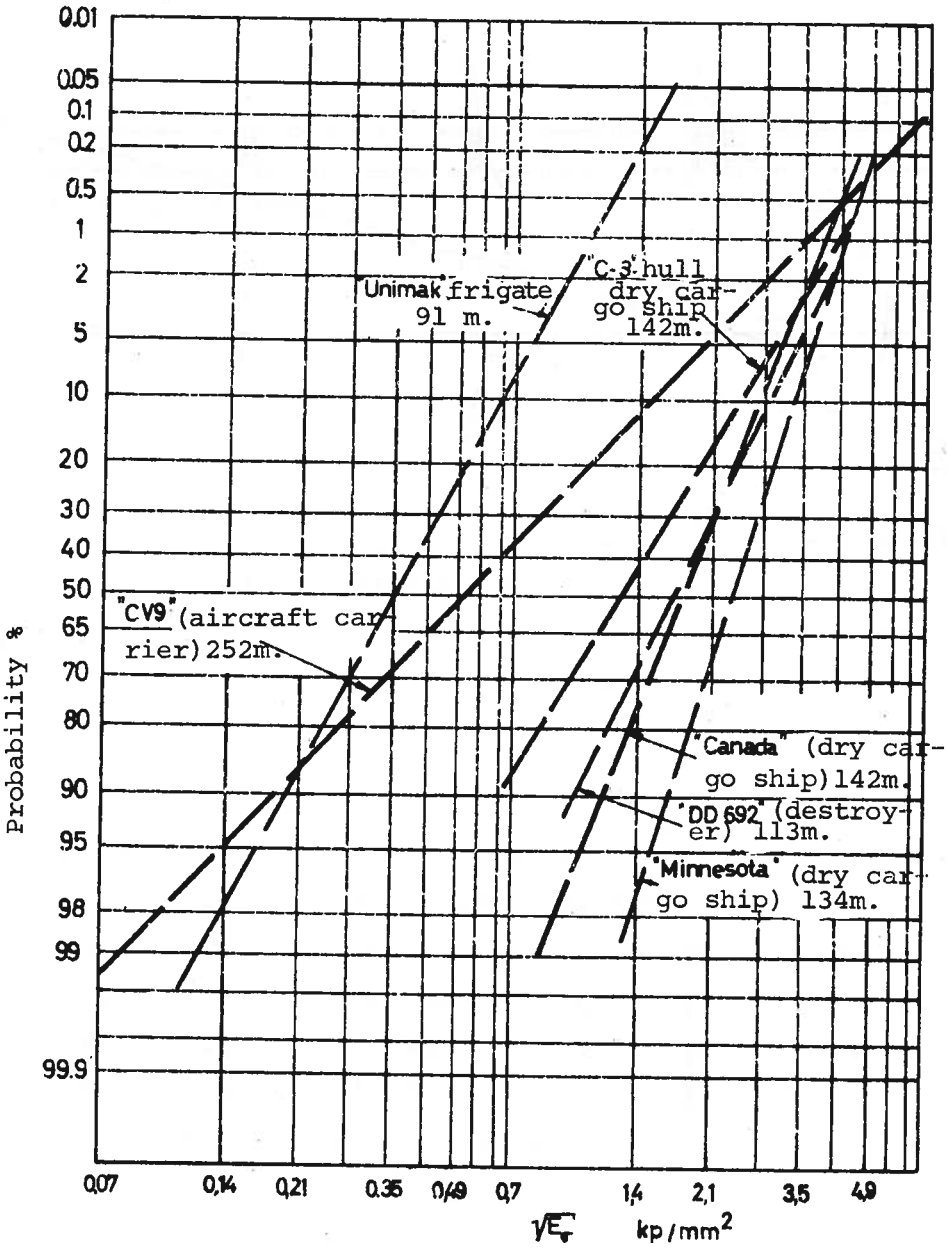
Probability %
0.01
0.05
0.1
0.2
0.5
1
2
5
10
20
30
40
50
65
70
80
90
95
98
99
99.9
0,07
0,14
0,21
0.35
0,49
0,7
1,4
2,1
3,5
4,9
√E_v kp/mm²
Unimak frigate 91 m.
"C-3 hull dry cargo ship 142m.
"CV9" (aircraft carrier) 252m.
"Canada" (dry cargo ship) 142m.
"DD 692" (destroyer) 113m.
"Minnesota" (dry cargo ship) 134m.

Fig .1.5.13

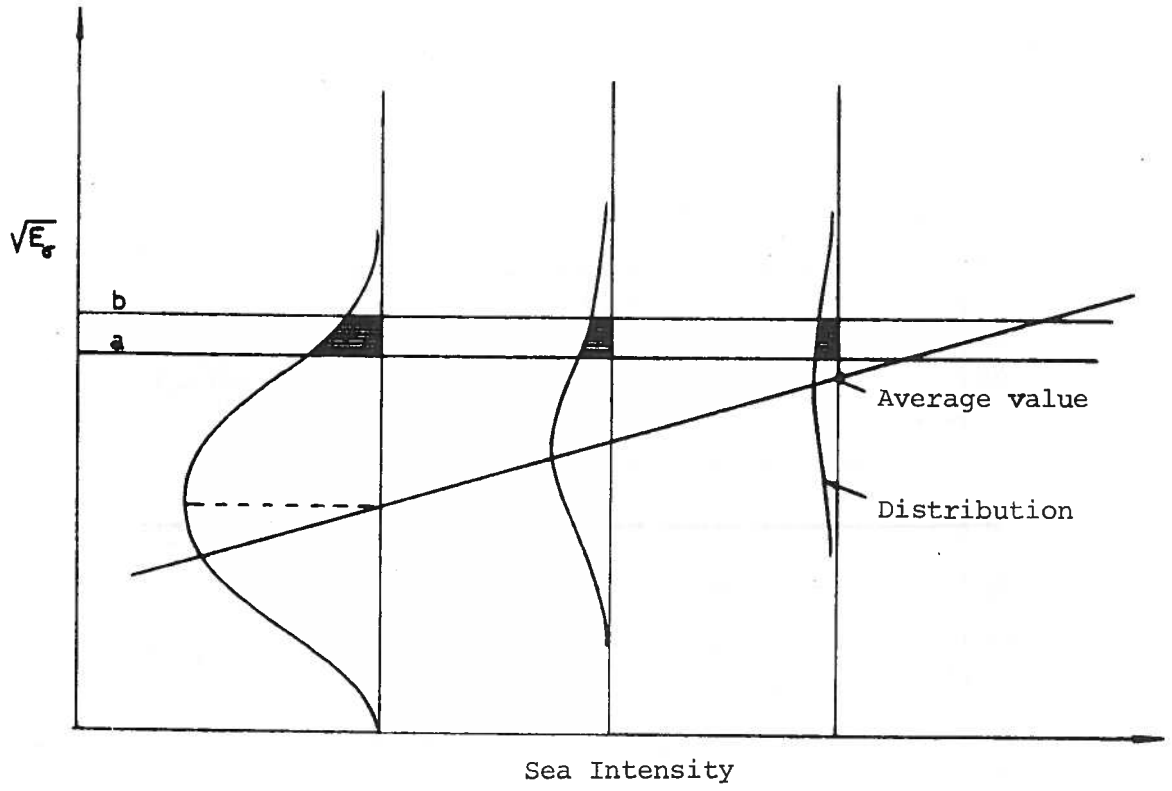

Fig. 1.5.14

When the distribution of $\sqrt{E}$ over a certain time period is known, the probable number of stresses up to any level may also be calculated. Fig. 1.5.15 shows such estimated probable distributions of the hull stresses for a couple of ships. The diagram includes two sets of dotted lines where the one to the left is for a time period of 30 days, whereas the other is for 20 years. For example, it is seen that the probable maximum stress reversal change for "Canada" during 20 years will be approximately 1530 kp/cm^2. It is then assumed that the vessel always sails the routes where the measurements were made.

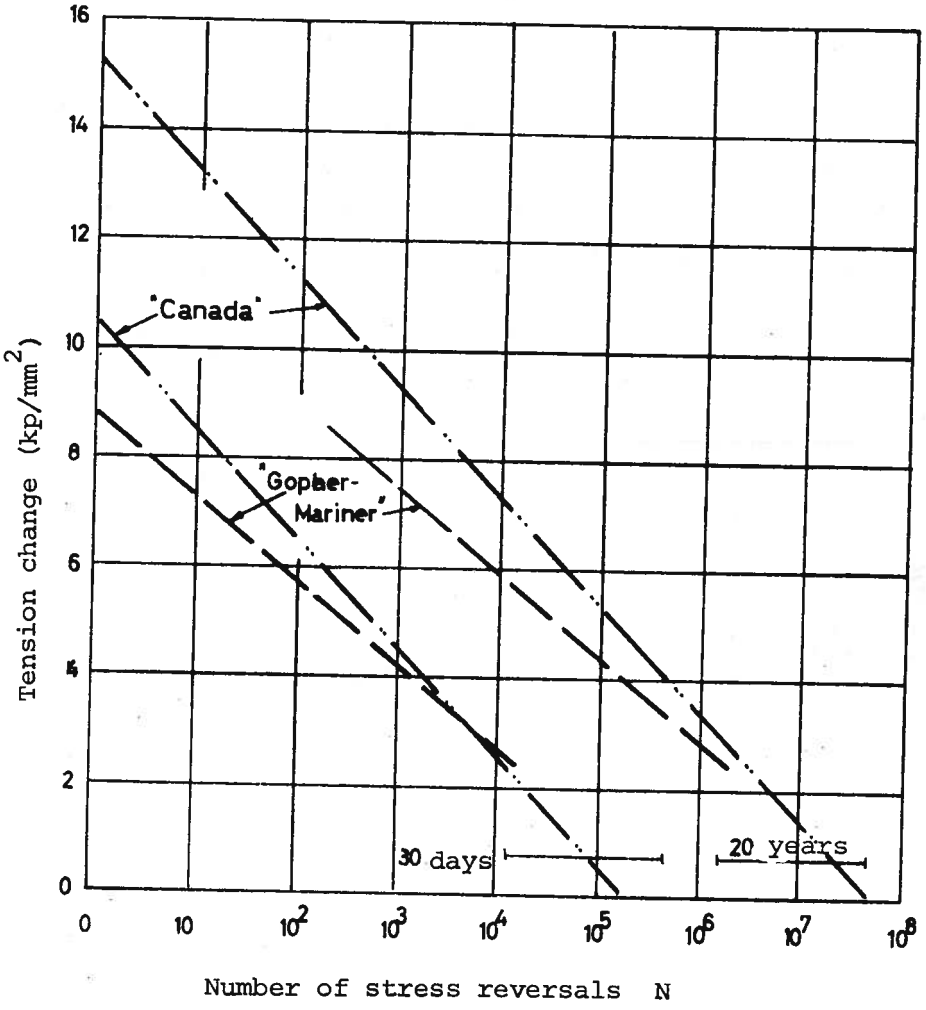

Fig. 1.5.15

1.5.8 Concluding remarks

Theoretically the objective is set up in the introduction to this chapter has been reached. Practically it is not so well off. Even though a number of observations at sea have been made during the last few years,

this is only the beginning. It should be assumed, however, that the statistical evaluations of stresses in ships in the years to come will be of an ever increasing importance[1,2,3].

To provide a sort of an overview of the material discussed in the sections 1.3, 1.4, and 1.5, a diagram is drawn in fig. 1.5.16 which tries to show how the various calculation steps may be assumed to fit into a rational analysis of longitudinal wave stresses.

Generally it may be said that practice followed until recent years is covered by the loop at the bottom of the figure. Since the beginning of the 1950's, the purpose has been to build out the upper part of the research shown in the figure. The problem may principally be solved in various ways, illustreated in fig. 1.5.16 by the various arrows. The higher up in the diagram the starting point is chosen, the more difficult it becomes perhaps to reach agreements between different approaches. On the other hand, the problem will constantly come closer to its complete solution as it becomes possible to include the whole problem set. There are all reasons in the world to follow the development of this field in the years to come. This development is very fast and is a requirement for the further development towards ever larger and relatively lighter ship hulls.

---

1) Bennet, R. : "Stresses and Motion Measurements at Sea". The Swedish Shipbuilding Research Foundation, Goteborg, 1958.

2) Nordenstrom, N.: "Statistics and Wave Loads". Goteborg 1964.

3) Johnson, A.J.: "Stresses in Ships in Service". RINA, Spring Meeting, 1963.

Fig. 1.5.16 Organizational Diagram for the Analysis of Wave Loads and Longitudinal Strength.